arXiv:1212.2891v1 [nucl-ex] 12 Dec 2012

# Elastic alpha scattering experiments and the alpha-nucleus optical potential at low energies

P. Mohr[a,b,*], G. G. Kiss[a], Zs. Fülöp[a], D. Galaviz[c], Gy. Gyürky[a], E. Somorjai[a]

[a] *Institute of Nuclear Research (ATOMKI), H-4001 Debrecen, Hungary*
[b] *Diakonie-Klinikum, D-74523 Schwäbisch Hall, Germany*
[c] *Centro de Física Nuclear, University of Lisbon, P-1649-003 Lisbon, Portugal*

---

## Abstract

High precision angular distribution data of ($\alpha$,$\alpha$) elastic scattering are presented for the nuclei $^{89}$Y, $^{92}$Mo, $^{106,110,116}$Cd, $^{112,124}$Sn, and $^{144}$Sm at energies around the Coulomb barrier. Such data with small experimental uncertainties over the full angular range (20-170 degrees) are the indispensable prerequisite for the extraction of local optical potentials and for the determination of the total reaction cross section $\sigma_{\rm reac}$.

A systematic fitting procedure was applied to the presented experimental scattering data to obtain comprehensive local potential parameter sets which are composed of a real folding potential and an imaginary potential of Woods-Saxon surface type. The obtained potential parameters were used in turn to construct a new systematic $\alpha$-nucleus potential with very few parameters. Although this new potential cannot reproduce the angular distributions with the same small deviations as the local potential, the new potential is able to predict the total reaction cross sections for all cases under study.

---

---

[*] Corresponding author.

*Email address:* `E-mail: mohr@atomki.mta.hu` (P. Mohr)

*Preprint submitted to Atomic Data and Nuclear Data Tables* *12.12.2012*

## Contents

1. Introduction . . . 3

2. Experimental technique . . . 4

    2.1. Beam properties and targets . . . 4

    2.2. Scattering chamber, detectors, and angular calibration . . . 4

    2.3. Data analysis . . . 5

3. Optical model analysis . . . 6

4. Summary and Conclusions . . . 8

A. Appendix: Suggestions for a new $\alpha$-nucleus potential . . . 9

References . . . 12

Explanation of Tables . . . 19

Explanation of Graphs . . . 20

Tables

1. Parameters of the energy dependence of the interaction. See page 19 for Explanation of Tables . . . 21

2. $^{89}$Y($\alpha$,$\alpha$)$^{89}$Y elastic scattering cross section (normalized to the Rutherford cross section) at the energy $E = 15.51$ MeV. See page 19 for Explanation of Tables . . . 22

3. $^{89}$Y($\alpha$,$\alpha$)$^{89}$Y elastic scattering cross section (normalized to the Rutherford cross section) at the energy $E = 18.63$ MeV. See page 19 for Explanation of Tables . . . 23

4. $^{92}$Mo($\alpha$,$\alpha$)$^{92}$Mo elastic scattering cross section (normalized to the Rutherford cross section) at the energy $E = 13.20$ MeV. See page 19 for Explanation of Tables . . . 24

5. $^{92}$Mo($\alpha$,$\alpha$)$^{92}$Mo elastic scattering cross section (normalized to the Rutherford cross section) at the energy $E = 15.69$ MeV. See page 19 for Explanation of Tables . . . 25

6. $^{92}$Mo($\alpha$,$\alpha$)$^{92}$Mo elastic scattering cross section (normalized to the Rutherford cross section) at the energy $E = 18.70$ MeV. See page 19 for Explanation of Tables . . . 26

7. $^{106}$Cd($\alpha$,$\alpha$)$^{106}$Cd elastic scattering cross section (normalized to the Rutherford cross section) at the energy $E = 15.55$ MeV. See page 19 for Explanation of Tables . . . 27

8. $^{106}$Cd($\alpha$,$\alpha$)$^{106}$Cd elastic scattering cross section (normalized to the Rutherford cross section) at the energy $E = 17.00$ MeV. See page 19 for Explanation of Tables . . . 28

9. $^{106}$Cd($\alpha$,$\alpha$)$^{106}$Cd elastic scattering cross section (normalized to the Rutherford cross section) at the energy $E = 18.88$ MeV. See page 19 for Explanation of Tables . . . 29

10. $^{110}$Cd($\alpha$,$\alpha$)$^{110}$Cd elastic scattering cross section (normalized to the Rutherford cross section) at the energy $E = 15.56$ MeV. See page 19 for Explanation of Tables . . . 30

$^{110}$Cd($\alpha$,$\alpha$)$^{110}$Cd elastic scattering cross section (normalized to the Rutherford cross section) at the energy $E = 18.76$ MeV. See page 19 for Explanation of Tables . . . 31

12. $^{116}$Cd($\alpha$,$\alpha$)$^{116}$Cd elastic scattering cross section (normalized to the Rutherford cross section) at the energy $E = 15.59$ MeV. See page 19 for Explanation of Tables . . . 32

13. $^{116}$Cd($\alpha$,$\alpha$)$^{116}$Cd elastic scattering cross section (normalized to the Rutherford cross section) at the energy $E = 18.80$ MeV. See page 19 for Explanation of Tables . . . 33

14. $^{112}$Sn($\alpha$,$\alpha$)$^{112}$Sn elastic scattering cross section (normalized to the Rutherford cross section) at the energy $E = 13.90$ MeV. See page 19 for Explanation of Tables . . . 34

15. $^{112}$Sn($\alpha$,$\alpha$)$^{112}$Sn elastic scattering cross section (normalized to the Rutherford cross section) at the energy $E = 18.84$ MeV. See page 19 for Explanation of Tables . . . . . 36
16. $^{124}$Sn($\alpha$,$\alpha$)$^{124}$Sn elastic scattering cross section (normalized to the Rutherford cross section) at the energy $E = 18.90$ MeV. See page 19 for Explanation of Tables . . . . . 37
17. $^{144}$Sm($\alpha$,$\alpha$)$^{144}$Sm elastic scattering cross section (normalized to the Rutherford cross section) at the energy $E = 19.45$ MeV. See page 19 for Explanation of Tables . . . . . 38

Graphs

1. Elastic ($\alpha$,$\alpha$) scattering angular distributions of $^{89}$Y and $^{92}$Mo. . . . . . 39
2. Elastic ($\alpha$,$\alpha$) scattering angular distributions of $^{106}$Cd and $^{110}$Cd. . . . . . 40
3. Elastic ($\alpha$,$\alpha$) scattering angular distributions of $^{116}$Cd, $^{112}$Sn, $^{124}$Sn, and $^{144}$Sm. . . . . . 41

## 1. Introduction

The $\alpha$-nucleus potential is the key ingredient for the calculation of $\alpha$-particle induced reaction cross sections. For intermediate mass and heavy target nuclei the reaction cross sections are typically calculated within the framework of the statistical model where the cross section $\sigma(\alpha,X)$ of an $\alpha$-induced reaction is given by the product of the compound formation cross section $\sigma_{CF}$ and the decay branching $b_X$ into the $X$ channel. Usually, the compound formation cross section $\sigma_{CF}$ is approximated by the total reaction cross section $\sigma_{\rm reac}$ which depends on the transmission coefficient $T_\alpha$ of the incoming $\alpha$-particle. The decay branching is given by $b_X = T_X / \sum_i T_i$ where the summation has to be performed over all open channels $i$ (including $T_\alpha$). This leads to the well-known proportionality

$$\sigma(\alpha,X) \sim \frac{T_\alpha T_X}{\sum_i T_i} \qquad . \tag{1}$$

In many cases it turns out that the transmission into other channels is much larger than the transmission into the $\alpha$ channel. This holds in particular for the neutron channel as soon as the energy exceeds the threshold of the ($\alpha$,n) reaction. In such cases we find $T_X \approx \sum_i T_i$, and the cross section $\sigma(\alpha,X)$ in Eq. (1) becomes proportional to $T_\alpha$, i.e. it is mainly defined by the transmission coefficient into the $\alpha$ channel and the underlying $\alpha$-nucleus potential. The full formalism of the statistical model is reviewed e.g. in [1, 2].

It has been noticed that predictions of $\alpha$-induced reaction cross sections at low energies have large uncertainties depending on the chosen $\alpha$-nucleus potential. This holds in particular for ($\alpha$,$\gamma$) capture reactions for targets with masses above $A \approx 100$ [3–10] but also for ($\alpha$,n) reactions as e.g. seen recently in [11, 12]. In addition, the uncertainties of ($\alpha$,$\gamma$) cross sections translate into similar uncertainties for the prediction of ($\gamma$,$\alpha$) cross sections and ($\gamma$,$\alpha$) reaction rates under the stellar conditions of the astrophysical *p*- or $\gamma$-process [13–15]. The stellar reaction rates of these photon-induced ($\gamma$,$\alpha$) reactions are usually determined from the inverse ($\alpha$,$\gamma$) capture cross sections using detailed balance because thermally excited states contribute significantly to the stellar reaction rate of photon-induced reactions [1, 16]; these thermally excited states are not accessible for ($\gamma$,$\alpha$) experiments in the laboratory.

Despite significant effort over the last decades, there is still no global potential available that is able to describe elastic scattering angular distributions and cross sections of $\alpha$-induced reactions simultaneously with high quality. Up to now, the four-parameter energy-independent potential by McFadden and Satchler is still widely used [17]. A many-parameter potential has been developed by Avrigeanu and coworkers over the last decade [18, 19]. A simple potential for higher energies is given by Kumar *et al.* [20] which has turned out to be inadequate at very low energies. A further global potential has been developed by Demetriou *et al.* [21], and a simple 6-parameter potential was optimized for reaction cross sections at low energies by Rauscher [22]. An attempt was made to find a common potential for $\alpha$ decay and $\alpha$ capture [23]. Very recently, a further regional potential in the cadmium/tin/tellurium region has been derived from elastic scattering data by the Notre Dame astrophysics group and coworkers [24, 25].

Elastic scattering is a standard method for the determination of $\alpha$-nucleus optical potentials. However, at energies close to the Coulomb barrier ambiguities are found for the derived potentials because of the dominating Rutherford contribution to the scattering cross section. It is obvious that experimental data have to be measured with high precision to reduce the ambiguities as much as possible. Here we present a summary of all the data that have been measured over the last 15 years at the cyclotron of ATOMKI, Debrecen, together with a new and consistent analysis within the optical model.

The paper is organized as follows: In Sect. 2 we briefly present our experimental set-up and the data analysis. Sect. 3 provides some information on the theoretical analysis and the derived local parameters of the optical potential. All experimental data are listed in the Tables at the end and are available as supplementary content. A suggestion for a new $\alpha$-nucleus potential is given in the Appendix (Sect. A). All energies are given as $E_{\mathrm{c.m.}}$ in the center-of-mass system except explicitly noted.

## 2. Experimental technique

### *2.1. Beam properties and targets*

All alpha elastic scattering experiments discussed in the present paper were carried out at the cyclotron laboratory of ATOMKI, Debrecen. In this paper a brief overview on the experimental technique is given. Further experimental details can be found in the original papers [26–32], conference proceedings [33, 34] and in a Ph.D. dissertation [35]. The proton and neutron number, the chemical form of the target material, isotopic enrichment of the target, the energy of the first excited states of the target nuclei and energies of the measured angular distributions are summarized in Table A.

The energies of the $^{4}\mathrm{He}^{++}$ beam — provided by the K20 cyclotron of ATOMKI — were between 13.8 and 20.0 MeV with typical beam currents of 300-500 enA. Since the imaginary part of the optical potential depends sensitively on the energy, it is important to have a well-defined beam energy. Therefore the beam was collimated by tight slits (1 mm wide) at the analyzing magnet; this corresponds to an overall energy spread of around 100 keV.

The targets were produced by evaporating isotopically highly enriched material ($\geq$ 95%, see Table A) onto thin carbon foils ($\approx$ 20 $\mu$g/cm$^2$). The target and backing thicknesses were determined via alpha particle energy loss measurement using a mixed alpha source which contains $^{239}$Pu, $^{241}$Am, and $^{244}$Cm radioactive nuclides. Typical energy losses in the carbon backing and the targets are about 15 keV and within 40 and 70 keV, respectively. These energy losses correspond to about 150-200 $\mu g$/cm$^2$ target thicknesses. The targets were mounted on a remotely controlled target ladder in the center of the scattering chamber. The stability of the targets was monitored continuously during the experiment using detectors (see below) built into the wall of the scattering chamber at $\pm$ 15° (with respect to the beam direction).

### *2.2. Scattering chamber, detectors, and angular calibration*

For carrying out the alpha elastic scattering experiments the 78.8 cm diameter scattering chamber was used. Ion implanted silicon detectors with active areas of 50 mm$^2$ and 500 $\mu$m thickness have been used to measure the yield of the scattered alpha particles. Two detectors were mounted on the wall of the scattering chamber at fixed angles $\vartheta = \pm 15^\circ$ left and right to the beam axis. These detectors were used as monitor detectors — their solid angles were 1.1 x $10^{-6}$ — during the whole experiment to normalize the measured angular distribution and to determine the precise position of the beam on the target. The detectors used to measure the alpha scattering angular distributions were mounted onto two independently movable turntables. On each of the turntables between 2 and 5 detectors were placed. The solid angles of these detectors varied between 1.36 x $10^{-4}$ and 1.93 x $10^{-4}$ (calculated from the known geometry), and the ratio of these solid angles was determined precisely by measurements at overlapping angles with good statistics ($\leq$1% uncertainty).

In order to derive precisely the scattering angle, the exact position of the beam on the target has to be known. For this reason, the following procedure was used. An aperture of 2 mm width and 6 mm height was mounted on the target ladder to check the beam position and size of the beam spot before and after every change of the beam energy or current. The beam was optimized until not more than 1% of the total beam current could be measured on this aperture. As a result of the procedure, the horizontal size of the beam spot was below 2 mm during the whole experiment.

The elastic scattering cross section at forward angles differs by several orders of magnitude from the one measured at backward angles (see below), this fact necessitates very different counting times at forward and backward angles. While at forward angles the spectra were collected for typically 5-30 minutes, at backward angles to achieve reasonable statistics the measuring times had to be typically within 3 and 6 hours. Furthermore, a reliable dead-time correction is also crucial. For this reason the automatically determined dead-time provided by the data acquisition system has been verified using a pulser in all spectra.

Knowledge of the exact angular position of the detectors is of crucial importance for the precision of a scattering experiment since the Rutherford cross section depends sensitively on the scattering angle especially at forward directions. The uncertainty in the angular distribution is dominated by the error of the scattering angles in the forward region. To determine the scattering angle precisely, kinematic coincidences were measured between elastically scattered alpha particles and the corresponding $^{12}$C recoil nuclei using a pure carbon backing as target. One detector was placed at a certain angle to measure the yield of the alpha particles scattered on $^{12}$C, and its signal was selected as a gate for the other detector which moved around the expected $^{12}$C recoil angle. A Gaussian had been fitted onto this experimental yield data. From the difference between the expected $^{12}$C recoil angle and the maximum of the Gaussian the angular offsets of the detectors can be calculated. In addition, in some experiments the steep kinematics of $^{1}$H($\alpha$,$\alpha$)$^{1}$H scattering was analyzed using a thin plastics $(CH_2)_n$ target.

This process was repeated for all detector pairs. The angular offset of each detector was less than 0.17° and the final angular uncertainty was found to be $\Delta\vartheta \leq 0.12°$ in the case of each detector. The given uncertainties of the measured cross sections contain the uncertainty of the scattering angle using standard error propagation; thus, the uncertainties of the scattering angle are not given explicitly in the tables.

### *2.3. Data analysis*

The elastic scattering peaks have to be well separated from the inelastic events and from alpha scattering on carbon (backing), oxygen, and other impurities of the target and/or backing. The energies of the first excited states of the target nuclei are listed in Table A. In principle, if the separation between the elastic and inelastic scattering is not properly done, it can lead to an overestimation of the elastic scattering peak. However, since our energy resolution is about 60-80 keV and the energies of the first excited states are far above 500 keV, typically around 1 MeV, the separation could be properly done. Furthermore, the peaks corresponding to elastic and/or inelastic alpha scattering on the carbon backing or on its oxygen contamination are also well separated from the elastic alpha scattering events of our interest because of the strong kinematic mass dependence of the energies of the scattered particles.

Angular distributions between 20° and 170° – 175° were measured at each energy listed in Table A (except for $^{92}$Mo at 15.69 MeV; due to technical problems at the end of the experiment, in this case the angular distribution was measured between 19.7° and 154.7°, and the very backward angles could not be covered), at angles below 100° in 1° steps and at angles above 100° in 2° – 2.5° angular steps. The statistical uncertainties varied typically between below 1% (forward angles) and 4% (backward angles). The count rates $N(\vartheta)$ have been normalized to the yield of the monitor detectors $N_{Mon.}(\vartheta=15°)$:

$$\left(\frac{d\sigma}{d\Omega}\right)(\vartheta) = \left(\frac{d\sigma}{d\Omega}\right)_{Mon.} \frac{N(\vartheta)}{N_{Mon.}} \frac{\Delta\Omega_{Mon.}}{\Delta\Omega}, \tag{2}$$

with $\Delta\Omega$ being the solid angles of the detectors, and $(\frac{d\sigma}{d\Omega})_{Mon.}$ is approximately given by the Rutherford cross section. Finally, the measured cross sections are converted to the center-of-mass system.

Whereas the Rutherford normalized cross section data cover about two orders of magnitude between the highest (forward angles at energies below the Coulomb barrier) and the lowest measured cross sections (backward angles at energies above the Coulomb barrier), the underlying cross sections cover more than four orders of magnitude. Over this huge range almost the same accuracy of about 2-5% total uncertainty could be achieved for each of the studied reactions. This error is mainly caused by the uncertainty of the determination of the scattering angle in the forward region and from the statistical uncertainty in the backward region.

The absolute normalization is done in two steps. In a first step the absolute normalization is taken from experiment, i.e. from the integrated beam current, the solid angle of the detectors, and the thickness of the target. This procedure has a relatively large uncertainty of the order of 10 % which is mainly based on the uncertainties of the target thickness. In a second step a “fine-tuning” of the absolute normalization is obtained by comparison to theoretical calculations at very forward angles. It is obvious that calculated cross sections from any reasonable potential practically do not deviate from the Rutherford cross section at the most forward angles; typical deviations are below 0.5 % for all potentials. This “fine-tuning” changed the first experimental normalization by only few per cent and thus confirmed the first normalization within the given errors.

## 3. Optical model analysis

The comprehensive analysis of the elastic scattering angular distributions is carried out within the framework of the optical model (OM). The interaction between the $\alpha$ projectile and the target nucleus is described by a complex OM potential

$$U_{\rm OM}(r) = V(r) + iW(r) + V_C(r) \tag{3}$$

where $V(r)$, $W(r)$, and $V_C(r)$ are the real part, imaginary part, and Coulomb part of the potential $U_{\rm OM}(r)$. The real part is calculated from the double-folding model with the widely used DDM3Y interaction [32, 36–39] where the folding potential $V_F(r)$ is modified by two parameters:

$$V(r) = \lambda \, V_F(r/w) \qquad . \tag{4}$$

$\lambda$ is the strength parameter of the order of $\lambda \approx 1.1 - 1.4$ leading to real volume integrals[1] of about $J_R \approx 350$ MeV fm$^3$. $w \approx 1$ is the width parameter which should remain very close to unity within about $1 - 2$ %; a larger deviation of $w$ from unity would indicate a failure of the underlying folding model. The folding potential is given by

$$V_F(r) = \int\int \rho_P(r_P)\, \rho_T(r_T)\, v_{\rm eff}(s, \rho, E_{\rm NN})\; d^3r_P\; d^3r_T \tag{5}$$

---

[1] As usual, the negative signs of the volume integrals $J_R$ and $J_I$ are omitted in the discussion.

with the nucleon densities $\rho_{P,T}(r_{P,T})$ and an effective energy- and density-dependent nucleon-nucleon (NN) interaction $v_{\rm eff}$ which factorizes into [37]

$$v_{\rm eff}(|\vec{s}|,\rho_P,\rho_T,E_{\rm NN}) = f(|\vec{s}|,E_{\rm NN})\cdot g(\rho_P,\rho_T,E_{\rm NN}) \qquad . \tag{6}$$

The energy $E_{\rm NN}$ in the NN interaction is usually taken from the energy per nucleon of the $\alpha$ projectile: $E_{\rm NN} = E_{\rm lab}/A_P$. $f(|\vec{s}|,E_{\rm NN})$ is composed of a short-range repulsive and a longer-range attractive part and a zero-range exchange part (e.g. [36]):

$$f(|\vec{s}|,E_{\rm NN}) = \left[7999\,\frac{e^{-4s}}{4s} - 2134\,\frac{e^{-2.5s}}{2.5s} - 276\,(1-0.005\,E_{\rm NN})\,\delta(s)\right]\ \text{MeV} \tag{7}$$

The geometrical definition of the interaction distance $s$ in Eq. (7) is shown e.g. in Fig. 1 of [38] ($s$ in fm). The density-dependent $g(\rho_P,\rho_T,E_{\rm NN})$ is given by

$$g(\rho_P,\rho_T,E_{\rm NN}) = C(E_{\rm NN})\cdot\left[1+\alpha(E_{\rm NN})\cdot e^{-\beta(E_{\rm NN})\cdot(\rho_P+\rho_T)}\right] \tag{8}$$

within the so-called frozen-density approximation. The parameters $C(E_{\rm NN})$, $\alpha(E_{\rm NN})$, and $\beta(E_{\rm NN})$ of the density dependence in Eq. (8) are fitted to reproduce the strength of an effective G-matrix interaction [40, 41]. The results for the parameters $C$, $\alpha$, and $\beta$ as adopted in [38] are listed in Table 1.

It has to be noted that the influence of the chosen parameters for the density dependence is minor for several reasons. First of all, the energy dependence of the parameters $C$, $\alpha$, and $\beta$ is minor: in the shown energy range in Tab. 1 ($5\,\text{MeV} \le E_{\rm lab} \le 40\,\text{MeV}$) the parameters $C$, $\alpha$, and $\beta$ do not vary by more than about 5 %; the energy range of the scattering experiments in this study is much smaller. Second, the parameter $C$ scales the total strength of the interaction; any arbitrary choice of the parameter $C$ will be compensated during the fitting procedure by the adjustment of the potential strength parameter $\lambda$. The parameters $\alpha$ and $\beta$ have some influence on the shape of the folding potential; however, this is at least partly compensated by fitting the potential width parameter $w$. Instead of discussing the parameters $\lambda$ and $w$ it is recommended to discuss the real volume integrals $J_R$ and root-mean-square radii $r_{R,rms}$ of the fitted real potential because these parameters are practically independent of the chosen parameters $C$, $\alpha$, and $\beta$ of the density dependence.

The basic ingredients in the calculation of the real folding potential are the nucleon densities of the colliding nuclei. They are derived from measured charge density distributions which are compiled in [42]. For the $\alpha$-particle the sum-of-Gaussian parameterization was chosen because the corresponding measurement covers by far the largest range of momentum transfer. For the target nuclei the average potential from all available density parameterizations was used. For $^{106}$Cd the two-parameter Fermi distribution of $^{110}$Cd (with $R_0$ scaled by $A^{1/3}$) had to be used because no data for $^{106}$Cd are listed in [42]. The variations of $R_0$ along the cadmium isotopic chain are of the order of 0.5 %; thus, the uncertainty of the extrapolated density distribution should remain small.

$W(r)$ is taken as Woods-Saxon potential (surface type):

$$W(r) = W_S \times \frac{d\,f_{WS}(x_S)}{dx_S} \tag{9}$$

with the potential depth[2] $W_S$ and

$$f_{WS}(x_S) = \frac{1}{1+\exp(x_S)} \tag{10}$$

and $x_S = (r - R_S \times A_T^{1/3})/a_S$ with the radius parameter $R_S$ and the diffuseness parameter $a_S$. It has been found in many studies that the surface contribution is dominating at low energies, and the volume part is small or even negligible [12, 31]; this finding has recently been confirmed in a microscopic calculation of the OM potential [43]. Finally, the Coulomb potential $V_C(r)$ has been calculated from a homogeneously charged sphere with a Coulomb radius $R_C$ identical to the root-mean-square radius $r_{R,rms}$ of the real folding potential (before adjusting the width parameter, i.e. $w = 1$).

---

[2] Note that maximum depth of the imaginary potential $W(r)$ at $r = R_S \times A_T^{1/3}$ is $W_{\rm max}(r) = -W_S/4$ in the definition of Eq. (9).

The above choice of the potential reduces the number of adjustable parameters. Three parameters of the imaginary part ($W_S$, $R_S$, $a_S$) and two parameters of the real part ($\lambda$, $w$) were fitted to the angular distributions using a standard $\chi^2$ search. However, because of ambiguities of the potential the parameter search was restricted to the above mentioned region of real volume integrals $J_R \approx 350\,\mathrm{MeV\,fm}^3$. The ambiguities increase towards lower energies, and in some cases very shallow minima in $\chi^2$ have been found with parameters $w$ which deviated by more than 3 % from unity. In such cases, the width parameter $w$ has been fixed either at $w = 1.0$ or at the average value found at the higher energies (note that typically this average value does not deviate by more than 1 % from unity). The fits are shown in Graphs 1, 2, and 3, and the parameters are listed in Table B.

In addition, the total reaction cross section $\sigma_{\rm reac}$ has been calculated from the obtained potential by the well-known formula

$$\sigma_{\rm reac} = \frac{\pi}{k^2} \sum_L (2L+1)\,(1-\eta_L^2) \tag{11}$$

where $k = \sqrt{2\mu E}/\hbar$ is the wave number, $E$ is the energy in the center-of-mass (c.m.) system, and $\eta_L$ are the real reflexion coefficients. The uncertainties of $\sigma_{\rm reac}$ have been estimated from phase shift fits using the model of [44] and are typically of the order of about 3 % (except at the lowest energies); see also the discussion of uncertainties of $\sigma_{\rm reac}$ in [45]. Minor differences between $\sigma_{\rm reac}$ in this work and our previous study [45] – typically within the uncertainties of this work – are due to the fact that $\sigma_{\rm reac}$ in [45] are calculated from different potential parameterizations (volume and surface Woods-Saxon in the imaginary part) whereas this work uses an imaginary Woods-Saxon potential of pure surface type.

For the comparison of total reaction cross sections $\sigma_{\rm reac}$ for various projectile-target systems at different energies it has been suggested to present the data as reduced cross sections $\sigma_{\rm red}$ versus the reduced energy $E_{\rm red}$ which are defined by

$$E_{\rm red} = \frac{(A_P^{1/3}+A_T^{1/3})E_{\rm c.m.}}{Z_P Z_T} \tag{12}$$

$$\sigma_{\rm red} = \frac{\sigma_{\rm reac}}{(A_P^{1/3}+A_T^{1/3})^2} \tag{13}$$

The reduced energy $E_{\rm red}$ takes into account the different heights of the Coulomb barrier in the systems under consideration, whereas the reduced reaction cross section $\sigma_{\rm red}$ scales the measured total reaction cross section $\sigma_{\rm reac}$ according to the geometrical size of the projectile-plus-target system. It is found that the reduced cross sections $\sigma_{\rm red}$ show a very similar behavior for all nuclei under study (see Fig. 1). Significantly different $\sigma_{\rm red}$ are found for weakly bound projectiles (like e.g. $^{6,7}$Li) or halo projectiles (e.g. $^{6}$He), see [46].

The results of this section are used as the basis for the construction of a new systematic $\alpha$-nucleus optical potential with very few adjustable parameters. Further details of the new potential are given in the Appendix (Sect.A).

## 4. Summary and Conclusions

The extraction of optical potentials from elastic scattering angular distributions requires experimental data with high precision. This holds in particular at relatively low energies around the Coulomb barrier where the repulsive Coulomb interaction governs the measured angular distribution. Increasing ambiguities of the derived potentials are found when the energy is lowered below the Coulomb barrier, e.g. when approaching astrophysically relevant energies.

Here we have presented a summary of the experimental scattering data for the nuclei $^{89}$Y, $^{92}$Mo, $^{106,110,116}$Cd, $^{112,124}$Sn, and $^{144}$Sm which were measured at ATOMKI, Debrecen in the last 15 years. The target nuclei were chosen to cover even-even and even-odd nuclei with magic and non-magic proton and neutron numbers. The measured angular distributions cover the full angular range from about $20^\circ$ to $170^\circ$ in small steps of $1^\circ - 2^\circ$ with uncertainties of a few per cent. These data are used to extract locally adjusted optical potentials, and from the obtained local potential parameters a new $\alpha$-nucleus potential is suggested which is able to reproduce the experimental total reaction cross section $\sigma_{\rm reac}$ at the measured energies with deviations of less than 5 % in most cases and less than 20 % in the worst case.

Elastic scattering data are the indispensable basis for the extraction of the optical potential, but this basis is unfortunately not complete yet. Angular distributions are available for targets in the mass range around $A \approx 100$, but complete angular distributions with small uncertainties are still missing for heavier targets above $A \approx 150$. There are significant complications of the analysis of scattering data at energies below the Coulomb barrier. Thus, in addition to the analysis of elastic scattering angular distributions, further experimental cross section data for $\alpha$-induced reactions are required to determine the weak energy dependence of the real part and the strong energy dependence of the imaginary part of the optical potential. Such a combined effort using elastic scattering and reaction cross sections should be able to resolve or at least to reduce the long-standing problem of $\alpha$-nucleus potentials at low energies and the resulting uncertainties in the prediction of $\alpha$-induced reaction cross sections in the near future.

## Acknowledgments

This work was supported by the EUROGENESIS research program, by OTKA (NN83261, K101328), by the European Research Council (grant agreement no. 203175). The authors thank for the collaboration to M. Avrigeanu, M. Babilon, Z. Elekes, J. Farkas, J. Görres, R. T. Güray, M. Jaeger, Z. Mátè, A. Kretschmer, S. Müller, H. Oberhummer, A. Ornelas, N. Özkan, T. Rauscher, K. Sonnabend, G. Staudt, C. Yalcin, A. Zilges, and L. Zolnai, and to the ATOMKI cyclotron staff for the stable beam in all the experiments.

## A. Appendix: Suggestions for a new $\alpha$-nucleus potential

In the following we present some suggestions for a new systematic $\alpha$-nucleus optical potential which is derived from the ATOMKI scattering data in this study. At present the potential is based on elastic scattering data in the mass range $89 \le A \le 144$ and in the energy range $13\,\mathrm{MeV} \lesssim E \lesssim 20\,\mathrm{MeV}$. The mass range can be extended in a standard way by measuring and analyzing angular distributions for targets with $A < 89$ and $A > 144$. As has been pointed out in [39], the $\alpha$-nucleus potential is not very sensitive to the mass of the target above $A \approx 60$; consequently, the new potential may be considered as valid for $A > 60$. An extension of the energy range to higher energies is not planned because it has been shown (see e.g. [12, 31, 43]) that the imaginary part of the potential changes from a dominating surface potential at low energies to a dominating volume potential at energies above $\approx 30 - 40\,\mathrm{MeV}$. An extension to lower energies is essential for the prediction of low-energy cross sections of $\alpha$-induced reactions. Such an extension cannot be done easily by elastic scattering because the cross section approaches the Rutherford cross section. Instead, experimental reaction cross sections have to be used to further constrain the $\alpha$-nucleus potential. It is interesting to note that under certain conditions the reaction cross section of a particular $(\alpha,X)$ reaction is almost entirely defined by the $\alpha$-nucleus potential.

The following suggestions for the new systematic potential are based on two new ideas. First, as a careful inspection of Table B shows, there is only a relatively weak variation of the potential parameters for all nuclei and all energies under study. Obviously such a finding is very helpful in the construction of a global potential. However, the relatively small variation of the potential parameters turns out to be non-systematic (except the increase of the imaginary volume integral $J_I$ with increasing energy) which complicates the determination of a global potential. We will accommodate this finding by a simple averaging procedure for the potential parameters as outlined below to keep the number of adjustable parameters as low as possible. Of course, a many-parameter global potential (as e.g. suggested in [18, 19, 24, 25]) will be able to reproduce elastic angular distributions with smaller deviations in $\chi^2$; however, because of the non-systematic behavior of the potential parameters any extrapolation using many-parameter global potentials may become uncertain.

Second, we suggest a new energy dependence of the imaginary volume integral. This suggestion is based on a new parametrization of the energy dependence of $J_I$ as a function of the reduced energy $E_{\rm red}$ (see Fig. 2).

We place special emphasis on the reproduction of the total reaction cross section $\sigma_{\rm reac}$ because $\sigma_{\rm reac}$ is the essential basis of any calculation of reaction cross sections within the statistical model. As will be shown, the deviation between the experimental $\sigma_{\rm reac}$ and the prediction from the suggested potential remains small in all cases under study.

Of course, the derived parameters and its uncertainties may be further improved by including more scattering data as e.g. from [12, 24, 25]. The suggested potential has to be tested against experimental cross sections of $\alpha$-induced reactions, in particular ($\alpha$,$\gamma$), ($\alpha$,n), and ($\alpha$,p) reactions. Such tests and further optimizations of this global potential are beyond the scope of the present paper and will be presented elsewhere.

The geometry of the real part of the potential can be determined from the folding procedure with very small uncertainties. From all angular distributions we find an average width parameter $w_{\rm all} = 1.0061 \pm 0.0095$. The analysis of all semi-magic (SM) target nuclei results in $w_{\rm SM} = 1.0104 \pm 0.0108$, and from the non-magic (NM) target nuclei we find $w_{\rm NM} = 1.0006 \pm 0.0025$. Thus, it is reasonable to adopt $w = 1.0$ for the global potential. It has to be noted that there are still significant uncertainties for the real part of the $\alpha$-nucleus potentials for unstable nuclei because density distributions from electron scattering are only available for stable nuclei [42].

The energy dependence of the real part of the $\alpha$-nucleus potential is expected to be very weak at low energies. The intrinsic energy dependence of the interaction, see Eqs. (7) and (8) above, leads to decreasing volume integrals $J_R$ with increasing energy. However, the coupling of the real and imaginary part by a dispersion relation leads to an opposite effect at low energies. No systematic trend for the energy dependence of the volume integrals $J_R$ can be found in our scattering data. Thus, we adopt an energy-independent strength of the real part of our global potential.

The strength parameter $\lambda$ of the real part has to be derived from the energy-independent volume integral $J_R$. Here we find the average values of $J_{R,\rm all} = 354.9 \pm 20.8\,\rm MeV\,fm^3$, $J_{R,\rm SM} = 342.4 \pm 9.6\,\rm MeV\,fm^3$, and $J_{R,\rm NM} = 371.0 \pm 20.6\,\rm MeV\,fm^3$. Because of the differences between $J_{R,\rm SM}$ and $J_{R,\rm NM}$ we recommend to use the lower value of $342.4\,\rm MeV\,fm^3$ for semi-magic targets and the higher value of $371.0\,\rm MeV\,fm^3$ for non-magic targets.

It is more difficult to provide a reasonable imaginary part for a global $\alpha$-nucleus potential because it is well-known that the imaginary part increases with energy because of the increasing number of open channels. (Note that the total reaction cross section $\sigma_{\rm reac}$ increases strongly with energy even if there is no energy dependence of the imaginary potential; this is simply due to the increasing tunneling probablility at higher energies.) We find from our scattering data that the geometry of the imaginary part is well constrained by the scattering angular distributions. The average radius parameters $R_S$ of the imaginary surface Woods-Saxon potential are $R_{S,\mathrm{all}} = 1.430 \pm 0.086\,\mathrm{fm}$, $R_{S,\mathrm{SM}} = 1.477 \pm 0.038\,\mathrm{fm}$, and $R_{S,\mathrm{NM}} = 1.370 \pm 0.094\,\mathrm{fm}$; the average diffuseness values are $a_{S,\mathrm{all}} = 0.470 \pm 0.100\,\mathrm{fm}$, $a_{S,\mathrm{SM}} = 0.423 \pm 0.056\,\mathrm{fm}$, and $a_{S,\mathrm{NM}} = 0.531 \pm 0.114\,\mathrm{fm}$. Because of the relatively small deviations between the results for semi-magic and non-magic nuclei we adopt the average values from all scattering data: $R_S = 1.430\,\mathrm{fm}$ and $a_S = 0.470\,\mathrm{fm}$.

The strength of the imaginary part is parametrized by the imaginary volume integral $J_I$. Here we find a relatively well-defined behavior for the $J_I$ vs. $E_{\mathrm{red}}$ dependence which can be fitted well by the following formula (similar to the phase shift behavior in a resonance):

$$J_I(E_{\mathrm{red}}) = \frac{1}{\pi}\, J_{I,0} \arctan \frac{\Gamma_{\mathrm{red}}}{2(E_{\mathrm{red},0} - E_{\mathrm{red}})} \tag{A.1}$$

with the saturation value $J_{I,0} = 92.0\,\mathrm{MeV\,fm}^3$, the turning point energy $E_{\mathrm{red},0} = 0.89594\,\mathrm{MeV}$, and the slope (or width) parameter $\Gamma_{\mathrm{red}} = 0.19659\,\mathrm{MeV}$. The data and the fit are shown in Fig. 2. The parametrization in Eq. (A.1) has been chosen because the widely used Brown-Rho parametrization of $J_I$ [47] has turned out to be inadequate for the description of low-energy reaction cross sections (see e.g. [3, 12]). A Fermi-type function for $J_I$ (with the parameters as e.g. used in [3, 11, 12]) has the disadvantage that $J_I$ almost vanishes at energies below 10 MeV, and thus the calculated total cross section $\sigma_{\mathrm{reac}}$ becomes smaller than the inelastic Coulomb excitation cross section. Eq. (A.1) is some kind of compromise between the intrinsically steep $J_I(E)$ from a Fermi-type function and the intrinsically shallow $J_I(E)$ from a Brown-Rho parametrization.

In the considered mass range $89 \le A \le 144$ the depth $W_S$ of the imaginary surface Woods-Saxon potential for the chosen geometry ($R_S = 1.43\,\mathrm{fm}$, $a_S = 0.47\,\mathrm{fm}$) is approximately related to the volume integral $J_I$ by

$$W_S \approx (0.8112 + 0.008363 A_T - 1.432 \times 10^{-5} A_T^2) \times J_I \tag{A.2}$$

with $W_S$ in MeV and $J_I$ in $\mathrm{MeV\,fm}^3$ in Eq. (A.2); this equation holds also for $50 \le A \le 210$ with small numerical deviations. The results from this new systematic potential are shown in Graphs 1, 2, and 3 as dashed lines, and the resulting deviations $\chi^2/F$ and total reaction cross sections $\sigma_{\mathrm{reac}}$ are listed in Table C. It is obvious that the global potential deviates stronger from the experimental data than the locally fitted potential. Nevertheless, the experimental total reaction cross sections $\sigma_{\mathrm{reac}}$ are well reproduced in all cases.

Here we provide a new $\alpha$-nucleus potential with a very limited number of parameters. The folding potential in the real part has to be scaled to the corresponding volume integral $J_R$ for semi-magic or non-magic targets (i.e., one parameter for the real part). The imaginary surface Woods-Saxon potential has an energy-independent geometry (i.e., two parameters for the imaginary geometry $R_S$ and $a_S$), and its energy-dependent strength is parametrized by the saturation value $J_{I,0}$, the turning point energy $E_{\mathrm{red},0}$, and the slope parameter $\Gamma_{\mathrm{red}}$ (i.e., three parameters for the imaginary energy dependence). The parameters for the calculation of the depth $W_S$ in Eq. (A.2) do not count here, because these parameters are only a technical help to calculate $W_S$ from a given $J_I$. This small number of parameters is close to the widely used 4-parameter potential by McFadden and Satchler [17], but significantly smaller than the recent many-parameter potentials by Avrigeanu *et al.* [18] or Palumbo *et al.* [25]. It follows the idea of [18] that the energy dependence of the imaginary part should be related to the height of the Coulomb barrier because the imaginary volume integrals $J_I$ are parametrized in dependence of the reduced energy $E_{\mathrm{red}}$.

The suggested new potential shows relatively poor $\chi^2$ for $^{124}$Sn and $^{144}$Sm and is also not perfect for $^{110,116}$Cd. The problems with $^{124}$Sn and $^{144}$Sm may simply be related to the fact that the derived average parameters are not very sensitive to the measurements of $^{124}$Sn and $^{144}$Sm because in these cases only one energy has been measured. It is obvious that the average parameters are most influenced by the many data points from the lower-mass target nuclei with $A \approx 100$. This clearly calls for further experimental data for heavier targets with masses far above $A \approx 100$, i.e. in the mass range $150 \leq A \leq 210$.

There is no simple explanation why the new global potential works well for $^{106}$Cd, but shows some problems with $^{110}$Cd and $^{116}$Cd. The angular distributions for $^{110}$Cd and $^{116}$Cd look similar (with about $\sigma/\sigma_R \approx 0.015$ at very backward angles in the 19 MeV angular distribution) whereas the elastic scattering cross section for $^{106}$Cd is almost a factor of two larger ($\sigma/\sigma_R \approx 0.03$). It has to be expected that any global potential with few smoothly varying parameters will show similar problems with the description of angular distributions along the cadmium isotopic chain.

Although this simple global potential is not perfect in the reproduction of the angular distributions, it nevertheless reproduces the total reaction cross sections $\sigma_{\rm reac}$ within the given uncertainties in most cases. Even in the worst case ($^{110}$Cd, $E = 15.56$ MeV) the deviation does not exceed 20 % for $\sigma_{\rm reac}$; such an agreement is the basic prerequisite for the prediction of $\alpha$-induced reaction cross sections. However, further studies beyond this paper are clearly necessary; the presented new potential should be considered as a first version which is based on the scattering data of this work only. The largest uncertainty of this global potential results from the parametrization of the energy dependence of the imaginary volume integral $J_I(E)$ in Eq. (A.1). Several parametrizations have been suggested in the literature for the energy dependence of $J_I$ but a strict theoretical derivation of this energy dependence is missing. In addition, the parameters of any $J_I$-vs.-$E_{\rm red}$ dependence cannot be fully constrained by elastic scattering experiments which are typically done only at energies around and above the turning point of Eq. (A.1), but not below; see also Fig. 2. The saturation value $J_{I,0} = 92$ MeV fm$^3$ is well defined from the elastic scattering data around the Coulomb barrier with about $10 - 15$ % uncertainty; this uncertainty has only minor influence on the prediction of reaction cross sections below the Coulomb barrier. The uncertainty of the turning point energy $E_{\rm red,0}$ is also of the order of 10 %; but together with the much larger uncertainty of the slope parameter $\Gamma_{\rm red}$ this leads to considerable uncertainties for $J_I(E)$ at energies below the Coulomb barrier which may exceed a factor of two or three at reduced energies below or around $E_{\rm red} \approx 0.7$ MeV which corresponds to energies of e.g. about 9 MeV for $^{89}$Y and about 13 MeV for $^{144}$Sm. This uncertainty of $J_I(E)$ has significant impact on the prediction of reaction cross sections at low energies. Consequently, reaction data have to be taken into account for better constraining these parameters $E_{\rm red,0}$ and $\Gamma_{\rm red}$ in particular at lower energies. Furthermore, as pointed out above, the radius $R_S$ and diffuseness $a_S$ seem to be slightly different for semi-magic and non-magic target nuclei. Of course it is also possible that the parameters $J_{I,0}$, $\Gamma_{\rm red}$, and $E_{\rm red,0}$ in Eq. (A.1) depend on whether the proton or neutron number of the target nucleus is magic or not. Such investigations will be presented in a forthcoming study.

## References

[1] T. Rauscher, Int. J. Mod. Phys. E **20**, 1071 (2011).

[2] T. Rauscher and F.-K. Thielemann, At. Data Nucl. Data Tables **75**, 1 (2000).

[3] E. Somorjai, Zs. Fülöp, A. Z. Kiss, C. E. Rolfs, H.-P. Trautvetter, U. Greife, M. Junker, S. Goriely, M. Arnould, M. Rayet, T. Rauscher, H. Oberhummer, Astron. Astrophys. **333**, 1112 (1998).

[4] Gy. Gyürky, G. G. Kiss, Z. Elekes, Zs. Fülöp, E. Somorjai, A. Palumbo, J. Görres, H. Y. Lee, W. Rapp, M. Wiescher, N. Özkan, R. T. Güray, G. Efe, T. Rauscher, Phys. Rev. C **74**, 025805 (2006).

[5] N. Özkan, G. Efe, R. T. Güray, A. Palumbo, J. Görres, H. Y. Lee, L. O. Lamm, W. Rapp, E. Stech, M. Wiescher, Gy. Gyürky, Zs. Fülöp, E. Somorjai, Phys. Rev. C **75**, 025801 (2007).

[6] I. Cata-Danil, D. Filipescu, M. Ivascu, D. Bucurescu, N. V. Zamfir, T. Glodariu, L. Stroe, G. Cata-Danil, D. G. Ghita, C. Mihai, G. Suliman, T. Sava, Phys. Rev. C **78**, 035803 (2008).

[7] C. Yalcin, R. T. Güray, N. Özkan, S. Kutlu, Gy. Gyürky, J. Farkas, G. G. Kiss, Zs. Fülüp, A. Simon, E. Somorjai, T. Rauscher, Phys. Rev. C **79**, 065801 (2009).

[8] Gy. Gyürky, Z. Elekes, J. Farkas, Zs. Fülöp, Z. Halász, G. G. Kiss, E. Somorjai, T. Szücs, R. T. Güray, N. Özkan, C. Yalcin, and T. Rauscher, J. Phys. G **37**, 115201 (2010).

[9] G. G. Kiss, T. Rauscher, T. Szücs, Zs. Kertész, Zs. Fülöp, Gy. Gyürky, C. Fröhlich, J. Farkas, Z. Elekes, E. Somorjai, Phys. Lett. B **695**, 419 (2011).

[10] G. G. Kiss, T. Szücs, Gy. Gyürky, Zs. Fülöp, J. Farkas, Zs. Kertész, E. Somorjai, M. Laubenstein, C. Fröhlich, and T. Rauscher, Nucl. Phys. **A867**, 52 (2011).

[11] A. Sauerwein, H. W. Becker, H. Dombrowski, M. Elvers, J. Endres, U. Giesen, J. Hasper, A. Hennig, L. Netterdon, T. Rauscher, D. Rogalla, K. O. Zell, A. Zilges, Phys. Rev. C, **84**, 045808 (2011).

[12] P. Mohr, Phys. Rev. C **84**, 055803 (2011).

[13] P. Mohr, Zs. Fülöp, and H. Utsunomiya, Eur. Phys. J. A **32**, 357 (2007).

[14] G. G. Kiss, T. Rauscher, Gy. Gyürky, A. Simon, Zs. Fülöp, and E. Somorjai, Phys. Rev. Lett. **101**, 191101 (2008).

[15] T. Rauscher, G. G. Kiss, Gy. Gyürky, A. Simon, Zs. Fülöp, and E. Somorjai, Phys. Rev. C **80**, 035801 (2009).

[16] P. Mohr, C. Angulo, P. Descouvemont, and H. Utsunomiya, Eur. Phys. J. A **27**, s01, 75 (2006).

[17] L. McFadden and G. R. Satchler, Nucl. Phys. **84**, 177 (1966).

[18] M. Avrigeanu and V. Avrigeanu, Phys. Rev. C **82**, 014606 (2010).

[19] M. Avrigeanu, A. C. Obreja, F. L. Roman, V. Avrigeanu, W. von Oertzen, At. Data Nucl. Data Tables **95**, 501 (2009).

[20] A. Kumar, S. Kailas, S. Rathi, K. Mahata, Nucl. Phys. **A776**, 105 (2006).

[21] P. Demetriou, C. Grama, and S. Goriely, Nucl. Phys. **A707**, 253 (2002).

[22] T. Rauscher, Nucl. Phys. **A719c**, 73 (2003); Erratum: Nucl. Phys. **A725**, 295 (2003).

[23] V. Yu. Denisov and A. A, Khudenko, At. Data Nucl. Data Tables **95**, 815 (2009).

[24] A. Palumbo *et al.*, *10th International Symposium on Nuclei in the Cosmos*, Mackinac Island, Michigan, USA, PoS(NIC X)046 (2008).

[25] A. Palumbo *et al.*, Phys. Rev. C **85**, 035808 (2012).

[26] Zs. Fülöp, Gy. Gyürky, Z. Máté, E. Somorjai, L. Zolnai, D. Galaviz, M. Babilon, P. Mohr, A. Zilges, T. Rauscher, H. Oberhummer, and G. Staudt, Phys. Rev. C **64**, 065805 (2001).

[27] G. G. Kiss, Zs. Fülöp, Gy. Gyürky, Z. Máté, E. Somorjai, D. Galaviz, A. Kretschmer, K. Sonnabend, and A. Zilges, Eur. Phys. J. **27**, 197 (2006).

[28] G. G. Kiss, Gy. Gyürky, Zs. Fülöp, E. Somorjai, D. Galaviz, A. Kretschmer, K. Sonnabend, A. Zilges, P. Mohr, and M. Avrigeanu, J. Physics G **35**, 014037 (2008).

[29] G. G. Kiss, P. Mohr, Zs. Fülöp, D. Galaviz, Gy. Gyürky, Z. Elekes, E. Somorjai, A. Kretschmer, K. Sonnabend, A. Zilges, and M. Avrigeanu, Phys. Rev. C **80**, 045807 (2009).

[30] G. G. Kiss, P. Mohr, Zs. Fülöp, Gy. Gyürky, Z. Elekes, J. Farkas, E. Somorjai, C. Yalcin, D. Galaviz, R. T. Güray, N. Özkan, and J. Görres, Phys. Rev. C **83**, 065807 (2011).

[31] D. Galaviz, Zs. Fülöp, Gy. Gyürky, Z. Máté, P. Mohr, T. Rauscher, E. Somorjai, A. Zilges, Phys. Rev. C **71**, 065802 (2005).

[32] P. Mohr, T. Rauscher, H. Oberhummer, Z. Máté, Zs. Fülöp, E. Somorjai, M. Jaeger, and G. Staudt, Phys. Rev. C **55**, 1523 (1997).

[33] Zs. Fülöp, D. Galaviz, Gy. Gyürky, G.G. Kiss, Z. Máté, P. Mohr, T. Rauscher, E. Somorjai, and A. Zilges AIP conference proceedings **847**, 351 (2006).

[34] G. G. Kiss, D. Galaviz, Gy. Gyürky, Z. Elekes, Zs. Fülöp, E. Somorjai, K. Sonnabend, A. Zilges, P. Mohr, J. Görres M. Wiescher, N. Özkan, T. Güray, C. Yalcin, and M. Avrigeanu AIP conference proceedings **1016**, 221 (2008).

[35] D. Galaviz, Ph.D. thesis, TU Darmstadt (2004).

[36] G. R. Satchler and W. G. Love, Phys. Rep. **55**, 183 (1979).

[37] A. M. Kobos, B. A. Brown, R. Lindsay, and G. R. Satchler, Nucl. Phys. **A425**, 205 (1984).

[38] H. Abele and G. Staudt, Phys. Rev. C **47**, 742 (1993).

[39] U. Atzrott, P. Mohr, H. Abele, C. Hillenmayer, and G. Staudt, Phys. Rev. C **53**, 1336 (1996).

[40] J. P. Jeukenne, A. Lejeune, C. Mahaux, Phys. Rev. C **16**, 80 (1977).

[41] J. P. Jeukenne, C. Mahaux, Z. Phys. A **302**, 233 (1981).

[42] H. de Vries, C. W. de Jager, and C. de Vries, Atomic Data and Nuclear Data Tables **36**, 495 (1987).

[43] H. Guo, Y. Xu, H. Liang, Y. Han, Q. Shen, Phys. Rev. C **83**, 064618 (2011).

[44] V. Chisté, R. Lichtenthäler, A. C. C. Villari, L. C. Gomes, Phys. Rev. C **54**, 784 (1996).

[45] P. Mohr, D. Galaviz, Zs. Fülöp, Gy. Gyürky, G. G. Kiss, E. Somorjai, Phys. Rev. C **82**, 047601 (2010).

[46] P. N. de Faria, R. Lichtenthäler, K. C. C. Pires, A. M. Moro, A. Lépine-Szily, V. Guimarães, D. R. Mendes, A. Arazi, M. Rodríguez-Gallardo, A. Barioni, V. Morcelle, M. C. Morais, O. Camargo, J. Alcantara Nuñez, M. Assunção, Phys. Rev. C **81**, 044605 (2010).

[47] G. E. Brown and M. Rho, Nucl. Phys. **A372**, 397 (1981).

## Figures

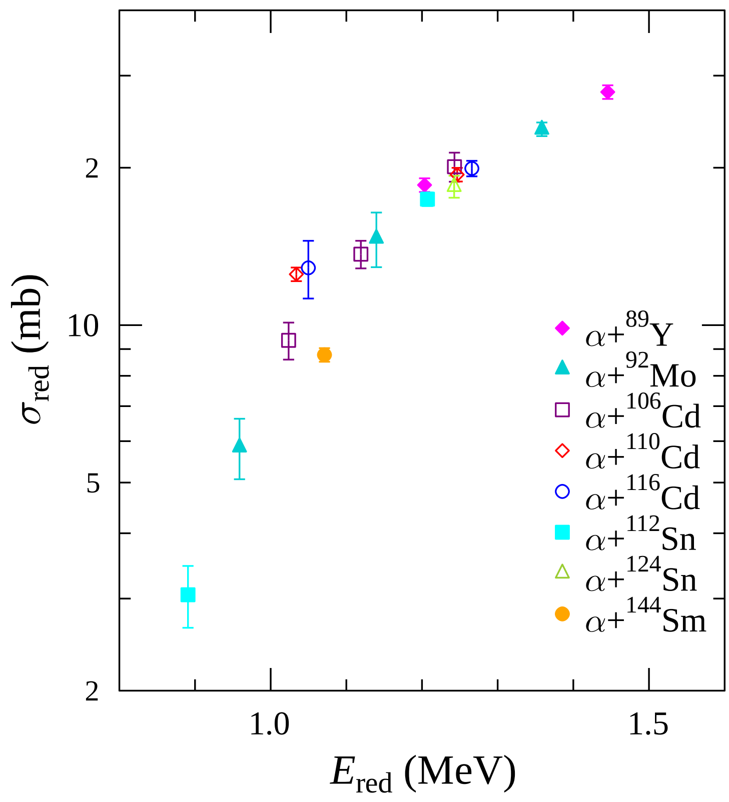

**Fig. 1**: Reduced cross section $\sigma_{\mathrm{red}}$ versus the reduced energy $E_{\mathrm{red}}$ for the data in Table B and Graphs 1, 2, and 3.

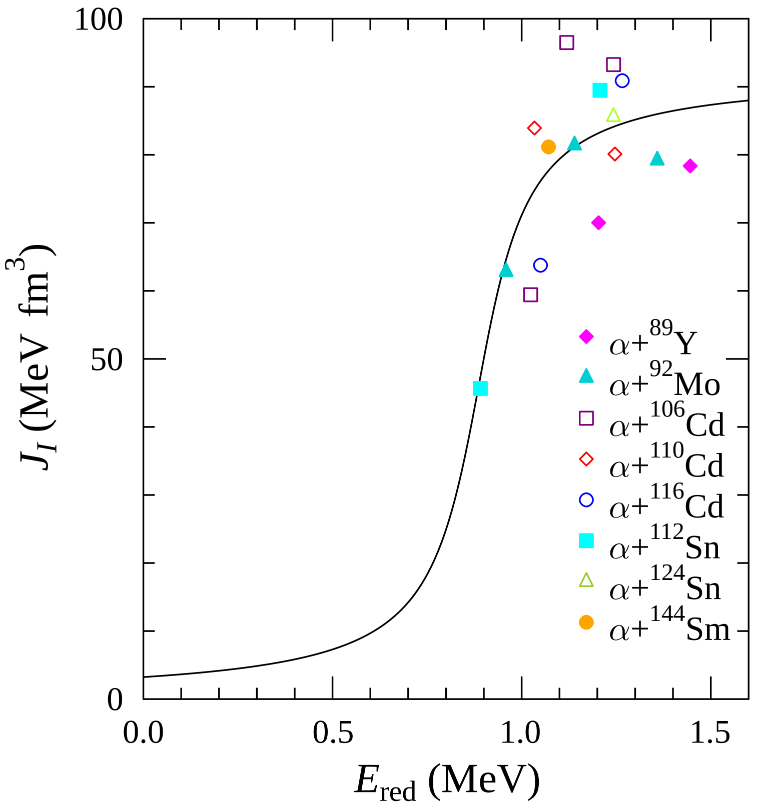

**Fig. 2**: Imaginary volume integrals $J_I$ versus the reduced energy $E_{\rm red}$. Further discussion see text.

Table A
Charge ($Z$) and neutron ($N$) number, chemical form, and isotopic enrichment of the target material, $E_{\mathrm{c.m.}}$ energies for each of the angular distributions studied at ATOMKI in the recent years. Furthermore, the energies of the first excited states of the target nuclei are listed, too.

| target nuclei | $Z$ | $N$ | chemical form | enrichment (%) | $E_{\mathrm{c.m.}}$ (MeV) | 1.st excited state (keV) | Ref. |
|---|---|---|---|---|---|---|---|
| $^{89}$Y | 39 | 50 | metallic | 100 | 15.51 | 908.97 | [29] |
| | | | | | 18.63 | | |
| $^{92}$Mo | 42 | 50 | oxide ($MoO_3$) | 97.3 | 13.20 | 1509.51 | [26] |
| | | | | | 15.69 | | |
| | | | | | 18.70 | | |
| $^{106}$Cd | 48 | 58 | metallic | 96.5 | 15.55 | 632.64 | [27, 35] |
| | | | | | 17.00 | | |
| | | | | | 18.88 | | |
| $^{110}$Cd | 48 | 62 | metallic | 95.7 | 15.56 | 657.76 | [30] |
| | | | | | 18.76 | | |
| $^{116}$Cd | 48 | 68 | metallic | 98.3 | 15.59 | 513.49 | [30] |
| | | | | | 18.80 | | |
| $^{112}$Sn | 50 | 62 | metallic | 99.6 | 13.90 | 1256.85 | [31] |
| | | | | | 18.84 | | |
| $^{124}$Sn | 50 | 74 | metallic | 97.4 | 18.90 | 1131.74 | [31] |
| $^{144}$Sm | 62 | 82 | oxide ($Sm_2O_3$) | 96.5 | 19.45 | 1660.03 | [32] |

Table B

Parameters of the optical potentials derived from the fits to the elastic scattering angular distributions (see Graphs 1, 2, and 3) and the total reaction cross section $\sigma_{\text{reac}}$ (see also Fig. 1).

| target | $E$ (MeV) | $\lambda$ (−) | $w$ (−) | $J_R$ (MeV fm$^3$) | $r_{rms,R}$ (fm) | $W_s$ (MeV) | $R_S$ (fm) | $a_S$ (fm) | $J_I$ (MeV fm$^3$) | $r_{rms,I}$ (fm) | $\sigma_{\text{reac}}$ (mb) | $\chi^2/F$ (−) |
|---|---|---|---|---|---|---|---|---|---|---|---|---|
| $^{89}$Y | 15.51 | 1.286 | 1.001 | 341.0 | 4.967 | 100.8 | 1.457 | 0.457 | 70.0 | 6.763 | 678.9±20.4 | 1.56 |
| | 18.63 | 1.214 | 1.016 | 337.0 | 5.042 | 107.7 | 1.481 | 0.464 | 78.4 | 6.871 | 1022.4±30.7 | 3.31 |
| $^{92}$Mo | 13.20 | 1.259 | 1.010 | 345.1 | 5.054 | 101.6 | 1.517 | 0.382 | 62.8 | 7.020 | 217.7±28.8 | 2.25 |
| | 15.69 | 1.190 | 1.008 | 323.7 | 5.041 | 126.5 | 1.464 | 0.426 | 81.4 | 6.828 | 545.9±65.4 | 4.62 |
| | 18.70 | 1.217 | 1.013 | 336.8 | 5.071 | 119.2 | 1.486 | 0.427 | 79.2 | 6.925 | 882.3±26.5 | 3.49 |
| $^{106}$Cd | 15.55 | 1.314 | 1.002 | 350.7 | 5.220 | 87.3 | 1.474 | 0.465 | 59.4 | 7.225 | 373.6±30.4 | 2.07 |
| | 17.00 | 1.373 | 1.004 | 368.9 | 5.232 | 166.3 | 1.464 | 0.403 | 96.5 | 7.116 | 546.0±33.1 | 0.87 |
| | 18.88 | 1.379 | 1.000 | 365.3 | 5.208 | 138.7 | 1.402 | 0.505 | 93.3 | 6.942 | 802.3±51.3 | 0.77 |
| $^{110}$Cd | 15.56 | 1.560 | 1.000 | 412.7 | 5.251 | 120.5 | 1.205 | 0.699 | 83.9 | 6.423 | 509.1±15.3 | 0.70 |
| | 18.76 | 1.387 | 0.996 | 362.9 | 5.232 | 129.7 | 1.381 | 0.485 | 80.1 | 6.901 | 789.6±23.8 | 0.32 |
| $^{116}$Cd | 15.59 | 1.442 | 1.000 | 379.6 | 5.303 | 82.8 | 1.298 | 0.684 | 63.8 | 6.905 | 537.8±68.0 | 0.27 |
| | 18.80 | 1.347 | 1.002 | 356.6 | 5.313 | 157.3 | 1.366 | 0.472 | 90.9 | 6.931 | 833.1±28.5 | 0.61 |
| $^{112}$Sn | 13.90 | 1.326 | 1.000 | 352.9 | 5.293 | 61.8 | 1.536 | 0.474 | 45.7 | 7.646 | 125.3±17.0 | 0.61 |
| | 18.84 | 1.354 | 0.996 | 356.5 | 5.273 | 146.9 | 1.423 | 0.455 | 89.5 | 7.101 | 715.1±21.5 | 0.63 |
| $^{124}$Sn | 18.90 | 1.251 | 1.020 | 344.9 | 5.444 | 153.0 | 1.428 | 0.430 | 85.6 | 7.330 | 795.8±38.5 | 1.12 |
| $^{144}$Sm | 19.45 | 1.207 | 1.030 | 343.7 | 5.742 | 204.8 | 1.499 | 0.293 | 81.2 | 7.944 | 409.2±12.3 | 1.82 |

Table C

Results for $\chi^2$ and $\sigma_{\text{reac}}$ from the simple global potential as suggested in Sec. A.

| | | experiment | global potential | |
|---|---|---|---|---|
| target | $E$ (MeV) | $\sigma_{\text{reac}}$ (mb) | $\chi^2/F$ (−) | $\sigma_{\text{reac}}$ (mb) |
| $^{89}$Y | 15.51 | 678.9±20.4 | 1.8 | 684.5 |
| | 18.63 | 1022.4±30.7 | 12.0 | 985.5 |
| $^{92}$Mo | 13.20 | 217.7±28.8 | 4.0 | 228.4 |
| | 15.69 | 545.9±65.4 | 9.6 | 564.0 |
| | 18.70 | 882.3±26.5 | 13.4 | 877.9 |
| $^{106}$Cd | 15.55 | 373.6±30.4 | 7.7 | 380.5 |
| | 17.00 | 546.0±33.1 | 5.9 | 572.7 |
| | 18.88 | 802.3±51.3 | 1.3 | 785.3 |
| $^{110}$Cd | 15.56 | 509.1±15.3 | 21.8 | 404.8 |
| | 18.76 | 789.6±23.8 | 16.9 | 801.1 |
| $^{116}$Cd | 15.59 | 537.8±68.0 | 13.3 | 439.0 |
| | 18.80 | 833.1±28.5 | 65.7 | 842.0 |
| $^{112}$Sn | 13.90 | 125.3±17.0 | 2.7 | 104.5 |
| | 18.84 | 715.1±21.5 | 2.0 | 725.0 |
| $^{124}$Sn | 18.90 | 795.8±38.5 | 498.2 | 769.4 |
| $^{144}$Sm | 19.45 | 409.2±12.3 | 347.5 | 431.6 |

## Explanation of Tables

### Table 1. Parameters $C(E_{\mathrm{NN}})$, $\alpha(E_{\mathrm{NN}})$, and $\beta(E_{\mathrm{NN}})$ of the density dependence of the chosen nucleon-nucleon interaction

| | |
|---|---|
| $E_{\mathrm{lab}}$ | Energy of the $\alpha$ projectile in the laboratory system in MeV |
| $E_{\mathrm{NN}}$ | Energy per nucleon in MeV: $E_{\mathrm{NN}} = E_{\mathrm{lab}}/A_P$ |
| $C(E_{\mathrm{NN}})$ | Coefficient $C$ in Eq. (8) |
| $\alpha(E_{\mathrm{NN}})$ | Coefficient $\alpha$ in Eq. (8) |
| $\beta(E_{\mathrm{NN}})$ | Coefficient $\beta$ in Eq. (8) in fm$^{-3}$ |

### Tables 2–17. Elastic ($\alpha$,$\alpha$) scattering cross sections (normalized to the Rutherford cross section)

| | |
|---|---|
| $\vartheta_{\mathrm{c.m.}}$ | Scattering angle in the center-of-mass system in degrees |
| $\sigma/\sigma_R$ | Ratio of experimental differential cross section $\left(\frac{d\sigma}{d\Omega}\right)_{\mathrm{exp}}$ to the Rutherford cross section $\left(\frac{d\sigma}{d\Omega}\right)_R$ |
| $\Delta(\sigma/\sigma_R)$ | Uncertainty of the ratio $\sigma/\sigma_R$; the uncertainty of the scattering angle $\vartheta_{\mathrm{c.m.}}$ is included in $\Delta(\sigma/\sigma_R)$ using standard error propagation |

## Explanation of Graphs

### Graphs 1–3. Elastic ($\alpha$,$\alpha$) scattering angular distributions for $^{89}$Y, $^{92}$Mo, $^{106,110,116}$Cd, $^{112,124}$Sn, and $^{144}$Sm, normalized to the Rutherford cross section.

The graphs show the experimental data of elastic $\alpha$ scattering which are also given in tabular form in Tables 2 – 17. The angular distributions are normalized to Rutherford scattering of point-like charges. The full lines result from a local fit with the parameters given in Table B. The dashed lines correspond to the global potential in the Appendix (Sect. A).

**Table 1**

Parameters of the energy dependence of the interaction. See page 19 for Explanation of Tables

| $E_{\text{lab}}$ (MeV) | $E_{\text{NN}}$ (MeV) | $C(E_{\text{NN}})$ | $\alpha(E_{\text{NN}})$ | $\beta(E_{\text{NN}})$ (fm$^{-3}$) |
|---|---|---|---|---|
| 5.0 | 1.25 | 0.4347 | 4.3023 | 10.5479 |
| 6.0 | 1.50 | 0.4344 | 4.3008 | 10.5336 |
| 7.0 | 1.75 | 0.4341 | 4.2992 | 10.5193 |
| 8.0 | 2.00 | 0.4338 | 4.2977 | 10.5049 |
| 9.0 | 2.25 | 0.4335 | 4.2961 | 10.4904 |
| 10.0 | 2.50 | 0.4331 | 4.2944 | 10.4758 |
| 11.0 | 2.75 | 0.4328 | 4.2927 | 10.4612 |
| 12.0 | 3.00 | 0.4325 | 4.2910 | 10.4465 |
| 13.0 | 3.25 | 0.4321 | 4.2893 | 10.4317 |
| 14.0 | 3.50 | 0.4317 | 4.2875 | 10.4168 |
| 15.0 | 3.75 | 0.4314 | 4.2858 | 10.4019 |
| 16.0 | 4.00 | 0.4310 | 4.2839 | 10.3869 |
| 17.0 | 4.25 | 0.4306 | 4.2821 | 10.3718 |
| 18.0 | 4.50 | 0.4302 | 4.2803 | 10.3567 |
| 19.0 | 4.75 | 0.4298 | 4.2784 | 10.3415 |
| 20.0 | 5.00 | 0.4294 | 4.2766 | 10.3262 |
| 21.0 | 5.25 | 0.4290 | 4.2747 | 10.3108 |
| 22.0 | 5.50 | 0.4286 | 4.2728 | 10.2954 |
| 23.0 | 5.75 | 0.4282 | 4.2709 | 10.2799 |
| 24.0 | 6.00 | 0.4277 | 4.2690 | 10.2643 |
| 25.0 | 6.25 | 0.4273 | 4.2671 | 10.2486 |
| 26.0 | 6.50 | 0.4269 | 4.2652 | 10.2329 |
| 27.0 | 6.75 | 0.4264 | 4.2633 | 10.2171 |
| 28.0 | 7.00 | 0.4259 | 4.2614 | 10.2012 |
| 29.0 | 7.25 | 0.4255 | 4.2595 | 10.1853 |
| 30.0 | 7.50 | 0.4250 | 4.2577 | 10.1692 |
| 31.0 | 7.75 | 0.4245 | 4.2558 | 10.1532 |
| 32.0 | 8.00 | 0.4240 | 4.2539 | 10.1370 |
| 33.0 | 8.25 | 0.4235 | 4.2521 | 10.1208 |
| 34.0 | 8.50 | 0.4230 | 4.2503 | 10.1044 |
| 35.0 | 8.75 | 0.4225 | 4.2484 | 10.0881 |
| 36.0 | 9.00 | 0.4220 | 4.2467 | 10.0716 |
| 37.0 | 9.25 | 0.4214 | 4.2449 | 10.0551 |
| 38.0 | 9.50 | 0.4209 | 4.2432 | 10.0385 |
| 39.0 | 9.75 | 0.4204 | 4.2414 | 10.0218 |
| 40.0 | 10.00 | 0.4198 | 4.2398 | 10.0051 |

**Table 2**
$^{89}$Y($\alpha$,$\alpha$)$^{89}$Y elastic scattering cross section (normalized to the Rutherford cross section) at the energy $E = 15.51$ MeV. See page 19 for Explanation of Tables

| $\vartheta_{\mathrm{c.m.}}$ (deg) | $\sigma/\sigma_R$ | $\Delta(\sigma/\sigma_R)$ |
|---:|---:|---:|
| 20.984 | 9.4408e-01 | 1.380e-02 |
| 21.991 | 9.2449e-01 | 1.350e-02 |
| 23.039 | 9.4977e-01 | 1.375e-02 |
| 24.040 | 9.1766e-01 | 1.339e-02 |
| 25.122 | 9.4139e-01 | 1.391e-02 |
| 26.158 | 9.3506e-01 | 1.387e-02 |
| 27.212 | 9.5078e-01 | 1.381e-02 |
| 28.223 | 9.4879e-01 | 1.392e-02 |
| 29.241 | 9.6027e-01 | 1.402e-02 |
| 30.351 | 9.8584e-01 | 1.426e-02 |
| 31.360 | 1.0026e+00 | 1.452e-02 |
| 31.383 | 1.0079e+00 | 1.397e-02 |
| 32.390 | 1.0156e+00 | 1.413e-02 |
| 33.433 | 1.0290e+00 | 1.409e-02 |
| 34.434 | 1.0425e+00 | 1.511e-02 |
| 35.509 | 1.0387e+00 | 1.587e-02 |
| 36.541 | 1.0657e+00 | 1.565e-02 |
| 37.589 | 1.0736e+00 | 1.504e-02 |
| 38.598 | 1.0776e+00 | 1.549e-02 |
| 39.615 | 1.0756e+00 | 1.530e-02 |
| 40.713 | 1.0791e+00 | 1.507e-02 |
| 41.720 | 1.0766e+00 | 1.513e-02 |
| 41.729 | 1.0771e+00 | 1.576e-02 |
| 42.763 | 1.0659e+00 | 1.554e-02 |
| 43.799 | 1.0482e+00 | 1.544e-02 |
| 44.827 | 1.0550e+00 | 1.543e-02 |
| 45.833 | 1.0322e+00 | 1.528e-02 |
| 46.847 | 1.0158e+00 | 1.512e-02 |
| 47.918 | 9.9623e-01 | 1.457e-02 |
| 48.930 | 9.8564e-01 | 1.450e-02 |
| 49.968 | 9.6576e-01 | 1.393e-02 |
| 50.995 | 9.4704e-01 | 1.377e-02 |
| 52.034 | 9.1898e-01 | 1.330e-02 |
| 52.035 | 9.2315e-01 | 1.357e-02 |
| 53.063 | 8.9483e-01 | 1.303e-02 |
| 54.093 | 8.7161e-01 | 1.304e-02 |
| 55.116 | 8.5435e-01 | 1.257e-02 |
| 56.121 | 8.1557e-01 | 1.239e-02 |
| 57.132 | 8.0395e-01 | 1.238e-02 |
| 58.189 | 7.9317e-01 | 1.168e-02 |
| 59.198 | 7.5655e-01 | 1.134e-02 |
| 60.228 | 7.3623e-01 | 1.049e-02 |
| 61.249 | 7.2003e-01 | 1.047e-02 |
| 62.187 | 6.9736e-01 | 1.015e-02 |
| 62.279 | 6.8706e-01 | 9.880e-03 |
| 63.200 | 6.8671e-01 | 1.055e-02 |
| 64.220 | 6.6338e-01 | 1.023e-02 |
| 65.240 | 6.4926e-01 | 9.930e-03 |
| 66.278 | 6.1746e-01 | 9.470e-03 |
| 67.293 | 6.0433e-01 | 9.330e-03 |
| 68.317 | 5.8072e-01 | 9.110e-03 |
| 69.376 | 5.5367e-01 | 8.690e-03 |
| 70.432 | 5.3451e-01 | 8.420e-03 |
| 71.445 | 5.2587e-01 | 8.200e-03 |
| 72.392 | 5.0447e-01 | 7.720e-03 |
| 72.462 | 5.0616e-01 | 8.010e-03 |
| 73.402 | 4.9137e-01 | 8.100e-03 |
| 74.416 | 4.8047e-01 | 7.950e-03 |
| 75.430 | 4.5732e-01 | 7.460e-03 |
| 76.455 | 4.4412e-01 | 7.240e-03 |
| 77.465 | 4.3029e-01 | 7.130e-03 |
| 78.480 | 4.0934e-01 | 6.990e-03 |
| 79.514 | 4.0158e-01 | 6.820e-03 |
| 80.546 | 3.8992e-01 | 6.660e-03 |
| 81.552 | 3.6613e-01 | 6.170e-03 |
| 82.557 | 3.5285e-01 | 5.820e-03 |
| 82.560 | 3.5216e-01 | 6.090e-03 |
| 83.561 | 3.3975e-01 | 5.570e-03 |
| 84.567 | 3.3009e-01 | 5.770e-03 |
| 85.571 | 3.0974e-01 | 5.090e-03 |
| 86.573 | 3.0324e-01 | 4.960e-03 |
| 87.575 | 2.9330e-01 | 4.710e-03 |
| 88.580 | 2.8679e-01 | 4.650e-03 |
| 89.581 | 2.7573e-01 | 4.350e-03 |
| 90.582 | 2.6922e-01 | 4.290e-03 |
| 91.583 | 2.5482e-01 | 4.100e-03 |
| 92.580 | 2.4846e-01 | 4.000e-03 |
| 92.580 | 2.5101e-01 | 4.620e-03 |
| 93.579 | 2.5058e-01 | 4.500e-03 |
| 94.576 | 2.3570e-01 | 4.710e-03 |
| 95.572 | 2.3133e-01 | 4.140e-03 |
| 96.569 | 2.2429e-01 | 4.000e-03 |
| 97.566 | 2.1999e-01 | 3.780e-03 |
| 98.556 | 2.1542e-01 | 3.750e-03 |
| 99.551 | 2.0691e-01 | 3.440e-03 |
| 100.540 | 1.9741e-01 | 3.360e-03 |
| 101.522 | 1.9640e-01 | 3.340e-03 |
| 102.516 | 1.9056e-01 | 3.250e-03 |
| 102.516 | 1.9048e-01 | 3.050e-03 |
| 103.993 | 1.8279e-01 | 3.280e-03 |
| 105.473 | 1.7555e-01 | 3.180e-03 |
| 106.952 | 1.5971e-01 | 3.580e-03 |
| 106.953 | 1.6324e-01 | 3.590e-03 |
| 108.432 | 1.5649e-01 | 3.000e-03 |
| 109.909 | 1.4548e-01 | 3.010e-03 |
| 111.359 | 1.3705e-01 | 2.920e-03 |
| 112.376 | 1.2961e-01 | 2.220e-03 |
| 112.827 | 1.2989e-01 | 2.890e-03 |
| 113.837 | 1.2518e-01 | 2.580e-03 |
| 114.369 | 1.2105e-01 | 2.670e-03 |
| 115.305 | 1.1882e-01 | 2.480e-03 |
| 115.894 | 1.2250e-01 | 2.620e-03 |
| 116.772 | 1.1246e-01 | 3.100e-03 |
| 116.774 | 1.1179e-01 | 3.030e-03 |
| 117.365 | 1.1336e-01 | 2.500e-03 |
| 118.243 | 1.1091e-01 | 2.450e-03 |
| 119.710 | 1.0589e-01 | 2.560e-03 |
| 121.137 | 1.0250e-01 | 2.550e-03 |
| 122.594 | 9.6380e-02 | 2.530e-03 |
| 124.155 | 9.6790e-02 | 2.460e-03 |
| 125.689 | 9.5580e-02 | 2.360e-03 |
| 127.149 | 9.9640e-02 | 2.450e-03 |
| 128.676 | 9.1990e-02 | 4.450e-03 |
| 130.142 | 8.9160e-02 | 4.340e-03 |
| 131.603 | 9.0170e-02 | 5.080e-03 |
| 131.605 | 8.5470e-02 | 4.930e-03 |
| 133.060 | 8.1920e-02 | 4.150e-03 |
| 134.516 | 8.5060e-02 | 4.450e-03 |
| 136.026 | 7.9820e-02 | 4.240e-03 |
| 137.488 | 7.4950e-02 | 4.110e-03 |
| 138.399 | 7.7140e-02 | 3.890e-03 |
| 139.857 | 6.9920e-02 | 3.650e-03 |
| 140.159 | 7.3010e-02 | 3.840e-03 |
| 141.309 | 6.7300e-02 | 4.150e-03 |
| 141.311 | 6.8230e-02 | 4.240e-03 |
| 141.612 | 7.0670e-02 | 3.780e-03 |
| 142.756 | 6.0900e-02 | 3.320e-03 |
| 144.203 | 6.1780e-02 | 3.550e-03 |
| 145.713 | 5.8380e-02 | 3.420e-03 |
| 147.167 | 5.9140e-02 | 3.540e-03 |
| 148.456 | 5.5380e-02 | 3.270e-03 |
| 149.790 | 5.3350e-02 | 3.080e-03 |
| 151.237 | 5.1430e-02 | 3.010e-03 |
| 153.311 | 6.0450e-02 | 2.670e-03 |
| 155.252 | 5.2120e-02 | 2.530e-03 |
| 157.151 | 5.3420e-02 | 2.400e-03 |
| 159.028 | 5.3050e-02 | 2.500e-03 |
| 160.879 | 5.7580e-02 | 2.710e-03 |
| 162.904 | 5.8800e-02 | 2.590e-03 |
| 164.840 | 5.4660e-02 | 2.630e-03 |
| 166.731 | 5.6030e-02 | 2.500e-03 |
| 168.601 | 5.6520e-02 | 2.630e-03 |
| 170.444 | 5.8400e-02 | 2.740e-03 |

**Table 3**

$^{89}$Y($\alpha$,$\alpha$)$^{89}$Y elastic scattering cross section (normalized to the Rutherford cross section) at the energy $E = 18.63$ MeV. See page 19 for Explanation of Tables

| $\vartheta_{\text{c.m.}}$ (deg) | $\sigma/\sigma_R$ | $\Delta(\sigma/\sigma_R)$ | $\vartheta_{\text{c.m.}}$ (deg) | $\sigma/\sigma_R$ | $\Delta(\sigma/\sigma_R)$ | $\vartheta_{\text{c.m.}}$ (deg) | $\sigma/\sigma_R$ | $\Delta(\sigma/\sigma_R)$ |
|---:|---:|---:|---:|---:|---:|---:|---:|---:|
| 20.659 | 9.5125e-01 | 9.920e-03 | 82.491 | 1.2239e-01 | 2.120e-03 | 131.350 | 2.3220e-02 | 9.332e-04 |
| 21.766 | 9.9453e-01 | 1.072e-02 | 82.507 | 1.2153e-01 | 2.020e-03 | 132.820 | 2.0460e-02 | 9.068e-04 |
| 22.835 | 1.0425e+00 | 1.156e-02 | 83.517 | 1.1809e-01 | 2.480e-03 | 134.266 | 1.9290e-02 | 8.859e-04 |
| 23.838 | 1.0640e+00 | 1.287e-02 | 83.518 | 1.1550e-01 | 2.130e-03 | 135.737 | 1.9310e-02 | 8.613e-04 |
| 24.837 | 1.0802e+00 | 1.293e-02 | 84.527 | 1.1077e-01 | 1.890e-03 | 137.169 | 1.8130e-02 | 8.847e-04 |
| 25.911 | 1.0865e+00 | 1.320e-02 | 85.543 | 1.0711e-01 | 1.830e-03 | 138.120 | 1.7260e-02 | 7.674e-04 |
| 26.983 | 1.0968e+00 | 1.377e-02 | 86.546 | 1.0170e-01 | 1.750e-03 | 138.591 | 1.9420e-02 | 8.431e-04 |
| 27.992 | 1.0956e+00 | 1.382e-02 | 87.549 | 9.6730e-02 | 1.680e-03 | 139.524 | 1.9210e-02 | 8.144e-04 |
| 29.018 | 1.0878e+00 | 1.368e-02 | 88.556 | 9.4130e-02 | 1.670e-03 | 140.036 | 2.0190e-02 | 8.564e-04 |
| 29.985 | 1.0828e+00 | 1.372e-02 | 89.567 | 8.9100e-02 | 1.580e-03 | 141.008 | 1.7780e-02 | 8.796e-04 |
| 31.063 | 1.0922e+00 | 1.398e-02 | 90.571 | 8.7000e-02 | 1.490e-03 | 141.484 | 1.9030e-02 | 8.742e-04 |
| 31.085 | 1.0922e+00 | 1.474e-02 | 91.576 | 8.5430e-02 | 1.500e-03 | 142.473 | 1.9450e-02 | 9.344e-04 |
| 32.184 | 1.0897e+00 | 1.469e-02 | 92.580 | 8.1580e-02 | 1.440e-03 | 143.911 | 2.0960e-02 | 9.561e-04 |
| 33.247 | 1.1049e+00 | 1.492e-02 | 92.580 | 8.2850e-02 | 1.570e-03 | 145.379 | 2.1500e-02 | 9.649e-04 |
| 34.251 | 1.0571e+00 | 1.431e-02 | 93.583 | 8.0130e-02 | 1.780e-03 | 146.802 | 2.2850e-02 | 1.040e-03 |
| 35.250 | 1.0313e+00 | 1.392e-02 | 93.583 | 8.1040e-02 | 2.170e-03 | 148.212 | 2.3210e-02 | 9.782e-04 |
| 36.319 | 9.8692e-01 | 1.334e-02 | 94.586 | 7.6730e-02 | 1.510e-03 | 149.651 | 2.2810e-02 | 9.831e-04 |
| 37.383 | 9.4953e-01 | 1.279e-02 | 95.584 | 7.3780e-02 | 1.460e-03 | 151.093 | 2.2140e-02 | 1.000e-03 |
| 38.392 | 9.1108e-01 | 1.235e-02 | 96.587 | 7.2850e-02 | 1.440e-03 | 151.118 | 2.4970e-02 | 5.310e-04 |
| 39.416 | 8.6945e-01 | 1.177e-02 | 97.591 | 7.1300e-02 | 1.410e-03 | 153.020 | 2.1910e-02 | 7.229e-04 |
| 40.389 | 8.1817e-01 | 1.106e-02 | 98.593 | 6.8770e-02 | 1.410e-03 | 154.945 | 2.0670e-02 | 5.528e-04 |
| 41.453 | 7.8544e-01 | 1.112e-02 | 99.583 | 6.6770e-02 | 1.350e-03 | 156.849 | 1.9790e-02 | 6.011e-04 |
| 41.459 | 7.8635e-01 | 1.064e-02 | 100.586 | 6.2890e-02 | 1.220e-03 | 158.804 | 1.8000e-02 | 5.193e-04 |
| 42.509 | 7.4609e-01 | 1.058e-02 | 101.586 | 6.1330e-02 | 1.240e-03 | 160.685 | 1.6410e-02 | 4.651e-04 |
| 43.559 | 7.3481e-01 | 1.043e-02 | 102.579 | 5.8500e-02 | 1.160e-03 | 160.696 | 1.7810e-02 | 4.337e-04 |
| 44.616 | 6.9786e-01 | 9.850e-03 | 102.582 | 5.7490e-02 | 1.170e-03 | 162.592 | 1.5060e-02 | 5.923e-04 |
| 45.614 | 6.7732e-01 | 9.650e-03 | 104.073 | 5.2780e-02 | 1.300e-03 | 164.513 | 1.4540e-02 | 4.544e-04 |
| 46.650 | 6.3328e-01 | 8.980e-03 | 104.074 | 5.4570e-02 | 2.010e-03 | 166.412 | 1.4590e-02 | 5.195e-04 |
| 47.708 | 6.1612e-01 | 8.820e-03 | 105.565 | 4.8880e-02 | 2.150e-03 | 168.366 | 1.5370e-02 | 4.836e-04 |
| 48.795 | 5.8703e-01 | 8.440e-03 | 105.566 | 4.7930e-02 | 1.230e-03 | 170.242 | 1.7950e-02 | 1.360e-03 |
| 49.797 | 5.5466e-01 | 8.000e-03 | 105.578 | 4.9240e-02 | 3.540e-03 | | | |
| 50.800 | 5.3303e-01 | 7.710e-03 | 107.055 | 4.4430e-02 | 1.260e-03 | | | |
| 51.805 | 5.1183e-01 | 7.130e-03 | 107.062 | 4.3590e-02 | 2.000e-03 | | | |
| 51.842 | 5.1006e-01 | 7.450e-03 | 108.530 | 4.2710e-02 | 2.030e-03 | | | |
| 52.853 | 4.7427e-01 | 6.640e-03 | 108.535 | 4.3670e-02 | 1.290e-03 | | | |
| 53.895 | 4.5507e-01 | 6.400e-03 | 110.023 | 3.9680e-02 | 1.220e-03 | | | |
| 54.943 | 4.2643e-01 | 5.900e-03 | 110.040 | 3.8450e-02 | 2.130e-03 | | | |
| 55.942 | 4.0746e-01 | 5.840e-03 | 111.497 | 3.9080e-02 | 1.180e-03 | | | |
| 56.973 | 3.8425e-01 | 5.500e-03 | 111.527 | 3.8800e-02 | 2.040e-03 | | | |
| 58.020 | 3.6299e-01 | 2.219e-02 | 112.499 | 3.8980e-02 | 9.373e-04 | | | |
| 59.091 | 3.4669e-01 | 5.110e-03 | 112.987 | 3.8900e-02 | 1.230e-03 | | | |
| 60.093 | 3.3142e-01 | 4.930e-03 | 112.995 | 3.7940e-02 | 2.190e-03 | | | |
| 61.097 | 3.2765e-01 | 4.910e-03 | 113.982 | 3.8280e-02 | 1.180e-03 | | | |
| 62.131 | 3.1269e-01 | 4.810e-03 | 113.984 | 3.7070e-02 | 1.820e-03 | | | |
| 62.144 | 3.0369e-01 | 4.750e-03 | 114.481 | 3.8080e-02 | 1.060e-03 | | | |
| 63.144 | 2.9485e-01 | 4.620e-03 | 115.462 | 3.9320e-02 | 2.200e-03 | | | |
| 64.161 | 2.8220e-01 | 4.390e-03 | 115.465 | 4.0490e-02 | 1.240e-03 | | | |
| 65.196 | 2.6939e-01 | 4.190e-03 | 115.484 | 4.0280e-02 | 3.700e-03 | | | |
| 66.194 | 2.5903e-01 | 4.060e-03 | 115.961 | 3.8380e-02 | 1.060e-03 | | | |
| 67.280 | 2.4596e-01 | 3.800e-03 | 116.941 | 3.9930e-02 | 1.290e-03 | | | |
| 68.283 | 2.2862e-01 | 3.540e-03 | 116.953 | 3.6940e-02 | 2.130e-03 | | | |
| 69.312 | 2.1768e-01 | 3.360e-03 | 117.437 | 3.6990e-02 | 1.080e-03 | | | |
| 70.301 | 2.0917e-01 | 3.230e-03 | 118.398 | 4.0420e-02 | 2.180e-03 | | | |
| 71.325 | 1.9676e-01 | 3.070e-03 | 118.406 | 3.8920e-02 | 1.340e-03 | | | |
| 72.325 | 1.8648e-01 | 2.910e-03 | 119.884 | 3.7420e-02 | 1.290e-03 | | | |
| 72.363 | 1.8670e-01 | 3.340e-03 | 119.909 | 3.5140e-02 | 2.320e-03 | | | |
| 73.365 | 1.8074e-01 | 3.250e-03 | 121.341 | 3.7720e-02 | 1.250e-03 | | | |
| 74.377 | 1.7184e-01 | 3.050e-03 | 121.386 | 4.0910e-02 | 2.360e-03 | | | |
| 75.402 | 1.6363e-01 | 2.880e-03 | 122.824 | 3.6000e-02 | 1.320e-03 | | | |
| 76.402 | 1.5940e-01 | 2.790e-03 | 122.835 | 3.6360e-02 | 2.350e-03 | | | |
| 77.457 | 1.5047e-01 | 2.600e-03 | 124.313 | 3.3850e-02 | 1.080e-03 | | | |
| 78.460 | 1.4870e-01 | 2.560e-03 | 125.782 | 3.2110e-02 | 1.040e-03 | | | |
| 79.478 | 1.3879e-01 | 2.380e-03 | 127.247 | 2.9510e-02 | 1.040e-03 | | | |
| 80.473 | 1.3569e-01 | 2.320e-03 | 128.445 | 2.6360e-02 | 9.284e-04 | | | |
| 81.489 | 1.2762e-01 | 2.220e-03 | 129.864 | 2.3980e-02 | 8.772e-04 | | | |

**Table 4**

$^{92}$Mo($\alpha$,$\alpha$)$^{92}$Mo elastic scattering cross section (normalized to the Rutherford cross section) at the energy $E = 13.20$ MeV. See page 19 for Explanation of Tables

| $\vartheta_{\text{c.m.}}$ (deg) | $\sigma/\sigma_R$ | $\Delta(\sigma/\sigma_R)$ |
|---|---|---|
| 20.145 | 9.4990e-01 | 2.168e-02 |
| 21.185 | 9.5014e-01 | 2.080e-02 |
| 22.226 | 9.5551e-01 | 2.011e-02 |
| 23.270 | 9.6942e-01 | 1.967e-02 |
| 24.311 | 9.6736e-01 | 1.897e-02 |
| 25.334 | 9.6642e-01 | 1.836e-02 |
| 26.374 | 9.7713e-01 | 1.801e-02 |
| 27.416 | 9.8018e-01 | 1.755e-02 |
| 28.469 | 9.7738e-01 | 1.703e-02 |
| 29.474 | 9.8811e-01 | 1.673e-02 |
| 30.508 | 9.9188e-01 | 1.638e-02 |
| 30.571 | 9.8403e-01 | 1.632e-02 |
| 31.609 | 9.8383e-01 | 1.595e-02 |
| 32.648 | 9.9168e-01 | 1.575e-02 |
| 33.690 | 9.8080e-01 | 1.527e-02 |
| 34.729 | 9.8410e-01 | 1.504e-02 |
| 35.751 | 9.8105e-01 | 1.474e-02 |
| 36.789 | 9.8230e-01 | 1.451e-02 |
| 37.828 | 9.8655e-01 | 1.434e-02 |
| 38.877 | 9.8608e-01 | 1.413e-02 |
| 39.883 | 9.9687e-01 | 1.395e-02 |
| 40.911 | 9.7951e-01 | 1.354e-02 |
| 40.915 | 9.8179e-01 | 1.351e-02 |
| 41.962 | 9.8453e-01 | 1.343e-02 |
| 43.002 | 9.9440e-01 | 1.340e-02 |
| 44.043 | 9.9292e-01 | 1.322e-02 |
| 45.083 | 9.9731e-01 | 1.314e-02 |
| 46.119 | 9.9673e-01 | 1.300e-02 |
| 47.150 | 1.0055e+00 | 1.297e-02 |
| 48.190 | 1.0029e+00 | 1.283e-02 |
| 49.223 | 1.0110e+00 | 1.280e-02 |
| 50.259 | 1.0162e+00 | 1.277e-02 |
| 51.282 | 1.0182e+00 | 1.272e-02 |
| 51.287 | 1.0116e+00 | 1.241e-02 |
| 52.326 | 1.0270e+00 | 1.274e-02 |
| 53.361 | 1.0296e+00 | 1.269e-02 |
| 54.397 | 1.0408e+00 | 1.274e-02 |
| 55.433 | 1.0443e+00 | 1.272e-02 |
| 56.463 | 1.0550e+00 | 1.278e-02 |
| 57.491 | 1.0481e+00 | 1.260e-02 |
| 58.525 | 1.0538e+00 | 1.265e-02 |
| 59.553 | 1.0669e+00 | 1.269e-02 |
| 60.584 | 1.0544e+00 | 1.253e-02 |
| 61.608 | 1.0704e+00 | 1.228e-02 |
| 61.641 | 1.0484e+00 | 1.223e-02 |
| 62.667 | 1.0576e+00 | 1.228e-02 |
| 63.692 | 1.0521e+00 | 1.218e-02 |
| 64.714 | 1.0551e+00 | 1.217e-02 |
| 65.747 | 1.0539e+00 | 1.213e-02 |
| 66.774 | 1.0524e+00 | 1.208e-02 |
| 67.799 | 1.0415e+00 | 1.193e-02 |
| 68.819 | 1.0532e+00 | 1.204e-02 |
| 69.848 | 1.0391e+00 | 1.186e-02 |
| 70.874 | 1.0324e+00 | 1.177e-02 |
| 71.893 | 1.0241e+00 | 1.165e-02 |
| 71.896 | 1.0406e+00 | 1.181e-02 |
| 72.913 | 1.0236e+00 | 1.163e-02 |
| 73.933 | 1.0253e+00 | 1.164e-02 |
| 74.950 | 1.0250e+00 | 1.163e-02 |
| 75.974 | 1.0060e+00 | 1.142e-02 |
| 76.994 | 1.0191e+00 | 1.156e-02 |
| 78.012 | 9.9317e-01 | 1.129e-02 |
| 79.027 | 9.9629e-01 | 1.133e-02 |
| 80.047 | 9.7285e-01 | 1.109e-02 |
| 81.065 | 9.4717e-01 | 1.083e-02 |
| 82.080 | 9.5869e-01 | 1.090e-02 |
| 82.081 | 9.5809e-01 | 1.073e-02 |
| 83.098 | 9.4920e-01 | 1.078e-02 |
| 84.107 | 9.3002e-01 | 1.006e-02 |
| 85.119 | 9.2954e-01 | 1.019e-02 |
| 86.132 | 9.1681e-01 | 9.890e-03 |
| 87.144 | 8.9780e-01 | 9.680e-03 |
| 88.154 | 8.9004e-01 | 9.610e-03 |
| 89.163 | 8.8060e-01 | 9.260e-03 |
| 90.173 | 8.6806e-01 | 9.100e-03 |
| 91.182 | 8.5819e-01 | 9.430e-03 |
| 92.190 | 8.4240e-01 | 9.640e-03 |
| 92.190 | 8.4699e-01 | 8.850e-03 |
| 93.196 | 8.3399e-01 | 9.760e-03 |
| 94.203 | 8.1807e-01 | 8.900e-03 |
| 95.208 | 8.1352e-01 | 9.060e-03 |
| 96.213 | 8.0087e-01 | 8.710e-03 |
| 97.216 | 7.9179e-01 | 8.610e-03 |
| 98.220 | 7.8641e-01 | 8.590e-03 |
| 99.223 | 7.6832e-01 | 8.070e-03 |
| 100.224 | 7.5428e-01 | 7.900e-03 |
| 101.223 | 7.4627e-01 | 8.400e-03 |
| 102.220 | 7.3137e-01 | 7.650e-03 |
| 102.223 | 7.3230e-01 | 7.790e-03 |
| 103.722 | 7.1128e-01 | 8.910e-03 |
| 105.213 | 6.9834e-01 | 7.540e-03 |
| 106.709 | 6.8667e-01 | 7.490e-03 |
| 108.201 | 6.7320e-01 | 7.230e-03 |
| 109.692 | 6.6514e-01 | 7.300e-03 |
| 111.182 | 6.4697e-01 | 7.010e-03 |
| 112.178 | 6.4326e-01 | 6.960e-03 |
| 112.669 | 6.3703e-01 | 6.970e-03 |
| 113.667 | 6.1142e-01 | 8.240e-03 |
| 114.160 | 6.0458e-01 | 6.760e-03 |
| 114.160 | 6.2482e-01 | 6.990e-03 |
| 114.160 | 6.2482e-01 | 6.990e-03 |
| 115.141 | 6.2560e-01 | 6.900e-03 |
| 115.652 | 5.9523e-01 | 6.500e-03 |
| 115.652 | 6.1515e-01 | 6.720e-03 |
| 115.652 | 6.1515e-01 | 6.720e-03 |
| 116.627 | 5.9944e-01 | 6.720e-03 |
| 117.146 | 5.7581e-01 | 6.200e-03 |
| 117.146 | 5.9508e-01 | 6.410e-03 |
| 117.146 | 5.9508e-01 | 6.410e-03 |
| 118.108 | 5.7252e-01 | 6.310e-03 |
| 119.587 | 5.7348e-01 | 6.500e-03 |
| 121.066 | 5.5714e-01 | 6.220e-03 |
| 122.542 | 5.5213e-01 | 6.230e-03 |
| 124.025 | 5.3944e-01 | 6.260e-03 |
| 125.509 | 5.2795e-01 | 5.950e-03 |
| 126.994 | 5.1415e-01 | 5.690e-03 |
| 127.162 | 5.1247e-01 | 5.990e-03 |
| 128.612 | 5.1172e-01 | 7.830e-03 |
| 130.080 | 5.0138e-01 | 6.010e-03 |
| 131.528 | 4.8378e-01 | 5.920e-03 |
| 132.979 | 4.7505e-01 | 5.660e-03 |
| 134.428 | 4.6044e-01 | 5.710e-03 |
| 135.875 | 4.6234e-01 | 5.580e-03 |
| 136.831 | 4.5246e-01 | 5.460e-03 |
| 137.323 | 4.5407e-01 | 5.560e-03 |
| 138.273 | 4.4265e-01 | 7.350e-03 |
| 138.758 | 4.4821e-01 | 5.680e-03 |
| 139.738 | 4.2651e-01 | 5.340e-03 |
| 140.189 | 4.4796e-01 | 5.440e-03 |
| 141.178 | 4.2817e-01 | 5.450e-03 |
| 141.615 | 4.3693e-01 | 5.190e-03 |
| 142.622 | 4.2179e-01 | 5.200e-03 |
| 144.065 | 4.1206e-01 | 5.310e-03 |
| 145.505 | 4.1225e-01 | 5.150e-03 |
| 146.947 | 4.0786e-01 | 5.170e-03 |
| 148.375 | 4.0670e-01 | 5.340e-03 |
| 149.798 | 4.0642e-01 | 5.090e-03 |
| 151.201 | 4.0148e-01 | 4.620e-03 |
| 151.217 | 4.0148e-01 | 4.880e-03 |
| 153.155 | 3.9947e-01 | 4.330e-03 |
| 155.087 | 4.0425e-01 | 4.570e-03 |
| 156.991 | 3.9490e-01 | 4.450e-03 |
| 158.909 | 3.9726e-01 | 4.940e-03 |
| 160.775 | 3.8411e-01 | 4.350e-03 |
| 160.841 | 3.8411e-01 | 4.640e-03 |
| 162.728 | 3.7799e-01 | 4.120e-03 |
| 164.658 | 3.7565e-01 | 4.300e-03 |
| 166.558 | 3.6926e-01 | 4.200e-03 |
| 168.474 | 3.6600e-01 | 4.640e-03 |
| 170.405 | 3.7529e-01 | 4.440e-03 |

**Table 5**

$^{92}$Mo($\alpha$,$\alpha$)$^{92}$Mo elastic scattering cross section (normalized to the Rutherford cross section) at the energy $E = 15.69$ MeV. See page 19 for Explanation of Tables

| $\vartheta_{\text{c.m.}}$ (deg) | $\sigma/\sigma_R$ | $\Delta(\sigma/\sigma_R)$ | $\vartheta_{\text{c.m.}}$ (deg) | $\sigma/\sigma_R$ | $\Delta(\sigma/\sigma_R)$ | $\vartheta_{\text{c.m.}}$ (deg) | $\sigma/\sigma_R$ | $\Delta(\sigma/\sigma_R)$ |
|---|---|---|---|---|---|---|---|---|
| 19.687 | 9.6174e-01 | 2.211e-02 | 80.972 | 5.4520e-01 | 6.100e-03 | 131.220 | 1.3984e-01 | 1.850e-03 |
| 20.730 | 9.7560e-01 | 2.148e-02 | 81.993 | 5.2115e-01 | 5.770e-03 | 132.663 | 1.3439e-01 | 1.930e-03 |
| 21.768 | 9.8174e-01 | 2.077e-02 | 81.994 | 5.2880e-01 | 5.990e-03 | 134.107 | 1.3244e-01 | 1.960e-03 |
| 22.817 | 9.7665e-01 | 1.989e-02 | 83.017 | 5.0550e-01 | 6.400e-03 | 135.549 | 1.3059e-01 | 1.920e-03 |
| 23.850 | 9.7427e-01 | 1.916e-02 | 84.039 | 4.9347e-01 | 5.500e-03 | 136.487 | 1.2878e-01 | 1.890e-03 |
| 24.903 | 9.5950e-01 | 1.825e-02 | 84.039 | 5.0465e-01 | 5.700e-03 | 136.984 | 1.2806e-01 | 1.850e-03 |
| 25.962 | 9.5684e-01 | 1.763e-02 | 85.060 | 4.7936e-01 | 5.340e-03 | 137.934 | 1.2528e-01 | 1.820e-03 |
| 26.998 | 9.4495e-01 | 1.691e-02 | 85.061 | 4.8557e-01 | 5.460e-03 | 138.421 | 1.2335e-01 | 1.780e-03 |
| 28.046 | 9.5222e-01 | 1.658e-02 | 86.080 | 4.6751e-01 | 5.230e-03 | 139.367 | 1.2242e-01 | 1.790e-03 |
| 29.090 | 9.5730e-01 | 1.624e-02 | 86.081 | 4.5994e-01 | 5.130e-03 | 139.863 | 1.2395e-01 | 1.740e-03 |
| 30.144 | 9.6157e-01 | 1.588e-02 | 87.100 | 4.4837e-01 | 4.900e-03 | 140.811 | 1.1712e-01 | 1.670e-03 |
| 30.148 | 9.7669e-01 | 1.617e-02 | 87.100 | 4.4853e-01 | 5.030e-03 | 141.304 | 1.1862e-01 | 1.690e-03 |
| 31.190 | 9.7704e-01 | 1.581e-02 | 88.117 | 4.3161e-01 | 4.740e-03 | 142.250 | 1.1187e-01 | 1.760e-03 |
| 32.229 | 9.9033e-01 | 1.569e-02 | 88.119 | 4.3699e-01 | 4.860e-03 | 143.689 | 1.1432e-01 | 1.830e-03 |
| 33.277 | 1.0007e+00 | 1.553e-02 | 89.136 | 4.1691e-01 | 4.590e-03 | 145.127 | 1.1181e-01 | 1.780e-03 |
| 34.310 | 1.0090e+00 | 1.537e-02 | 89.137 | 4.2171e-01 | 4.700e-03 | 146.557 | 1.0697e-01 | 1.680e-03 |
| 35.361 | 1.0086e+00 | 1.509e-02 | 90.154 | 3.9596e-01 | 4.360e-03 | 147.989 | 1.0496e-01 | 1.630e-03 |
| 36.417 | 1.0397e+00 | 1.529e-02 | 90.155 | 4.1299e-01 | 4.570e-03 | 149.429 | 1.0117e-01 | 1.540e-03 |
| 37.453 | 1.0457e+00 | 1.513e-02 | 91.171 | 3.9934e-01 | 4.320e-03 | 150.866 | 1.0541e-01 | 1.520e-03 |
| 38.499 | 1.0539e+00 | 1.503e-02 | 91.171 | 3.9725e-01 | 4.390e-03 | 150.868 | 1.0541e-01 | 1.840e-03 |
| 39.541 | 1.0737e+00 | 1.510e-02 | 92.187 | 3.8908e-01 | 4.200e-03 | 152.776 | 1.1090e-01 | 1.390e-03 |
| 40.593 | 1.0670e+00 | 1.473e-02 | 92.187 | 3.7280e-01 | 4.130e-03 | 154.691 | 1.1219e-01 | 1.430e-03 |
| 40.601 | 1.0754e+00 | 1.475e-02 | 92.187 | 3.8609e-01 | 4.280e-03 | | | |
| 41.645 | 1.0843e+00 | 1.468e-02 | 92.187 | 3.8609e-01 | 4.280e-03 | | | |
| 42.677 | 1.0873e+00 | 1.454e-02 | 92.187 | 3.8637e-01 | 4.490e-03 | | | |
| 43.722 | 1.0855e+00 | 1.430e-02 | 93.202 | 3.5813e-01 | 3.960e-03 | | | |
| 44.771 | 1.0899e+00 | 1.425e-02 | 93.202 | 3.7090e-01 | 4.110e-03 | | | |
| 45.812 | 1.0871e+00 | 1.407e-02 | 93.202 | 3.7090e-01 | 4.110e-03 | | | |
| 46.852 | 1.0823e+00 | 1.388e-02 | 94.216 | 3.7248e-01 | 4.490e-03 | | | |
| 47.897 | 1.0910e+00 | 1.387e-02 | 94.217 | 3.6884e-01 | 4.330e-03 | | | |
| 48.945 | 1.1025e+00 | 1.389e-02 | 94.217 | 3.5035e-01 | 3.930e-03 | | | |
| 49.975 | 1.0846e+00 | 1.357e-02 | 94.217 | 3.6283e-01 | 4.070e-03 | | | |
| 51.015 | 1.0715e+00 | 1.302e-02 | 94.217 | 3.6283e-01 | 4.070e-03 | | | |
| 51.022 | 1.0705e+00 | 1.330e-02 | 95.230 | 3.5525e-01 | 4.260e-03 | | | |
| 52.062 | 1.0631e+00 | 1.312e-02 | 95.230 | 3.5156e-01 | 4.150e-03 | | | |
| 53.092 | 1.0511e+00 | 1.290e-02 | 96.243 | 3.4184e-01 | 4.050e-03 | | | |
| 54.134 | 1.0353e+00 | 1.254e-02 | 96.243 | 3.4548e-01 | 4.110e-03 | | | |
| 55.177 | 1.0165e+00 | 1.236e-02 | 97.255 | 3.3045e-01 | 3.950e-03 | | | |
| 56.215 | 1.0062e+00 | 1.219e-02 | 97.255 | 3.3091e-01 | 3.800e-03 | | | |
| 57.251 | 9.7598e-01 | 1.180e-02 | 98.266 | 3.1918e-01 | 3.780e-03 | | | |
| 58.291 | 9.6515e-01 | 1.164e-02 | 102.310 | 2.9855e-01 | 3.280e-03 | | | |
| 59.333 | 9.4442e-01 | 1.137e-02 | 103.819 | 2.9159e-01 | 3.200e-03 | | | |
| 60.361 | 9.3839e-01 | 1.128e-02 | 105.329 | 2.7874e-01 | 3.070e-03 | | | |
| 61.397 | 8.9813e-01 | 1.028e-02 | 106.834 | 2.6700e-01 | 2.920e-03 | | | |
| 61.402 | 9.1335e-01 | 1.059e-02 | 108.338 | 2.6046e-01 | 2.960e-03 | | | |
| 62.433 | 8.9040e-01 | 1.030e-02 | 109.840 | 2.4884e-01 | 2.890e-03 | | | |
| 63.469 | 8.5810e-01 | 9.630e-03 | 111.340 | 2.3694e-01 | 2.760e-03 | | | |
| 64.506 | 8.2774e-01 | 9.310e-03 | 112.351 | 2.2985e-01 | 2.670e-03 | | | |
| 65.535 | 8.0942e-01 | 9.110e-03 | 112.842 | 2.2950e-01 | 2.660e-03 | | | |
| 66.568 | 7.9315e-01 | 8.880e-03 | 113.845 | 2.2241e-01 | 2.580e-03 | | | |
| 67.603 | 7.5847e-01 | 8.500e-03 | 114.340 | 2.1700e-01 | 2.520e-03 | | | |
| 68.631 | 7.3847e-01 | 8.250e-03 | 115.344 | 2.1466e-01 | 2.510e-03 | | | |
| 69.669 | 7.2423e-01 | 8.080e-03 | 115.833 | 2.1095e-01 | 2.420e-03 | | | |
| 70.701 | 7.1149e-01 | 7.880e-03 | 116.835 | 2.0492e-01 | 2.360e-03 | | | |
| 71.730 | 6.7951e-01 | 7.900e-03 | 117.324 | 2.0417e-01 | 2.370e-03 | | | |
| 71.730 | 6.9114e-01 | 7.690e-03 | 118.326 | 1.9992e-01 | 2.440e-03 | | | |
| 72.757 | 6.7174e-01 | 7.830e-03 | 119.815 | 1.8961e-01 | 2.390e-03 | | | |
| 72.760 | 6.6939e-01 | 7.910e-03 | 121.302 | 1.8976e-01 | 2.370e-03 | | | |
| 73.786 | 6.6134e-01 | 7.320e-03 | 122.791 | 1.8388e-01 | 2.280e-03 | | | |
| 74.816 | 6.3405e-01 | 7.100e-03 | 124.278 | 1.7666e-01 | 2.190e-03 | | | |
| 75.841 | 6.2485e-01 | 7.070e-03 | 125.757 | 1.7324e-01 | 2.110e-03 | | | |
| 76.868 | 6.0727e-01 | 6.870e-03 | 126.881 | 1.5762e-01 | 2.120e-03 | | | |
| 77.895 | 5.9434e-01 | 6.680e-03 | 127.236 | 1.6880e-01 | 2.080e-03 | | | |
| 78.918 | 5.7673e-01 | 6.480e-03 | 128.332 | 1.5351e-01 | 2.050e-03 | | | |
| 79.947 | 5.6116e-01 | 6.330e-03 | 129.771 | 1.4487e-01 | 1.960e-03 | | | |

**Table 6**

$^{92}$Mo($\alpha$,$\alpha$)$^{92}$Mo elastic scattering cross section (normalized to the Rutherford cross section) at the energy $E = 18.70$ MeV. See page 19 for Explanation of Tables

| $\vartheta_{\text{c.m.}}$ (deg) | $\sigma/\sigma_R$ | $\Delta(\sigma/\sigma_R)$ |
|---:|---:|---:|
| 20.388 | 9.2461e-01 | 2.174e-02 |
| 21.420 | 9.4039e-01 | 2.124e-02 |
| 22.467 | 9.5479e-01 | 2.077e-02 |
| 23.498 | 9.7596e-01 | 2.050e-02 |
| 24.561 | 1.0033e+00 | 2.037e-02 |
| 25.573 | 1.0211e+00 | 2.015e-02 |
| 26.634 | 1.0474e+00 | 2.009e-02 |
| 27.625 | 1.0512e+00 | 1.964e-02 |
| 28.702 | 1.0711e+00 | 1.953e-02 |
| 29.738 | 1.0708e+00 | 1.912e-02 |
| 30.790 | 1.1004e+00 | 1.908e-02 |
| 30.795 | 1.0923e+00 | 1.907e-02 |
| 31.824 | 1.1150e+00 | 1.903e-02 |
| 32.869 | 1.1219e+00 | 1.878e-02 |
| 33.897 | 1.1206e+00 | 1.841e-02 |
| 34.955 | 1.1112e+00 | 1.789e-02 |
| 35.967 | 1.0937e+00 | 1.741e-02 |
| 37.022 | 1.0893e+00 | 1.714e-02 |
| 38.015 | 1.0578e+00 | 1.640e-02 |
| 39.085 | 1.0340e+00 | 1.589e-02 |
| 40.117 | 1.0050e+00 | 1.536e-02 |
| 41.164 | 9.6594e-01 | 1.438e-02 |
| 41.168 | 9.6490e-01 | 1.432e-02 |
| 41.474 | 9.7081e-01 | 1.442e-02 |
| 42.489 | 9.4387e-01 | 1.373e-02 |
| 43.574 | 9.1902e-01 | 1.327e-02 |
| 44.587 | 8.8231e-01 | 1.267e-02 |
| 45.625 | 8.4927e-01 | 1.213e-02 |
| 46.640 | 8.2753e-01 | 1.163e-02 |
| 47.699 | 8.1376e-01 | 1.170e-02 |
| 48.721 | 7.8152e-01 | 1.095e-02 |
| 49.746 | 7.5966e-01 | 1.047e-02 |
| 50.783 | 7.2190e-01 | 1.006e-02 |
| 51.497 | 6.8835e-01 | 9.830e-03 |
| 51.753 | 7.0357e-01 | 1.014e-02 |
| 51.796 | 6.9532e-01 | 9.890e-03 |
| 52.764 | 6.6113e-01 | 9.200e-03 |
| 53.834 | 6.4249e-01 | 9.030e-03 |
| 54.844 | 5.9671e-01 | 8.470e-03 |
| 55.874 | 5.7080e-01 | 8.180e-03 |
| 56.885 | 5.3964e-01 | 7.580e-03 |
| 57.932 | 5.1708e-01 | 7.890e-03 |
| 58.948 | 4.8828e-01 | 7.110e-03 |
| 59.967 | 4.7179e-01 | 6.670e-03 |
| 60.994 | 4.4358e-01 | 6.620e-03 |
| 61.743 | 4.3216e-01 | 6.460e-03 |
| 62.003 | 4.2745e-01 | 6.750e-03 |
| 62.750 | 4.2322e-01 | 5.300e-03 |
| 62.766 | 4.2419e-01 | 5.560e-03 |
| 63.765 | 4.1259e-01 | 5.150e-03 |
| 64.774 | 3.9844e-01 | 4.960e-03 |
| 65.799 | 3.8261e-01 | 4.770e-03 |
| 66.784 | 3.6549e-01 | 4.550e-03 |
| 67.827 | 3.5560e-01 | 4.440e-03 |
| 68.832 | 3.3219e-01 | 4.150e-03 |
| 69.863 | 3.2505e-01 | 4.070e-03 |
| 70.884 | 3.0773e-01 | 3.870e-03 |
| 71.903 | 2.9984e-01 | 3.760e-03 |
| 71.963 | 2.6952e-01 | 4.940e-03 |
| 72.969 | 2.7418e-01 | 3.510e-03 |
| 72.980 | 2.7819e-01 | 3.920e-03 |
| 73.981 | 2.6626e-01 | 3.400e-03 |
| 74.988 | 2.5425e-01 | 3.260e-03 |
| 76.007 | 2.4316e-01 | 3.140e-03 |
| 77.000 | 2.3308e-01 | 3.020e-03 |
| 78.029 | 2.1927e-01 | 2.880e-03 |
| 79.034 | 2.1144e-01 | 2.800e-03 |
| 80.055 | 2.0495e-01 | 2.740e-03 |
| 81.070 | 1.9479e-01 | 2.630e-03 |
| 82.083 | 1.8778e-01 | 2.530e-03 |
| 82.086 | 1.9002e-01 | 2.570e-03 |
| 84.107 | 1.7900e-01 | 2.500e-03 |
| 85.127 | 1.7262e-01 | 2.480e-03 |
| 86.130 | 1.6188e-01 | 2.360e-03 |
| 87.149 | 1.5919e-01 | 2.320e-03 |
| 88.157 | 1.5006e-01 | 2.140e-03 |
| 89.165 | 1.4832e-01 | 2.140e-03 |
| 90.172 | 1.4231e-01 | 2.060e-03 |
| 91.181 | 1.3897e-01 | 1.970e-03 |
| 92.189 | 1.3626e-01 | 2.000e-03 |
| 92.190 | 1.3112e-01 | 2.020e-03 |
| 94.203 | 1.2370e-01 | 1.990e-03 |
| 95.206 | 1.1853e-01 | 2.010e-03 |
| 96.214 | 1.1460e-01 | 1.960e-03 |
| 97.212 | 1.1079e-01 | 1.920e-03 |
| 98.215 | 1.0520e-01 | 1.740e-03 |
| 99.220 | 1.0209e-01 | 1.730e-03 |
| 100.227 | 1.0070e-01 | 1.700e-03 |
| 101.232 | 9.6010e-02 | 1.590e-03 |
| 102.189 | 8.6740e-02 | 1.460e-03 |
| 102.232 | 9.1490e-02 | 1.610e-03 |
| 103.686 | 8.1050e-02 | 1.430e-03 |
| 105.173 | 7.7310e-02 | 1.380e-03 |
| 106.650 | 7.3050e-02 | 1.380e-03 |
| 108.148 | 6.5890e-02 | 1.250e-03 |
| 109.613 | 6.6670e-02 | 1.250e-03 |
| 111.101 | 6.0650e-02 | 1.170e-03 |
| 112.111 | 6.1730e-02 | 1.260e-03 |
| 112.581 | 5.9950e-02 | 1.230e-03 |
| 113.600 | 5.9760e-02 | 1.270e-03 |
| 114.078 | 5.8130e-02 | 1.160e-03 |
| 114.078 | 6.0310e-02 | 1.210e-03 |
| 114.078 | 6.0310e-02 | 1.210e-03 |
| 115.073 | 5.8130e-02 | 1.230e-03 |
| 115.606 | 5.3580e-02 | 1.090e-03 |
| 115.606 | 5.5600e-02 | 1.130e-03 |
| 115.606 | 5.5600e-02 | 1.130e-03 |
| 116.530 | 5.5290e-02 | 1.240e-03 |
| 117.108 | 5.4990e-02 | 9.190e-04 |
| 117.108 | 5.7060e-02 | 9.530e-04 |
| 117.108 | 5.7060e-02 | 9.530e-04 |
| 118.024 | 5.5570e-02 | 1.220e-03 |
| 119.467 | 5.4780e-02 | 1.170e-03 |
| 120.947 | 5.4450e-02 | 1.160e-03 |
| 122.414 | 5.1250e-02 | 1.200e-03 |
| 123.909 | 5.1130e-02 | 1.170e-03 |
| 125.445 | 4.6840e-02 | 1.090e-03 |
| 126.944 | 4.5470e-02 | 8.590e-04 |
| 127.272 | 4.5470e-02 | 1.160e-03 |
| 128.719 | 4.4200e-02 | 1.200e-03 |
| 130.187 | 4.4550e-02 | 1.190e-03 |
| 131.675 | 3.9500e-02 | 1.140e-03 |
| 133.103 | 3.6340e-02 | 1.060e-03 |
| 134.603 | 3.4540e-02 | 1.010e-03 |
| 136.044 | 3.3010e-02 | 9.660e-04 |
| 136.966 | 3.0700e-02 | 1.010e-03 |
| 137.500 | 3.0700e-02 | 9.820e-04 |
| 138.403 | 3.1630e-02 | 1.040e-03 |
| 138.915 | 2.9890e-02 | 9.520e-04 |
| 139.866 | 2.9140e-02 | 9.800e-04 |
| 140.274 | 3.0920e-02 | 9.450e-04 |
| 141.352 | 2.9660e-02 | 1.040e-03 |
| 141.682 | 3.1520e-02 | 7.390e-04 |
| 142.768 | 3.1070e-02 | 1.020e-03 |
| 144.268 | 2.8560e-02 | 9.600e-04 |
| 145.701 | 2.8850e-02 | 9.500e-04 |
| 147.150 | 3.3200e-02 | 1.090e-03 |
| 148.554 | 3.0880e-02 | 1.010e-03 |
| 149.895 | 3.3580e-02 | 1.040e-03 |
| 151.292 | 3.2280e-02 | 7.800e-04 |
| 151.787 | 3.0810e-02 | 1.210e-03 |
| 153.365 | 2.8330e-02 | 1.680e-03 |
| 155.178 | 3.2690e-02 | 6.970e-04 |
| 157.027 | 2.9230e-02 | 6.700e-04 |
| 158.786 | 3.3340e-02 | 8.790e-04 |
| 160.829 | 2.8060e-02 | 6.100e-04 |
| 161.409 | 2.5840e-02 | 1.150e-03 |
| 162.953 | 2.2640e-02 | 1.510e-03 |
| 164.756 | 2.5660e-02 | 6.190e-04 |
| 166.597 | 2.7020e-02 | 6.500e-04 |
| 168.345 | 1.9540e-02 | 2.980e-03 |
| 170.393 | 2.3100e-02 | 5.500e-04 |

**Table 7**

$^{106}$Cd($\alpha$,$\alpha$)$^{106}$Cd elastic scattering cross section (normalized to the Rutherford cross section) at the energy $E = 15.55$ MeV. See page 19 for Explanation of Tables

| $\vartheta_{\text{c.m.}}$ (deg) | $\sigma/\sigma_R$ | $\Delta(\sigma/\sigma_R)$ |
|---:|---:|---:|
| 20.653 | 9.7300e-01 | 4.072e-02 |
| 21.684 | 9.8571e-01 | 3.955e-02 |
| 22.715 | 9.9891e-01 | 3.852e-02 |
| 23.746 | 9.9569e-01 | 3.698e-02 |
| 24.777 | 9.9469e-01 | 3.569e-02 |
| 25.807 | 9.9107e-01 | 3.434e-02 |
| 26.837 | 9.9741e-01 | 3.348e-02 |
| 27.867 | 1.0020e+00 | 3.264e-02 |
| 28.897 | 9.9694e-01 | 3.156e-02 |
| 29.927 | 9.9801e-01 | 3.075e-02 |
| 30.956 | 9.9361e-01 | 2.987e-02 |
| 31.985 | 1.0026e+00 | 2.944e-02 |
| 33.014 | 1.0009e+00 | 2.870e-02 |
| 34.042 | 9.8698e-01 | 2.767e-02 |
| 35.070 | 9.7797e-01 | 2.690e-02 |
| 36.098 | 9.7830e-01 | 2.627e-02 |
| 37.126 | 9.7796e-01 | 2.576e-02 |
| 38.153 | 9.7616e-01 | 2.525e-02 |
| 39.180 | 9.9268e-01 | 2.473e-02 |
| 40.206 | 9.9851e-01 | 2.446e-02 |
| 41.232 | 1.0069e+00 | 2.427e-02 |
| 42.258 | 1.0097e+00 | 2.398e-02 |
| 43.284 | 1.0099e+00 | 2.362e-02 |
| 44.309 | 1.0216e+00 | 2.355e-02 |
| 45.333 | 1.0230e+00 | 2.329e-02 |
| 46.358 | 1.0221e+00 | 2.296e-02 |
| 47.382 | 1.0425e+00 | 2.315e-02 |
| 48.405 | 1.0547e+00 | 2.316e-02 |
| 49.428 | 1.0548e+00 | 2.291e-02 |
| 50.451 | 1.0575e+00 | 2.271e-02 |
| 51.473 | 1.0573e+00 | 2.240e-02 |
| 52.495 | 1.0565e+00 | 2.228e-02 |
| 53.516 | 1.0550e+00 | 2.201e-02 |
| 54.537 | 1.0708e+00 | 2.213e-02 |
| 55.558 | 1.0588e+00 | 2.176e-02 |
| 56.578 | 1.0624e+00 | 2.162e-02 |
| 57.597 | 1.0633e+00 | 2.152e-02 |
| 58.616 | 1.0746e+00 | 2.160e-02 |
| 59.635 | 1.0622e+00 | 2.123e-02 |
| 60.653 | 1.0595e+00 | 2.101e-02 |
| 61.671 | 1.0522e+00 | 2.040e-02 |
| 62.688 | 1.0574e+00 | 2.029e-02 |
| 63.704 | 1.0488e+00 | 2.000e-02 |
| 64.720 | 1.0451e+00 | 1.977e-02 |
| 65.735 | 1.0520e+00 | 1.964e-02 |
| 66.750 | 1.0288e+00 | 1.938e-02 |
| 67.764 | 1.0373e+00 | 1.898e-02 |
| 68.778 | 1.0183e+00 | 1.853e-02 |
| 69.791 | 1.0093e+00 | 1.829e-02 |
| 70.804 | 9.8704e-01 | 1.780e-02 |
| 71.815 | 9.7097e-01 | 1.749e-02 |
| 72.826 | 9.4651e-01 | 1.693e-02 |
| 73.837 | 9.3520e-01 | 1.667e-02 |
| 74.847 | 9.2139e-01 | 1.631e-02 |
| 75.855 | 9.0042e-01 | 1.627e-02 |
| 76.863 | 8.8681e-01 | 1.643e-02 |
| 77.871 | 8.8047e-01 | 1.553e-02 |
| 78.877 | 8.6082e-01 | 1.514e-02 |
| 79.882 | 8.4271e-01 | 1.480e-02 |
| 80.885 | 8.3482e-01 | 1.435e-02 |
| 81.887 | 8.3276e-01 | 1.542e-02 |
| 82.887 | 8.1594e-01 | 1.390e-02 |
| 83.884 | 7.9640e-01 | 1.361e-02 |
| 84.877 | 7.8437e-01 | 1.332e-02 |
| 85.863 | 7.7136e-01 | 1.305e-02 |
| 86.837 | 7.5361e-01 | 1.276e-02 |
| 87.783 | 7.3586e-01 | 1.248e-02 |
| 88.643 | 7.2327e-01 | 1.213e-02 |
| 90.886 | 6.9154e-01 | 1.176e-02 |
| 91.317 | 6.9152e-01 | 1.158e-02 |
| 92.166 | 6.6226e-01 | 1.214e-02 |
| 93.107 | 6.4761e-01 | 1.102e-02 |
| 94.075 | 6.3464e-01 | 1.090e-02 |
| 95.056 | 6.2092e-01 | 1.059e-02 |
| 96.042 | 6.1382e-01 | 1.042e-02 |
| 97.031 | 6.0355e-01 | 1.030e-02 |
| 98.022 | 5.7831e-01 | 9.926e-03 |
| 99.014 | 5.6280e-01 | 9.505e-03 |
| 100.006 | 5.4732e-01 | 9.479e-03 |
| 100.999 | 5.4137e-01 | 9.165e-03 |
| 101.991 | 5.2268e-01 | 9.906e-03 |
| 103.479 | 4.9851e-01 | 9.429e-03 |
| 104.967 | 4.7438e-01 | 9.174e-03 |
| 106.454 | 4.6345e-01 | 9.271e-03 |
| 107.940 | 4.4185e-01 | 8.690e-03 |
| 109.425 | 4.3159e-01 | 8.349e-03 |
| 110.909 | 4.2815e-01 | 7.979e-03 |
| 111.897 | 4.1659e-01 | 8.550e-03 |
| 112.391 | 4.1712e-01 | 8.017e-03 |
| 113.379 | 4.0237e-01 | 8.167e-03 |
| 113.873 | 4.0328e-01 | 7.736e-03 |
| 114.860 | 3.8450e-01 | 8.038e-03 |
| 115.353 | 3.8971e-01 | 7.498e-03 |
| 116.339 | 3.5771e-01 | 7.928e-03 |
| 116.832 | 3.7403e-01 | 7.198e-03 |
| 117.817 | 3.6208e-01 | 7.719e-03 |
| 119.294 | 3.5019e-01 | 7.317e-03 |
| 120.770 | 3.4120e-01 | 6.949e-03 |
| 122.245 | 3.3751e-01 | 7.131e-03 |
| 123.718 | 3.2144e-01 | 6.801e-03 |
| 125.191 | 3.0994e-01 | 6.580e-03 |
| 126.662 | 3.0631e-01 | 7.253e-03 |
| 128.131 | 2.8250e-01 | 7.531e-03 |
| 129.600 | 2.8383e-01 | 7.697e-03 |
| 131.068 | 2.8695e-01 | 8.053e-03 |
| 132.534 | 2.8455e-01 | 7.228e-03 |
| 134.000 | 2.9917e-01 | 7.284e-03 |
| 135.464 | 2.8849e-01 | 6.871e-03 |
| 136.440 | 2.6757e-01 | 7.005e-03 |
| 136.927 | 2.7535e-01 | 6.834e-03 |
| 137.902 | 2.7219e-01 | 7.046e-03 |
| 138.390 | 2.7197e-01 | 6.691e-03 |
| 139.364 | 2.6021e-01 | 6.955e-03 |
| 139.851 | 2.6098e-01 | 6.439e-03 |
| 140.824 | 2.4918e-01 | 7.040e-03 |
| 141.311 | 2.5858e-01 | 6.318e-03 |
| 142.284 | 2.5402e-01 | 6.826e-03 |
| 143.743 | 2.3785e-01 | 6.290e-03 |
| 145.201 | 2.3186e-01 | 5.953e-03 |
| 146.657 | 2.3335e-01 | 6.181e-03 |
| 148.113 | 2.2209e-01 | 5.873e-03 |
| 149.569 | 2.2761e-01 | 5.926e-03 |
| 151.023 | 2.2431e-01 | 5.052e-03 |
| 152.961 | 2.2275e-01 | 4.396e-03 |
| 154.898 | 2.2217e-01 | 4.287e-03 |
| 156.834 | 2.1660e-01 | 4.198e-03 |
| 158.768 | 2.1552e-01 | 4.537e-03 |
| 160.701 | 2.0666e-01 | 4.014e-03 |
| 162.634 | 2.0350e-01 | 3.962e-03 |
| 164.566 | 2.0478e-01 | 3.882e-03 |
| 166.497 | 2.0154e-01 | 3.836e-03 |
| 168.427 | 1.9976e-01 | 4.162e-03 |
| 170.357 | 1.9959e-01 | 3.983e-03 |

**Table 8**
$^{106}$Cd($\alpha$,$\alpha$)$^{106}$Cd elastic scattering cross section (normalized to the Rutherford cross section) at the energy $E = 17.00$ MeV. See page 19 for Explanation of Tables

| $\vartheta_{\text{c.m.}}$ (deg) | $\sigma/\sigma_R$ | $\Delta(\sigma/\sigma_R)$ | $\vartheta_{\text{c.m.}}$ (deg) | $\sigma/\sigma_R$ | $\Delta(\sigma/\sigma_R)$ | $\vartheta_{\text{c.m.}}$ (deg) | $\sigma/\sigma_R$ | $\Delta(\sigma/\sigma_R)$ |
|---:|---:|---:|---:|---:|---:|---:|---:|---:|
| 20.804 | 9.9992e-01 | 1.381e-02 | 82.140 | 5.4214e-01 | 8.042e-03 | 151.026 | 1.0101e-01 | 3.197e-03 |
| 21.832 | 1.0135e+00 | 1.394e-02 | 82.143 | 5.4672e-01 | 8.178e-03 | 151.064 | 8.9107e-02 | 2.051e-03 |
| 22.875 | 1.0163e+00 | 1.399e-02 | 83.145 | 5.2660e-01 | 7.758e-03 | 151.146 | 1.0069e-01 | 3.840e-03 |
| 23.891 | 1.0058e+00 | 1.384e-02 | 84.146 | 5.1823e-01 | 7.480e-03 | 153.058 | 9.8905e-02 | 3.644e-03 |
| 24.928 | 9.9453e-01 | 1.363e-02 | 85.153 | 4.9951e-01 | 7.368e-03 | 154.982 | 9.7807e-02 | 3.701e-03 |
| 25.956 | 9.8697e-01 | 1.345e-02 | 86.153 | 4.8068e-01 | 7.123e-03 | 156.900 | 9.5861e-02 | 5.296e-03 |
| 27.034 | 9.4819e-01 | 1.288e-02 | 87.159 | 4.5839e-01 | 6.791e-03 | 158.833 | 9.1021e-02 | 3.396e-03 |
| 28.029 | 9.5908e-01 | 1.301e-02 | 88.159 | 4.5435e-01 | 6.702e-03 | 160.679 | 8.8638e-02 | 3.115e-03 |
| 29.116 | 9.4768e-01 | 1.287e-02 | 89.163 | 4.4445e-01 | 6.711e-03 | 160.720 | 8.8201e-02 | 2.094e-03 |
| 30.115 | 9.4769e-01 | 1.281e-02 | 90.164 | 4.2925e-01 | 6.463e-03 | 160.734 | 9.0958e-02 | 3.345e-03 |
| 31.141 | 9.8322e-01 | 1.334e-02 | 91.165 | 4.1152e-01 | 6.236e-03 | 160.809 | 9.0769e-02 | 2.842e-03 |
| 31.175 | 9.8108e-01 | 1.327e-02 | 92.166 | 4.0222e-01 | 6.040e-03 | 162.713 | 8.8268e-02 | 2.618e-03 |
| 32.166 | 9.9274e-01 | 1.344e-02 | 92.166 | 4.0548e-01 | 6.529e-03 | 164.632 | 8.8184e-02 | 2.713e-03 |
| 33.206 | 9.9098e-01 | 1.347e-02 | 93.165 | 3.8680e-01 | 6.183e-03 | 166.545 | 8.6337e-02 | 3.963e-03 |
| 34.220 | 9.8838e-01 | 1.344e-02 | 94.164 | 3.7874e-01 | 5.894e-03 | 168.474 | 8.5550e-02 | 2.543e-03 |
| 35.254 | 9.9510e-01 | 1.354e-02 | 95.161 | 3.6372e-01 | 5.848e-03 | 170.369 | 8.2967e-02 | 2.415e-03 |
| 36.279 | 9.9790e-01 | 1.356e-02 | 96.161 | 3.5385e-01 | 5.702e-03 | | | |
| 37.349 | 1.0170e+00 | 1.369e-02 | 97.156 | 3.3965e-01 | 5.451e-03 | | | |
| 38.344 | 1.0324e+00 | 1.388e-02 | 98.156 | 3.3595e-01 | 5.367e-03 | | | |
| 39.421 | 1.0449e+00 | 1.406e-02 | 99.150 | 3.2494e-01 | 5.359e-03 | | | |
| 40.420 | 1.0535e+00 | 1.416e-02 | 100.148 | 3.2123e-01 | 5.259e-03 | | | |
| 41.473 | 1.0672e+00 | 1.433e-02 | 101.144 | 3.0559e-01 | 5.085e-03 | | | |
| 41.479 | 1.0602e+00 | 1.434e-02 | 102.131 | 2.9743e-01 | 4.963e-03 | | | |
| 42.489 | 1.0660e+00 | 1.438e-02 | 102.132 | 2.9211e-01 | 4.803e-03 | | | |
| 43.461 | 1.0754e+00 | 1.454e-02 | 103.616 | 2.8592e-01 | 5.117e-03 | | | |
| 44.513 | 1.0879e+00 | 1.472e-02 | 105.105 | 2.7360e-01 | 4.904e-03 | | | |
| 45.558 | 1.0845e+00 | 1.466e-02 | 106.596 | 2.6153e-01 | 4.559e-03 | | | |
| 46.561 | 1.0947e+00 | 1.485e-02 | 108.078 | 2.4981e-01 | 4.216e-03 | | | |
| 47.581 | 1.0917e+00 | 1.483e-02 | 109.555 | 2.3545e-01 | 4.072e-03 | | | |
| 48.610 | 1.0927e+00 | 1.482e-02 | 111.049 | 2.2960e-01 | 4.021e-03 | | | |
| 49.623 | 1.0904e+00 | 1.481e-02 | 112.032 | 2.1438e-01 | 4.116e-03 | | | |
| 50.676 | 1.0982e+00 | 1.489e-02 | 112.524 | 2.1803e-01 | 3.839e-03 | | | |
| 51.658 | 1.0748e+00 | 1.468e-02 | 113.504 | 2.1353e-01 | 4.413e-03 | | | |
| 51.732 | 1.0893e+00 | 1.476e-02 | 114.003 | 2.1237e-01 | 3.767e-03 | | | |
| 52.740 | 1.0854e+00 | 1.472e-02 | 114.984 | 2.0728e-01 | 4.317e-03 | | | |
| 53.716 | 1.0709e+00 | 1.445e-02 | 115.480 | 2.0089e-01 | 3.782e-03 | | | |
| 54.759 | 1.0608e+00 | 1.443e-02 | 116.469 | 1.9134e-01 | 3.852e-03 | | | |
| 55.796 | 1.0333e+00 | 1.406e-02 | 116.952 | 1.9334e-01 | 3.547e-03 | | | |
| 56.798 | 1.0249e+00 | 1.402e-02 | 117.940 | 1.8828e-01 | 3.582e-03 | | | |
| 57.814 | 1.0195e+00 | 1.390e-02 | 119.405 | 1.8464e-01 | 3.598e-03 | | | |
| 58.837 | 1.0022e+00 | 1.372e-02 | 120.897 | 1.7498e-01 | 3.472e-03 | | | |
| 59.847 | 9.7912e-01 | 1.346e-02 | 122.360 | 1.6718e-01 | 3.344e-03 | | | |
| 60.889 | 9.6875e-01 | 1.330e-02 | 123.829 | 1.6308e-01 | 3.276e-03 | | | |
| 61.875 | 9.3002e-01 | 1.289e-02 | 125.297 | 1.5697e-01 | 3.396e-03 | | | |
| 61.881 | 9.3540e-01 | 1.281e-02 | 126.759 | 1.5413e-01 | 3.206e-03 | | | |
| 62.894 | 9.3779e-01 | 1.290e-02 | 126.779 | 1.4612e-01 | 5.764e-03 | | | |
| 63.933 | 9.1066e-01 | 1.263e-02 | 128.259 | 1.4767e-01 | 6.072e-03 | | | |
| 64.958 | 8.8120e-01 | 1.236e-02 | 129.722 | 1.4235e-01 | 5.831e-03 | | | |
| 65.964 | 8.5827e-01 | 1.199e-02 | 131.173 | 1.4305e-01 | 5.719e-03 | | | |
| 66.969 | 8.4253e-01 | 1.180e-02 | 132.644 | 1.3698e-01 | 5.322e-03 | | | |
| 67.998 | 8.2272e-01 | 1.157e-02 | 134.120 | 1.3517e-01 | 5.302e-03 | | | |
| 69.010 | 8.0910e-01 | 1.136e-02 | 135.554 | 1.2911e-01 | 5.111e-03 | | | |
| 70.035 | 7.7302e-01 | 1.083e-02 | 136.537 | 1.2785e-01 | 4.352e-03 | | | |
| 71.045 | 7.5172e-01 | 1.070e-02 | 137.026 | 1.2617e-01 | 4.963e-03 | | | |
| 72.039 | 7.2790e-01 | 1.027e-02 | 138.012 | 1.2234e-01 | 4.496e-03 | | | |
| 72.055 | 7.4007e-01 | 1.048e-02 | 138.487 | 1.2237e-01 | 4.858e-03 | | | |
| 73.048 | 7.1501e-01 | 1.016e-02 | 139.468 | 1.1888e-01 | 4.319e-03 | | | |
| 74.073 | 6.9583e-01 | 1.005e-02 | 139.947 | 1.1659e-01 | 4.800e-03 | | | |
| 75.090 | 6.8553e-01 | 1.010e-02 | 140.909 | 1.1590e-01 | 4.055e-03 | | | |
| 76.093 | 6.6123e-01 | 9.656e-03 | 142.374 | 1.1000e-01 | 3.699e-03 | | | |
| 77.095 | 6.3633e-01 | 9.362e-03 | 143.845 | 1.0675e-01 | 3.664e-03 | | | |
| 78.113 | 6.1538e-01 | 9.135e-03 | 145.268 | 1.0826e-01 | 3.702e-03 | | | |
| 79.120 | 6.1045e-01 | 9.017e-03 | 146.736 | 1.0997e-01 | 3.720e-03 | | | |
| 80.133 | 5.8281e-01 | 8.576e-03 | 148.190 | 1.0144e-01 | 3.464e-03 | | | |
| 81.138 | 5.6401e-01 | 8.547e-03 | 149.645 | 1.0604e-01 | 3.745e-03 | | | |

**Table 9**

$^{106}$Cd($\alpha$,$\alpha$)$^{106}$Cd elastic scattering cross section (normalized to the Rutherford cross section) at the energy $E = 18.88$ MeV. See page 19 for Explanation of Tables

| $\vartheta_{\text{c.m.}}$ (deg) | $\sigma/\sigma_R$ | $\Delta(\sigma/\sigma_R)$ | $\vartheta_{\text{c.m.}}$ (deg) | $\sigma/\sigma_R$ | $\Delta(\sigma/\sigma_R)$ | $\vartheta_{\text{c.m.}}$ (deg) | $\sigma/\sigma_R$ | $\Delta(\sigma/\sigma_R)$ |
|---:|---:|---:|---:|---:|---:|---:|---:|---:|
| 20.715 | 9.5450e-01 | 4.471e-02 | 89.150 | 2.1613e-01 | 4.677e-03 | 170.303 | 2.9448e-02 | 8.698e-04 |
| 21.749 | 9.6545e-01 | 4.626e-02 | 90.115 | 2.1062e-01 | 4.447e-03 | | | |
| 22.783 | 9.5007e-01 | 4.356e-02 | 91.077 | 1.9701e-01 | 4.139e-03 | | | |
| 23.817 | 9.5505e-01 | 4.373e-02 | 92.076 | 1.9301e-01 | 4.274e-03 | | | |
| 24.851 | 9.5502e-01 | 4.507e-02 | 93.076 | 1.8926e-01 | 4.505e-03 | | | |
| 25.884 | 9.6959e-01 | 4.357e-02 | 94.076 | 1.8049e-01 | 4.247e-03 | | | |
| 26.917 | 9.7426e-01 | 4.293e-02 | 95.075 | 1.7476e-01 | 4.064e-03 | | | |
| 27.950 | 9.8297e-01 | 4.260e-02 | 96.074 | 1.6626e-01 | 3.800e-03 | | | |
| 28.983 | 9.9316e-01 | 3.916e-02 | 97.073 | 1.6190e-01 | 3.724e-03 | | | |
| 30.015 | 1.0113e+00 | 3.666e-02 | 98.070 | 1.5093e-01 | 3.426e-03 | | | |
| 31.048 | 1.0206e+00 | 3.660e-02 | 99.067 | 1.4578e-01 | 3.276e-03 | | | |
| 32.079 | 1.0520e+00 | 3.882e-02 | 100.064 | 1.4525e-01 | 3.121e-03 | | | |
| 33.111 | 1.0723e+00 | 3.828e-02 | 101.060 | 1.4100e-01 | 2.888e-03 | | | |
| 34.142 | 1.0775e+00 | 4.019e-02 | 102.055 | 1.3916e-01 | 2.806e-03 | | | |
| 36.204 | 1.1175e+00 | 4.219e-02 | 103.546 | 1.3197e-01 | 2.640e-03 | | | |
| 37.234 | 1.1382e+00 | 4.263e-02 | 105.036 | 1.2341e-01 | 2.606e-03 | | | |
| 38.264 | 1.1439e+00 | 4.266e-02 | 106.525 | 1.1368e-01 | 2.373e-03 | | | |
| 39.294 | 1.1277e+00 | 3.951e-02 | 108.012 | 1.0939e-01 | 2.302e-03 | | | |
| 40.323 | 1.1277e+00 | 3.587e-02 | 109.497 | 1.0231e-01 | 2.043e-03 | | | |
| 42.380 | 1.1133e+00 | 4.210e-02 | 110.981 | 1.0003e-01 | 2.133e-03 | | | |
| 43.408 | 1.0871e+00 | 3.815e-02 | 111.970 | 9.4752e-02 | 2.104e-03 | | | |
| 44.436 | 1.0601e+00 | 3.872e-02 | 112.464 | 9.1332e-02 | 1.935e-03 | | | |
| 45.463 | 1.0504e+00 | 3.774e-02 | 113.452 | 9.2572e-02 | 2.003e-03 | | | |
| 46.490 | 1.0279e+00 | 3.765e-02 | 113.945 | 8.8142e-02 | 1.801e-03 | | | |
| 47.517 | 1.0130e+00 | 3.643e-02 | 114.932 | 8.5995e-02 | 2.040e-03 | | | |
| 48.543 | 9.8628e-01 | 3.487e-02 | 115.425 | 8.6756e-02 | 1.715e-03 | | | |
| 49.568 | 9.7562e-01 | 3.377e-02 | 116.410 | 8.2547e-02 | 1.923e-03 | | | |
| 50.593 | 9.4203e-01 | 3.153e-02 | 116.903 | 8.4217e-02 | 1.724e-03 | | | |
| 51.618 | 9.2336e-01 | 3.223e-02 | 117.888 | 8.1606e-02 | 1.906e-03 | | | |
| 52.642 | 9.1077e-01 | 3.294e-02 | 119.364 | 7.5913e-02 | 1.667e-03 | | | |
| 53.666 | 8.6389e-01 | 2.883e-02 | 120.838 | 7.3901e-02 | 1.765e-03 | | | |
| 54.689 | 8.2650e-01 | 2.886e-02 | 122.311 | 6.6982e-02 | 1.590e-03 | | | |
| 55.712 | 8.1422e-01 | 2.813e-02 | 123.783 | 6.4989e-02 | 1.472e-03 | | | |
| 56.735 | 7.8029e-01 | 2.761e-02 | 125.253 | 6.4695e-02 | 1.407e-03 | | | |
| 57.757 | 7.5295e-01 | 2.621e-02 | 126.722 | 6.1842e-02 | 1.576e-03 | | | |
| 58.778 | 7.1535e-01 | 2.444e-02 | 128.190 | 5.8312e-02 | 1.614e-03 | | | |
| 59.799 | 6.9774e-01 | 2.344e-02 | 129.657 | 5.7003e-02 | 1.742e-03 | | | |
| 60.819 | 6.6324e-01 | 2.152e-02 | 131.122 | 5.1797e-02 | 1.577e-03 | | | |
| 61.839 | 6.4672e-01 | 2.254e-02 | 132.586 | 4.8585e-02 | 1.503e-03 | | | |
| 62.858 | 6.1909e-01 | 2.539e-02 | 134.048 | 4.9100e-02 | 1.394e-03 | | | |
| 63.877 | 6.0614e-01 | 2.254e-02 | 135.510 | 4.6616e-02 | 1.450e-03 | | | |
| 64.895 | 5.7656e-01 | 2.193e-02 | 136.483 | 4.3823e-02 | 1.400e-03 | | | |
| 65.913 | 5.6115e-01 | 2.042e-02 | 136.970 | 4.5618e-02 | 1.378e-03 | | | |
| 66.930 | 5.3133e-01 | 1.834e-02 | 137.943 | 4.0699e-02 | 1.280e-03 | | | |
| 67.946 | 5.1552e-01 | 1.788e-02 | 138.429 | 4.2242e-02 | 1.230e-03 | | | |
| 68.962 | 4.8954e-01 | 1.699e-02 | 139.401 | 4.4238e-02 | 1.530e-03 | | | |
| 69.978 | 4.7426e-01 | 1.528e-02 | 139.887 | 4.2496e-02 | 1.186e-03 | | | |
| 70.993 | 4.6029e-01 | 1.444e-02 | 140.858 | 4.0461e-02 | 1.392e-03 | | | |
| 72.007 | 4.3572e-01 | 1.491e-02 | 141.344 | 4.1924e-02 | 1.211e-03 | | | |
| 73.021 | 4.2178e-01 | 1.749e-02 | 142.314 | 3.9570e-02 | 1.364e-03 | | | |
| 74.034 | 4.1106e-01 | 1.536e-02 | 143.769 | 3.9618e-02 | 1.241e-03 | | | |
| 75.046 | 3.8006e-01 | 1.460e-02 | 145.224 | 3.8294e-02 | 1.322e-03 | | | |
| 76.058 | 3.6673e-01 | 1.344e-02 | 146.677 | 3.6789e-02 | 1.235e-03 | | | |
| 77.069 | 3.4621e-01 | 1.204e-02 | 148.129 | 3.5337e-02 | 1.123e-03 | | | |
| 78.080 | 3.3078e-01 | 1.162e-02 | 149.580 | 3.8870e-02 | 1.147e-03 | | | |
| 79.090 | 3.2838e-01 | 1.152e-02 | 151.030 | 3.5310e-02 | 1.107e-03 | | | |
| 80.099 | 3.1722e-01 | 1.006e-02 | 152.963 | 3.3644e-02 | 1.235e-03 | | | |
| 81.108 | 3.0293e-01 | 9.375e-03 | 154.894 | 3.3090e-02 | 8.424e-04 | | | |
| 82.116 | 2.8838e-01 | 7.700e-03 | 156.824 | 3.2773e-02 | 7.424e-04 | | | |
| 83.124 | 2.7533e-01 | 6.361e-03 | 158.752 | 3.2374e-02 | 1.000e-03 | | | |
| 84.131 | 2.6606e-01 | 6.060e-03 | 160.679 | 3.1808e-02 | 1.159e-03 | | | |
| 85.137 | 2.5374e-01 | 5.706e-03 | 162.606 | 3.0526e-02 | 1.196e-03 | | | |
| 86.142 | 2.4543e-01 | 5.415e-03 | 164.531 | 2.8708e-02 | 7.690e-04 | | | |
| 87.146 | 2.3453e-01 | 5.213e-03 | 166.456 | 3.0291e-02 | 7.033e-04 | | | |
| 88.150 | 2.2703e-01 | 4.964e-03 | 168.379 | 2.9936e-02 | 9.665e-04 | | | |

**Table 10**

$^{110}$Cd($\alpha$,$\alpha$)$^{110}$Cd elastic scattering cross section (normalized to the Rutherford cross section) at the energy $E = 15.56$ MeV. See page 19 for Explanation of Tables

| $\vartheta_{\text{c.m.}}$ (deg) | $\sigma/\sigma_R$ | $\Delta(\sigma/\sigma_R)$ |
|---:|---:|---:|
| 20.799 | 9.9861e-01 | 4.249e-02 |
| 21.832 | 1.0017e+00 | 4.262e-02 |
| 22.865 | 1.0025e+00 | 4.266e-02 |
| 23.898 | 1.0074e+00 | 4.287e-02 |
| 24.930 | 1.0033e+00 | 4.271e-02 |
| 25.962 | 1.0084e+00 | 4.295e-02 |
| 26.994 | 1.0124e+00 | 4.312e-02 |
| 28.026 | 1.0142e+00 | 4.322e-02 |
| 29.058 | 1.0112e+00 | 4.310e-02 |
| 30.089 | 1.0008e+00 | 4.269e-02 |
| 31.114 | 1.0012e+00 | 4.275e-02 |
| 32.139 | 9.9733e-01 | 4.257e-02 |
| 33.170 | 9.8618e-01 | 4.212e-02 |
| 34.200 | 9.8711e-01 | 4.218e-02 |
| 35.230 | 9.6531e-01 | 4.127e-02 |
| 36.259 | 9.7518e-01 | 4.176e-02 |
| 37.288 | 9.7399e-01 | 4.170e-02 |
| 38.317 | 9.6815e-01 | 4.151e-02 |
| 39.345 | 9.6772e-01 | 4.151e-02 |
| 40.374 | 9.7998e-01 | 4.211e-02 |
| 41.407 | 9.7352e-01 | 4.167e-02 |
| 42.440 | 9.7300e-01 | 4.152e-02 |
| 43.467 | 9.8634e-01 | 4.205e-02 |
| 44.494 | 9.8923e-01 | 4.223e-02 |
| 45.520 | 9.9141e-01 | 4.234e-02 |
| 47.571 | 1.0031e+00 | 4.350e-02 |
| 49.621 | 1.0050e+00 | 4.396e-02 |
| 51.663 | 1.0060e+00 | 4.365e-02 |
| 52.681 | 1.0158e+00 | 4.354e-02 |
| 53.704 | 1.0131e+00 | 4.334e-02 |
| 54.726 | 1.0170e+00 | 4.363e-02 |
| 55.748 | 1.0210e+00 | 4.382e-02 |
| 57.791 | 1.0256e+00 | 4.538e-02 |
| 59.831 | 1.0247e+00 | 4.605e-02 |
| 61.870 | 1.0055e+00 | 4.561e-02 |
| 64.935 | 9.8207e-01 | 4.216e-02 |
| 65.952 | 9.6937e-01 | 4.166e-02 |
| 66.968 | 9.5248e-01 | 4.101e-02 |
| 67.984 | 9.4511e-01 | 4.082e-02 |
| 68.999 | 9.3807e-01 | 4.058e-02 |
| 70.014 | 9.1225e-01 | 3.945e-02 |
| 71.028 | 9.0567e-01 | 3.924e-02 |
| 72.042 | 8.8478e-01 | 3.821e-02 |
| 75.068 | 8.2766e-01 | 3.587e-02 |
| 76.079 | 8.1597e-01 | 3.543e-02 |
| 77.090 | 7.8826e-01 | 3.435e-02 |
| 78.100 | 7.7588e-01 | 3.401e-02 |
| 79.110 | 7.6593e-01 | 3.366e-02 |
| 80.119 | 7.4610e-01 | 3.277e-02 |
| 81.127 | 7.3655e-01 | 3.246e-02 |
| 82.140 | 7.1893e-01 | 3.202e-02 |
| 84.159 | 7.0199e-01 | 3.175e-02 |
| 86.170 | 6.6382e-01 | 3.060e-02 |
| 88.177 | 6.4158e-01 | 2.946e-02 |
| 89.785 | 5.8152e-01 | 2.681e-02 |
| 92.188 | 5.6686e-01 | 2.678e-02 |
| 94.182 | 5.3410e-01 | 2.540e-02 |
| 96.180 | 5.0814e-01 | 2.488e-02 |
| 98.176 | 4.5922e-01 | 2.251e-02 |
| 100.170 | 4.2586e-01 | 2.089e-02 |
| 102.161 | 3.8203e-01 | 1.961e-02 |
| 104.657 | 3.6560e-01 | 1.687e-02 |
| 107.138 | 3.3183e-01 | 1.617e-02 |
| 109.615 | 3.1248e-01 | 1.520e-02 |
| 112.089 | 3.0204e-01 | 1.435e-02 |
| 114.547 | 2.7345e-01 | 1.329e-02 |
| 117.013 | 2.6117e-01 | 1.363e-02 |
| 119.482 | 2.3777e-01 | 1.301e-02 |
| 121.932 | 2.2044e-01 | 1.121e-02 |
| 124.397 | 2.0393e-01 | 1.016e-02 |
| 126.848 | 1.9562e-01 | 1.017e-02 |
| 129.284 | 1.8326e-01 | 1.140e-02 |
| 131.739 | 1.8652e-01 | 9.384e-03 |
| 134.169 | 1.7826e-01 | 9.364e-03 |
| 136.606 | 1.6907e-01 | 9.548e-03 |
| 139.040 | 1.6603e-01 | 7.377e-03 |
| 141.471 | 1.5353e-01 | 7.487e-03 |
| 143.899 | 1.4923e-01 | 6.684e-03 |
| 146.325 | 1.4526e-01 | 6.486e-03 |
| 148.748 | 1.3962e-01 | 6.220e-03 |
| 151.168 | 1.3451e-01 | 5.976e-03 |
| 153.587 | 1.3179e-01 | 5.970e-03 |
| 156.003 | 1.2347e-01 | 5.581e-03 |
| 158.417 | 1.2817e-01 | 6.152e-03 |
| 160.830 | 1.2345e-01 | 5.500e-03 |
| 163.241 | 1.1729e-01 | 5.693e-03 |
| 165.651 | 1.1828e-01 | 5.283e-03 |
| 168.059 | 1.1316e-01 | 5.387e-03 |
| 170.467 | 1.1605e-01 | 5.139e-03 |
| 172.874 | 1.1174e-01 | 5.468e-03 |
| 175.280 | 1.1563e-01 | 5.173e-03 |

**Table 11**
$^{110}$Cd($\alpha$,$\alpha$)$^{110}$Cd elastic scattering cross section (normalized to the Rutherford cross section) at the energy $E = 18.76$ MeV. See page 19 for Explanation of Tables

| $\vartheta_{\mathrm{c.m.}}$ (deg) | $\sigma/\sigma_R$ | $\Delta(\sigma/\sigma_R)$ | $\vartheta_{\mathrm{c.m.}}$ (deg) | $\sigma/\sigma_R$ | $\Delta(\sigma/\sigma_R)$ | $\vartheta_{\mathrm{c.m.}}$ (deg) | $\sigma/\sigma_R$ | $\Delta(\sigma/\sigma_R)$ |
|---:|---:|---:|---:|---:|---:|---:|---:|---:|
| 20.799 | 9.9928e-01 | 4.258e-02 | 92.188 | 1.7828e-01 | 8.803e-03 | | | |
| 21.832 | 9.9744e-01 | 4.252e-02 | 93.182 | 1.7726e-01 | 8.590e-03 | | | |
| 22.865 | 9.8590e-01 | 4.204e-02 | 94.182 | 1.6466e-01 | 8.288e-03 | | | |
| 23.898 | 9.8193e-01 | 4.190e-02 | 96.180 | 1.4559e-01 | 8.127e-03 | | | |
| 24.930 | 9.6942e-01 | 4.141e-02 | 98.176 | 1.4387e-01 | 7.888e-03 | | | |
| 25.962 | 9.7365e-01 | 4.158e-02 | 100.170 | 1.2732e-01 | 7.227e-03 | | | |
| 26.994 | 9.7199e-01 | 4.154e-02 | 102.161 | 1.1692e-01 | 6.611e-03 | | | |
| 28.026 | 9.8868e-01 | 4.230e-02 | 104.657 | 1.0127e-01 | 5.634e-03 | | | |
| 29.058 | 1.0065e+00 | 4.311e-02 | 109.615 | 8.3396e-02 | 4.648e-03 | | | |
| 30.089 | 1.0191e+00 | 4.369e-02 | 111.984 | 7.8943e-02 | 3.682e-03 | | | |
| 31.114 | 1.0423e+00 | 4.475e-02 | 114.547 | 6.3688e-02 | 4.294e-03 | | | |
| 32.139 | 1.0734e+00 | 4.617e-02 | 116.919 | 6.4801e-02 | 3.118e-03 | | | |
| 33.170 | 1.0890e+00 | 4.687e-02 | 119.381 | 6.2507e-02 | 3.081e-03 | | | |
| 34.200 | 1.1040e+00 | 4.755e-02 | 121.839 | 5.4938e-02 | 2.672e-03 | | | |
| 35.230 | 1.0937e+00 | 4.727e-02 | 124.293 | 5.1256e-02 | 2.644e-03 | | | |
| 36.259 | 1.1121e+00 | 4.795e-02 | 126.744 | 4.5142e-02 | 2.257e-03 | | | |
| 37.288 | 1.1218e+00 | 4.847e-02 | 129.192 | 4.3512e-02 | 2.342e-03 | | | |
| 38.317 | 1.1238e+00 | 4.871e-02 | 131.635 | 3.9738e-02 | 2.012e-03 | | | |
| 39.345 | 1.1334e+00 | 4.922e-02 | 134.076 | 3.2466e-02 | 1.813e-03 | | | |
| 40.374 | 1.1263e+00 | 4.900e-02 | 136.513 | 3.0881e-02 | 1.613e-03 | | | |
| 41.407 | 1.1292e+00 | 4.876e-02 | 138.947 | 3.2722e-02 | 1.782e-03 | | | |
| 42.440 | 1.1046e+00 | 4.740e-02 | 141.379 | 3.3125e-02 | 1.919e-03 | | | |
| 43.467 | 1.0819e+00 | 4.644e-02 | 143.807 | 3.1677e-02 | 1.776e-03 | | | |
| 44.494 | 1.0786e+00 | 4.637e-02 | 146.233 | 2.9589e-02 | 1.798e-03 | | | |
| 45.520 | 1.0514e+00 | 4.531e-02 | 148.656 | 2.5836e-02 | 1.524e-03 | | | |
| 46.546 | 1.0465e+00 | 4.493e-02 | 151.077 | 2.4937e-02 | 1.620e-03 | | | |
| 47.571 | 1.0199e+00 | 4.389e-02 | 153.495 | 2.3427e-02 | 1.381e-03 | | | |
| 48.596 | 1.0081e+00 | 4.345e-02 | 155.911 | 2.2335e-02 | 1.439e-03 | | | |
| 49.621 | 9.8347e-01 | 4.229e-02 | 158.326 | 2.0906e-02 | 1.232e-03 | | | |
| 50.645 | 9.5702e-01 | 4.117e-02 | 160.738 | 2.0512e-02 | 1.122e-03 | | | |
| 51.663 | 9.3258e-01 | 4.028e-02 | 163.150 | 2.1292e-02 | 1.264e-03 | | | |
| 52.681 | 8.9845e-01 | 3.917e-02 | 165.559 | 1.9108e-02 | 1.070e-03 | | | |
| 53.704 | 8.6463e-01 | 3.773e-02 | 167.968 | 2.0562e-02 | 1.236e-03 | | | |
| 54.726 | 8.5471e-01 | 3.744e-02 | 170.376 | 1.9273e-02 | 1.080e-03 | | | |
| 55.748 | 8.2144e-01 | 3.620e-02 | 172.782 | 1.8336e-02 | 1.097e-03 | | | |
| 56.770 | 7.8558e-01 | 3.428e-02 | 175.189 | 1.7743e-02 | 9.949e-04 | | | |
| 57.791 | 7.5831e-01 | 3.332e-02 | | | | | | |
| 58.811 | 7.1869e-01 | 3.173e-02 | | | | | | |
| 59.831 | 7.0347e-01 | 3.085e-02 | | | | | | |
| 60.851 | 6.6673e-01 | 2.928e-02 | | | | | | |
| 61.870 | 6.4330e-01 | 2.828e-02 | | | | | | |
| 62.899 | 6.2671e-01 | 2.704e-02 | | | | | | |
| 63.917 | 5.9342e-01 | 2.585e-02 | | | | | | |
| 64.935 | 5.8088e-01 | 2.510e-02 | | | | | | |
| 65.952 | 5.4687e-01 | 2.398e-02 | | | | | | |
| 66.968 | 5.3780e-01 | 2.335e-02 | | | | | | |
| 67.984 | 5.0335e-01 | 2.204e-02 | | | | | | |
| 68.999 | 4.8880e-01 | 2.120e-02 | | | | | | |
| 70.014 | 4.6315e-01 | 2.034e-02 | | | | | | |
| 71.028 | 4.4958e-01 | 1.972e-02 | | | | | | |
| 73.044 | 4.0149e-01 | 1.773e-02 | | | | | | |
| 74.056 | 3.9528e-01 | 1.781e-02 | | | | | | |
| 75.068 | 3.8477e-01 | 1.703e-02 | | | | | | |
| 76.079 | 3.5533e-01 | 1.626e-02 | | | | | | |
| 77.090 | 3.4583e-01 | 1.546e-02 | | | | | | |
| 78.100 | 3.2830e-01 | 1.496e-02 | | | | | | |
| 79.110 | 3.2209e-01 | 1.434e-02 | | | | | | |
| 80.119 | 3.0184e-01 | 1.382e-02 | | | | | | |
| 81.127 | 2.9263e-01 | 1.336e-02 | | | | | | |
| 82.146 | 2.7587e-01 | 1.256e-02 | | | | | | |
| 83.153 | 2.6427e-01 | 1.201e-02 | | | | | | |
| 84.159 | 2.5007e-01 | 1.159e-02 | | | | | | |
| 86.170 | 2.2660e-01 | 1.112e-02 | | | | | | |
| 88.177 | 2.0952e-01 | 1.027e-02 | | | | | | |
| 89.785 | 1.9461e-01 | 9.685e-03 | | | | | | |

**Table 12**
$^{116}$Cd($\alpha$,$\alpha$)$^{116}$Cd elastic scattering cross section (normalized to the Rutherford cross section) at the energy $E = 15.59$ MeV. See page 19 for Explanation of Tables

| $\vartheta_{\text{c.m.}}$ (deg) | $\sigma/\sigma_R$ | $\Delta(\sigma/\sigma_R)$ | $\vartheta_{\text{c.m.}}$ (deg) | $\sigma/\sigma_R$ | $\Delta(\sigma/\sigma_R)$ | $\vartheta_{\text{c.m.}}$ (deg) | $\sigma/\sigma_R$ | $\Delta(\sigma/\sigma_R)$ |
|---|---|---|---|---|---|---|---|---|
| 20.764 | 1.0064e+00 | 4.286e-02 | 87.068 | 6.1461e-01 | 2.717e-02 | | | |
| 21.796 | 9.9886e-01 | 4.255e-02 | 88.071 | 6.0103e-01 | 2.660e-02 | | | |
| 22.827 | 9.9380e-01 | 4.234e-02 | 89.071 | 5.7731e-01 | 2.559e-02 | | | |
| 23.858 | 9.9514e-01 | 4.241e-02 | 89.874 | 5.5913e-01 | 2.472e-02 | | | |
| 24.889 | 1.0040e+00 | 4.280e-02 | 91.086 | 5.5104e-01 | 2.435e-02 | | | |
| 25.919 | 1.0062e+00 | 4.290e-02 | 92.080 | 5.3365e-01 | 2.392e-02 | | | |
| 26.950 | 1.0054e+00 | 4.288e-02 | 93.074 | 5.1455e-01 | 2.317e-02 | | | |
| 27.980 | 1.0109e+00 | 4.311e-02 | 94.074 | 5.0988e-01 | 2.309e-02 | | | |
| 29.010 | 1.0022e+00 | 4.275e-02 | 95.073 | 4.8197e-01 | 2.142e-02 | | | |
| 30.040 | 1.0014e+00 | 4.271e-02 | 96.072 | 4.6990e-01 | 2.122e-02 | | | |
| 31.063 | 9.9445e-01 | 4.246e-02 | 97.043 | 4.6002e-01 | 2.028e-02 | | | |
| 32.087 | 9.8400e-01 | 4.206e-02 | 98.068 | 4.5304e-01 | 2.066e-02 | | | |
| 33.116 | 9.7456e-01 | 4.167e-02 | 99.065 | 4.3126e-01 | 1.975e-02 | | | |
| 34.144 | 9.6188e-01 | 4.117e-02 | 99.469 | 4.3623e-01 | 1.903e-02 | | | |
| 35.172 | 9.6814e-01 | 4.145e-02 | 100.062 | 4.3191e-01 | 1.964e-02 | | | |
| 36.200 | 9.5883e-01 | 4.108e-02 | 101.058 | 4.0182e-01 | 1.831e-02 | | | |
| 37.228 | 9.5707e-01 | 4.103e-02 | 101.959 | 3.9752e-01 | 1.747e-02 | | | |
| 38.255 | 9.6302e-01 | 4.126e-02 | 102.053 | 3.9026e-01 | 1.783e-02 | | | |
| 39.282 | 9.5600e-01 | 4.100e-02 | 104.445 | 3.5795e-01 | 1.576e-02 | | | |
| 40.309 | 9.6099e-01 | 4.118e-02 | 106.927 | 3.3899e-01 | 1.498e-02 | | | |
| 41.341 | 9.5873e-01 | 4.111e-02 | 107.021 | 3.4739e-01 | 1.514e-02 | | | |
| 42.373 | 9.7264e-01 | 4.170e-02 | 109.405 | 3.1539e-01 | 1.390e-02 | | | |
| 43.398 | 9.8073e-01 | 4.205e-02 | 111.880 | 2.9591e-01 | 1.323e-02 | | | |
| 44.424 | 9.9108e-01 | 4.255e-02 | 114.351 | 2.8554e-01 | 1.281e-02 | | | |
| 45.449 | 9.9914e-01 | 4.294e-02 | 116.818 | 2.6990e-01 | 1.218e-02 | | | |
| 46.473 | 9.8981e-01 | 4.245e-02 | 119.282 | 2.6289e-01 | 1.160e-02 | | | |
| 47.497 | 1.0071e+00 | 4.327e-02 | 121.742 | 2.4740e-01 | 1.094e-02 | | | |
| 48.521 | 1.0138e+00 | 4.357e-02 | 124.199 | 2.2456e-01 | 1.000e-02 | | | |
| 49.544 | 1.0199e+00 | 4.380e-02 | 126.652 | 2.1350e-01 | 9.528e-03 | | | |
| 50.567 | 1.0190e+00 | 4.364e-02 | 129.102 | 2.0270e-01 | 9.013e-03 | | | |
| 51.584 | 1.0128e+00 | 4.355e-02 | 131.549 | 1.9053e-01 | 8.488e-03 | | | |
| 52.601 | 1.0082e+00 | 4.359e-02 | 133.992 | 1.7752e-01 | 8.070e-03 | | | |
| 53.622 | 1.0009e+00 | 4.327e-02 | 136.433 | 1.7105e-01 | 7.782e-03 | | | |
| 54.644 | 1.0058e+00 | 4.360e-02 | 138.871 | 1.6829e-01 | 7.394e-03 | | | |
| 55.664 | 1.0129e+00 | 4.399e-02 | 141.305 | 1.5804e-01 | 6.907e-03 | | | |
| 56.685 | 1.0175e+00 | 4.398e-02 | 143.737 | 1.5099e-01 | 6.668e-03 | | | |
| 57.705 | 1.0215e+00 | 4.431e-02 | 146.167 | 1.4613e-01 | 6.408e-03 | | | |
| 58.724 | 1.0052e+00 | 4.363e-02 | 148.594 | 1.4126e-01 | 6.214e-03 | | | |
| 59.743 | 9.9795e-01 | 4.328e-02 | 151.019 | 1.3369e-01 | 5.847e-03 | | | |
| 60.761 | 9.8509e-01 | 4.245e-02 | 153.442 | 1.3189e-01 | 5.874e-03 | | | |
| 61.785 | 9.9162e-01 | 4.265e-02 | 155.863 | 1.2563e-01 | 5.549e-03 | | | |
| 62.808 | 9.9128e-01 | 4.248e-02 | 158.282 | 1.2333e-01 | 5.424e-03 | | | |
| 63.825 | 9.7175e-01 | 4.166e-02 | 160.699 | 1.2413e-01 | 5.694e-03 | | | |
| 64.842 | 9.6891e-01 | 4.157e-02 | 163.115 | 1.2037e-01 | 5.560e-03 | | | |
| 65.858 | 9.5451e-01 | 4.099e-02 | 165.529 | 1.1661e-01 | 5.378e-03 | | | |
| 66.873 | 9.3744e-01 | 4.021e-02 | 167.943 | 1.1157e-01 | 5.170e-03 | | | |
| 67.888 | 9.2501e-01 | 3.979e-02 | 170.355 | 1.1436e-01 | 5.203e-03 | | | |
| 68.903 | 8.9677e-01 | 3.860e-02 | 172.767 | 1.1420e-01 | 5.235e-03 | | | |
| 69.917 | 8.9275e-01 | 3.845e-02 | 175.178 | 1.1175e-01 | 5.176e-03 | | | |
| 70.930 | 8.7853e-01 | 3.792e-02 | 177.589 | 1.1102e-01 | 5.427e-03 | | | |
| 71.937 | 8.5259e-01 | 3.683e-02 | | | | | | |
| 72.944 | 8.2857e-01 | 3.575e-02 | | | | | | |
| 73.956 | 8.0960e-01 | 3.495e-02 | | | | | | |
| 74.967 | 7.9159e-01 | 3.424e-02 | | | | | | |
| 75.978 | 7.8506e-01 | 3.401e-02 | | | | | | |
| 76.988 | 7.7041e-01 | 3.330e-02 | | | | | | |
| 77.998 | 7.5166e-01 | 3.268e-02 | | | | | | |
| 79.007 | 7.3594e-01 | 3.201e-02 | | | | | | |
| 80.015 | 7.2104e-01 | 3.141e-02 | | | | | | |
| 81.023 | 7.0757e-01 | 3.094e-02 | | | | | | |
| 82.036 | 6.8773e-01 | 3.021e-02 | | | | | | |
| 83.048 | 6.5771e-01 | 2.889e-02 | | | | | | |
| 84.054 | 6.5506e-01 | 2.886e-02 | | | | | | |
| 85.059 | 6.3491e-01 | 2.767e-02 | | | | | | |
| 86.064 | 6.2795e-01 | 2.760e-02 | | | | | | |

**Table 13**
$^{116}$Cd($\alpha$,$\alpha$)$^{116}$Cd elastic scattering cross section (normalized to the Rutherford cross section) at the energy $E = 18.80$ MeV. See page 19 for Explanation of Tables

| $\vartheta_{\text{c.m.}}$ (deg) | $\sigma/\sigma_R$ | $\Delta(\sigma/\sigma_R)$ |
|---:|---:|---:|
| 20.764 | 1.0072e+00 | 4.292e-02 |
| 21.796 | 9.9159e-01 | 4.226e-02 |
| 22.827 | 9.8241e-01 | 4.188e-02 |
| 23.858 | 9.6449e-01 | 4.116e-02 |
| 24.889 | 9.7731e-01 | 4.172e-02 |
| 25.919 | 1.0084e+00 | 4.305e-02 |
| 26.950 | 1.0085e+00 | 4.308e-02 |
| 27.980 | 1.0294e+00 | 4.398e-02 |
| 29.010 | 1.0440e+00 | 4.465e-02 |
| 30.040 | 1.0593e+00 | 4.533e-02 |
| 31.063 | 1.0630e+00 | 4.545e-02 |
| 32.087 | 1.0892e+00 | 4.660e-02 |
| 33.116 | 1.1017e+00 | 4.719e-02 |
| 34.144 | 1.1118e+00 | 4.774e-02 |
| 35.172 | 1.1201e+00 | 4.816e-02 |
| 36.200 | 1.1371e+00 | 4.887e-02 |
| 37.228 | 1.1445e+00 | 4.926e-02 |
| 38.255 | 1.1631e+00 | 5.003e-02 |
| 39.282 | 1.1526e+00 | 4.972e-02 |
| 40.309 | 1.1400e+00 | 4.924e-02 |
| 41.341 | 1.1249e+00 | 4.829e-02 |
| 42.373 | 1.1067e+00 | 4.744e-02 |
| 43.398 | 1.0930e+00 | 4.681e-02 |
| 44.424 | 1.0689e+00 | 4.581e-02 |
| 45.449 | 1.0417e+00 | 4.468e-02 |
| 46.473 | 1.0335e+00 | 4.441e-02 |
| 47.497 | 9.9166e-01 | 4.258e-02 |
| 48.521 | 9.6830e-01 | 4.161e-02 |
| 49.544 | 9.4818e-01 | 4.075e-02 |
| 50.567 | 9.2046e-01 | 3.951e-02 |
| 51.584 | 8.8396e-01 | 3.810e-02 |
| 52.601 | 8.6362e-01 | 3.751e-02 |
| 53.622 | 8.2399e-01 | 3.569e-02 |
| 54.644 | 7.8777e-01 | 3.420e-02 |
| 55.664 | 7.6150e-01 | 3.312e-02 |
| 56.685 | 7.5789e-01 | 3.311e-02 |
| 57.705 | 7.1070e-01 | 3.099e-02 |
| 58.724 | 6.7491e-01 | 2.951e-02 |
| 59.743 | 6.5321e-01 | 2.856e-02 |
| 60.761 | 6.2581e-01 | 2.726e-02 |
| 61.785 | 6.0999e-01 | 2.646e-02 |
| 62.808 | 5.8578e-01 | 2.546e-02 |
| 63.825 | 5.6371e-01 | 2.444e-02 |
| 64.842 | 5.2928e-01 | 2.293e-02 |
| 65.858 | 5.1631e-01 | 2.241e-02 |
| 66.873 | 4.9630e-01 | 2.164e-02 |
| 67.888 | 4.8479e-01 | 2.118e-02 |
| 68.903 | 4.6084e-01 | 1.998e-02 |
| 69.917 | 4.2735e-01 | 1.867e-02 |
| 70.930 | 4.0698e-01 | 1.784e-02 |
| 71.937 | 3.9083e-01 | 1.728e-02 |
| 72.944 | 3.7143e-01 | 1.668e-02 |
| 73.956 | 3.6092e-01 | 1.610e-02 |
| 74.967 | 3.3723e-01 | 1.501e-02 |
| 75.978 | 3.3505e-01 | 1.495e-02 |
| 76.988 | 3.0596e-01 | 1.383e-02 |
| 77.998 | 3.0154e-01 | 1.369e-02 |
| 79.007 | 2.8846e-01 | 1.284e-02 |
| 80.015 | 2.7540e-01 | 1.246e-02 |
| 81.023 | 2.6228e-01 | 1.195e-02 |
| 82.036 | 2.4199e-01 | 1.115e-02 |
| 83.048 | 2.3366e-01 | 1.066e-02 |
| 84.054 | 2.2115e-01 | 1.010e-02 |
| 85.059 | 2.1406e-01 | 9.901e-03 |
| 86.064 | 2.0907e-01 | 9.726e-03 |
| 87.068 | 1.9946e-01 | 9.432e-03 |
| 88.071 | 1.8615e-01 | 9.050e-03 |
| 89.071 | 1.7876e-01 | 8.759e-03 |
| 89.874 | 1.7302e-01 | 8.249e-03 |
| 91.086 | 1.6651e-01 | 7.875e-03 |
| 92.080 | 1.5707e-01 | 7.816e-03 |
| 93.074 | 1.4978e-01 | 7.355e-03 |
| 94.074 | 1.4642e-01 | 7.164e-03 |
| 95.073 | 1.4330e-01 | 7.159e-03 |
| 96.072 | 1.3756e-01 | 6.958e-03 |
| 97.070 | 1.2337e-01 | 6.483e-03 |
| 98.068 | 1.2732e-01 | 6.884e-03 |
| 99.065 | 1.1108e-01 | 6.181e-03 |
| 100.062 | 1.1215e-01 | 5.924e-03 |
| 101.058 | 9.9650e-02 | 5.245e-03 |
| 102.053 | 1.0039e-01 | 5.584e-03 |
| 104.550 | 9.6386e-02 | 5.532e-03 |
| 106.979 | 7.9937e-02 | 4.150e-03 |
| 109.510 | 7.2907e-02 | 4.610e-03 |
| 111.880 | 6.6710e-02 | 3.048e-03 |
| 114.445 | 5.9335e-02 | 4.129e-03 |
| 116.849 | 5.4348e-02 | 2.991e-03 |
| 119.329 | 4.4610e-02 | 2.870e-03 |
| 121.742 | 4.1471e-02 | 2.006e-03 |
| 124.199 | 3.9101e-02 | 1.981e-03 |
| 126.652 | 3.6111e-02 | 1.910e-03 |
| 129.102 | 3.0569e-02 | 1.638e-03 |
| 131.549 | 2.9801e-02 | 1.758e-03 |
| 133.992 | 2.4477e-02 | 1.347e-03 |
| 136.433 | 2.5492e-02 | 1.506e-03 |
| 138.871 | 2.7440e-02 | 1.468e-03 |
| 141.305 | 2.5421e-02 | 1.279e-03 |
| 143.737 | 2.3957e-02 | 1.337e-03 |
| 146.167 | 2.0995e-02 | 1.101e-03 |
| 148.594 | 2.2121e-02 | 1.269e-03 |
| 151.019 | 1.9898e-02 | 1.061e-03 |
| 153.442 | 1.7378e-02 | 1.033e-03 |
| 155.863 | 1.6579e-02 | 8.984e-04 |
| 158.282 | 1.6544e-02 | 9.127e-04 |
| 160.699 | 1.6815e-02 | 9.260e-04 |
| 163.115 | 1.6006e-02 | 8.977e-04 |
| 165.529 | 1.6082e-02 | 9.020e-04 |
| 167.943 | 1.6846e-02 | 9.366e-04 |
| 170.355 | 1.5591e-02 | 8.834e-04 |
| 172.767 | 1.4305e-02 | 8.018e-04 |
| 175.178 | 1.3574e-02 | 7.705e-04 |

**Table 14**

$^{112}$Sn($\alpha$,$\alpha$)$^{112}$Sn elastic scattering cross section (normalized to the Rutherford cross section) at the energy $E = 13.90$ MeV. See page 19 for Explanation of Tables

| $\vartheta_{\text{c.m.}}$ (deg) | $\sigma/\sigma_R$ | $\Delta(\sigma/\sigma_R)$ | $\vartheta_{\text{c.m.}}$ (deg) | $\sigma/\sigma_R$ | $\Delta(\sigma/\sigma_R)$ | $\vartheta_{\text{c.m.}}$ (deg) | $\sigma/\sigma_R$ | $\Delta(\sigma/\sigma_R)$ |
|---:|---:|---:|---:|---:|---:|---:|---:|---:|
| 20.892 | 1.0000e+00 | 1.563e-02 | 82.050 | 9.9177e-01 | 1.565e-02 | 132.399 | 7.0151e-01 | 1.083e-02 |
| 21.892 | 9.8908e-01 | 1.545e-02 | 82.052 | 1.0025e+00 | 1.398e-02 | 133.396 | 7.1576e-01 | 1.108e-02 |
| 22.921 | 9.9991e-01 | 1.559e-02 | 83.054 | 1.0096e+00 | 1.597e-02 | 134.334 | 7.0760e-01 | 1.106e-02 |
| 23.984 | 1.0025e+00 | 1.561e-02 | 84.055 | 9.7749e-01 | 1.547e-02 | 134.572 | 7.1015e-01 | 1.424e-02 |
| 24.994 | 9.8886e-01 | 1.543e-02 | 85.067 | 1.0045e+00 | 1.578e-02 | 135.293 | 6.9623e-01 | 1.089e-02 |
| 26.058 | 1.0034e+00 | 1.683e-02 | 86.074 | 9.9044e-01 | 1.575e-02 | 135.594 | 7.0221e-01 | 1.478e-02 |
| 27.045 | 9.9602e-01 | 1.556e-02 | 87.069 | 9.9833e-01 | 1.587e-02 | 136.283 | 7.0071e-01 | 1.066e-02 |
| 28.086 | 9.9342e-01 | 1.552e-02 | 88.062 | 9.7902e-01 | 1.555e-02 | 136.616 | 6.9411e-01 | 1.344e-02 |
| 29.121 | 9.8425e-01 | 1.532e-02 | 89.065 | 9.8480e-01 | 1.573e-02 | 137.236 | 6.9038e-01 | 1.056e-02 |
| 30.171 | 9.9666e-01 | 1.551e-02 | 90.056 | 9.9251e-01 | 1.576e-02 | 137.612 | 6.9061e-01 | 1.342e-02 |
| 31.200 | 1.0028e+00 | 1.357e-02 | 91.055 | 9.7367e-01 | 1.548e-02 | 138.272 | 6.7536e-01 | 1.058e-02 |
| 31.219 | 1.0067e+00 | 1.627e-02 | 92.050 | 9.4878e-01 | 1.505e-02 | 138.523 | 6.8515e-01 | 1.347e-02 |
| 32.200 | 9.9987e-01 | 1.358e-02 | 92.050 | 9.6956e-01 | 1.371e-02 | 139.191 | 6.8609e-01 | 1.070e-02 |
| 33.226 | 1.0081e+00 | 1.370e-02 | 93.046 | 9.7411e-01 | 1.384e-02 | 139.551 | 6.8854e-01 | 1.351e-02 |
| 34.283 | 1.0053e+00 | 1.365e-02 | 94.042 | 9.4440e-01 | 1.343e-02 | 140.167 | 6.7785e-01 | 1.062e-02 |
| 35.291 | 9.9697e-01 | 1.361e-02 | 95.033 | 9.5495e-01 | 1.340e-02 | 140.521 | 6.8194e-01 | 1.343e-02 |
| 36.348 | 1.0055e+00 | 1.506e-02 | 96.021 | 9.4628e-01 | 1.357e-02 | 141.137 | 6.8120e-01 | 1.175e-02 |
| 37.336 | 1.0043e+00 | 1.379e-02 | 97.015 | 9.4515e-01 | 1.356e-02 | 141.154 | 6.6444e-01 | 1.049e-02 |
| 38.372 | 9.9636e-01 | 1.373e-02 | 98.013 | 9.3352e-01 | 1.332e-02 | 141.480 | 6.7517e-01 | 1.333e-02 |
| 39.403 | 9.9393e-01 | 1.370e-02 | 98.993 | 9.3486e-01 | 1.347e-02 | 141.497 | 6.7322e-01 | 1.078e-02 |
| 40.447 | 9.9241e-01 | 1.364e-02 | 100.000 | 9.0972e-01 | 1.302e-02 | 142.104 | 6.7237e-01 | 1.164e-02 |
| 41.489 | 1.0088e+00 | 1.389e-02 | 100.987 | 9.1023e-01 | 1.314e-02 | 142.475 | 6.8807e-01 | 1.103e-02 |
| 41.496 | 1.0060e+00 | 1.544e-02 | 101.967 | 9.0711e-01 | 1.477e-02 | 143.075 | 6.6952e-01 | 1.177e-02 |
| 42.479 | 9.8823e-01 | 1.516e-02 | 101.978 | 8.9320e-01 | 1.287e-02 | 143.448 | 6.7039e-01 | 1.091e-02 |
| 43.499 | 9.7554e-01 | 1.499e-02 | 102.970 | 8.9637e-01 | 1.457e-02 | 144.032 | 6.6552e-01 | 1.172e-02 |
| 44.577 | 1.0008e+00 | 1.541e-02 | 103.948 | 9.0229e-01 | 1.462e-02 | 144.434 | 6.6417e-01 | 1.085e-02 |
| 45.570 | 9.9338e-01 | 1.525e-02 | 104.943 | 8.9430e-01 | 1.464e-02 | 145.029 | 6.8574e-01 | 1.207e-02 |
| 46.586 | 9.9710e-01 | 1.531e-02 | 105.935 | 8.9673e-01 | 1.464e-02 | 145.380 | 6.6738e-01 | 1.094e-02 |
| 47.578 | 9.7511e-01 | 1.498e-02 | 106.922 | 8.9290e-01 | 1.456e-02 | 146.005 | 6.4756e-01 | 1.143e-02 |
| 48.679 | 1.0055e+00 | 1.545e-02 | 107.912 | 8.7817e-01 | 1.442e-02 | 146.345 | 6.5535e-01 | 1.071e-02 |
| 49.658 | 9.8411e-01 | 1.513e-02 | 108.876 | 8.6437e-01 | 1.424e-02 | 146.937 | 6.5105e-01 | 1.137e-02 |
| 50.724 | 1.0161e+00 | 1.575e-02 | 109.861 | 8.5013e-01 | 1.406e-02 | 147.354 | 6.5013e-01 | 1.054e-02 |
| 51.720 | 9.9796e-01 | 1.340e-02 | 110.829 | 8.5794e-01 | 1.422e-02 | 147.940 | 6.4440e-01 | 1.150e-02 |
| 51.725 | 9.9495e-01 | 1.545e-02 | 111.825 | 8.3592e-01 | 1.241e-02 | 148.292 | 6.4734e-01 | 1.073e-02 |
| 52.705 | 9.6890e-01 | 1.300e-02 | 111.826 | 8.3773e-01 | 1.391e-02 | 148.869 | 6.4038e-01 | 1.145e-02 |
| 53.721 | 9.6817e-01 | 1.304e-02 | 112.835 | 8.3187e-01 | 1.231e-02 | 149.303 | 6.4963e-01 | 1.077e-02 |
| 54.784 | 9.9599e-01 | 1.344e-02 | 113.798 | 8.1278e-01 | 1.204e-02 | 149.877 | 6.4552e-01 | 1.158e-02 |
| 55.777 | 9.8229e-01 | 1.323e-02 | 114.793 | 8.3587e-01 | 1.248e-02 | 150.234 | 6.4495e-01 | 1.073e-02 |
| 56.789 | 9.8476e-01 | 1.327e-02 | 115.783 | 8.2659e-01 | 1.237e-02 | 150.822 | 6.3406e-01 | 1.003e-02 |
| 57.782 | 9.7734e-01 | 1.318e-02 | 116.764 | 8.1927e-01 | 1.216e-02 | 150.874 | 6.2724e-01 | 1.129e-02 |
| 58.862 | 9.8862e-01 | 1.334e-02 | 117.751 | 7.9380e-01 | 1.193e-02 | 151.175 | 6.4515e-01 | 1.071e-02 |
| 59.844 | 9.8066e-01 | 1.325e-02 | 118.697 | 8.0560e-01 | 1.212e-02 | 151.212 | 6.3333e-01 | 9.500e-03 |
| 60.895 | 1.0169e+00 | 1.402e-02 | 119.676 | 7.9311e-01 | 1.200e-02 | 151.227 | 6.3413e-01 | 1.256e-02 |
| 61.852 | 9.9511e-01 | 1.540e-02 | 120.631 | 7.8075e-01 | 1.187e-02 | 151.785 | 6.3584e-01 | 1.007e-02 |
| 61.895 | 9.9797e-01 | 1.380e-02 | 121.630 | 7.8101e-01 | 1.187e-02 | 151.810 | 6.2502e-01 | 1.108e-02 |
| 62.854 | 9.8610e-01 | 1.525e-02 | 121.641 | 7.7423e-01 | 1.302e-02 | 152.176 | 6.3198e-01 | 1.038e-02 |
| 63.857 | 9.8774e-01 | 1.531e-02 | 122.640 | 7.6397e-01 | 1.287e-02 | 152.201 | 6.4858e-01 | 1.284e-02 |
| 64.877 | 9.8839e-01 | 1.534e-02 | 123.637 | 7.6924e-01 | 1.297e-02 | 152.249 | 6.1835e-01 | 9.430e-03 |
| 65.893 | 9.8256e-01 | 1.526e-02 | 124.587 | 7.6597e-01 | 1.299e-02 | 152.753 | 6.2492e-01 | 1.008e-02 |
| 66.949 | 1.0086e+00 | 1.565e-02 | 124.778 | 7.6190e-01 | 1.231e-02 | 153.170 | 6.2233e-01 | 1.249e-02 |
| 67.965 | 1.0114e+00 | 1.573e-02 | 125.553 | 7.6249e-01 | 1.294e-02 | 153.174 | 6.2535e-01 | 9.220e-03 |
| 68.931 | 9.9184e-01 | 1.543e-02 | 125.796 | 7.6544e-01 | 1.310e-02 | 153.706 | 6.3207e-01 | 1.022e-02 |
| 69.989 | 1.0018e+00 | 1.560e-02 | 126.543 | 7.5703e-01 | 1.262e-02 | 154.152 | 6.2717e-01 | 9.280e-03 |
| 70.970 | 1.0176e+00 | 1.584e-02 | 126.815 | 7.5093e-01 | 1.160e-02 | 154.154 | 6.2877e-01 | 1.263e-02 |
| 71.979 | 1.0070e+00 | 1.379e-02 | 127.504 | 7.4390e-01 | 1.247e-02 | 154.704 | 6.3452e-01 | 1.032e-02 |
| 71.993 | 1.0184e+00 | 1.592e-02 | 127.812 | 7.4070e-01 | 1.149e-02 | 155.092 | 6.1792e-01 | 1.247e-02 |
| 72.979 | 1.0096e+00 | 1.380e-02 | 128.533 | 7.2390e-01 | 1.234e-02 | 155.144 | 6.0416e-01 | 8.980e-03 |
| 73.980 | 9.9514e-01 | 1.366e-02 | 128.740 | 7.3307e-01 | 1.156e-02 | 155.678 | 6.1661e-01 | 1.000e-02 |
| 74.993 | 9.9932e-01 | 1.375e-02 | 129.465 | 7.3486e-01 | 1.250e-02 | 156.053 | 6.2119e-01 | 1.247e-02 |
| 76.002 | 1.0067e+00 | 1.385e-02 | 129.765 | 7.3204e-01 | 1.154e-02 | 156.099 | 6.2210e-01 | 9.260e-03 |
| 77.035 | 1.0046e+00 | 1.381e-02 | 130.445 | 7.3919e-01 | 1.258e-02 | 156.604 | 6.1319e-01 | 9.800e-03 |
| 78.043 | 9.9806e-01 | 1.379e-02 | 130.741 | 7.3116e-01 | 1.155e-02 | 157.001 | 6.3420e-01 | 9.490e-03 |
| 79.022 | 9.8401e-01 | 1.360e-02 | 131.398 | 7.2548e-01 | 1.118e-02 | 157.062 | 6.2174e-01 | 1.238e-02 |
| 80.054 | 9.9669e-01 | 1.380e-02 | 131.433 | 7.3259e-01 | 1.252e-02 | 157.608 | 6.1851e-01 | 1.015e-02 |
| 81.042 | 1.0012e+00 | 1.386e-02 | 131.707 | 7.2321e-01 | 1.148e-02 | 157.939 | 6.0549e-01 | 9.130e-03 |

**Table 14** (continued)

| $\vartheta_{\text{c.m.}}$ (deg) | $\sigma/\sigma_R$ | $\Delta(\sigma/\sigma_R)$ | $\vartheta_{\text{c.m.}}$ (deg) | $\sigma/\sigma_R$ | $\Delta(\sigma/\sigma_R)$ | $\vartheta_{\text{c.m.}}$ (deg) | $\sigma/\sigma_R$ | $\Delta(\sigma/\sigma_R)$ |
|---|---|---|---|---|---|---|---|---|
| 157.993 | 6.2314e-01 | 1.260e-02 | | | | | | |
| 158.531 | 6.1439e-01 | 1.013e-02 | | | | | | |
| 158.905 | 6.1730e-01 | 9.300e-03 | | | | | | |
| 159.004 | 6.1945e-01 | 1.254e-02 | | | | | | |
| 159.540 | 6.1779e-01 | 1.018e-02 | | | | | | |
| 159.903 | 6.1067e-01 | 9.310e-03 | | | | | | |
| 159.928 | 6.0559e-01 | 1.233e-02 | | | | | | |
| 160.483 | 6.0987e-01 | 1.107e-02 | | | | | | |
| 160.537 | 6.0153e-01 | 9.940e-03 | | | | | | |
| 160.864 | 6.1568e-01 | 1.249e-02 | | | | | | |
| 160.904 | 6.0672e-01 | 1.141e-02 | | | | | | |
| 160.914 | 6.1492e-01 | 1.013e-02 | | | | | | |
| 160.918 | 6.0040e-01 | 1.014e-02 | | | | | | |
| 161.476 | 5.9917e-01 | 1.080e-02 | | | | | | |
| 161.858 | 6.0441e-01 | 1.008e-02 | | | | | | |
| 161.864 | 6.1360e-01 | 1.229e-02 | | | | | | |
| 161.942 | 5.9866e-01 | 1.138e-02 | | | | | | |
| 162.428 | 6.2162e-01 | 1.126e-02 | | | | | | |
| 162.837 | 6.1121e-01 | 1.030e-02 | | | | | | |
| 162.860 | 5.9879e-01 | 1.112e-02 | | | | | | |
| 163.393 | 6.0759e-01 | 1.052e-02 | | | | | | |
| 163.805 | 6.0774e-01 | 9.750e-03 | | | | | | |
| 163.836 | 6.0155e-01 | 1.119e-02 | | | | | | |
| 164.342 | 6.0256e-01 | 1.055e-02 | | | | | | |
| 164.786 | 6.0118e-01 | 9.780e-03 | | | | | | |
| 164.827 | 5.7799e-01 | 1.079e-02 | | | | | | |
| 165.778 | 6.0103e-01 | 1.123e-02 | | | | | | |
| 166.673 | 6.0974e-01 | 1.144e-02 | | | | | | |
| 167.607 | 5.8933e-01 | 1.110e-02 | | | | | | |
| 168.570 | 6.0029e-01 | 1.129e-02 | | | | | | |
| 169.568 | 5.8848e-01 | 1.117e-02 | | | | | | |
| 170.128 | 6.0288e-01 | 9.950e-03 | | | | | | |
| 170.578 | 5.9434e-01 | 1.191e-02 | | | | | | |
| 170.582 | 6.0564e-01 | 1.230e-02 | | | | | | |
| 171.121 | 5.8586e-01 | 9.610e-03 | | | | | | |
| 171.519 | 5.9078e-01 | 1.194e-02 | | | | | | |
| 172.072 | 5.9372e-01 | 9.830e-03 | | | | | | |
| 172.497 | 5.9238e-01 | 1.205e-02 | | | | | | |
| 173.036 | 5.9254e-01 | 9.250e-03 | | | | | | |
| 173.462 | 5.9345e-01 | 1.166e-02 | | | | | | |
| 173.984 | 5.8776e-01 | 9.320e-03 | | | | | | |
| 174.443 | 5.9358e-01 | 1.176e-02 | | | | | | |

**Table 15**

$^{112}$Sn($\alpha$,$\alpha$)$^{112}$Sn elastic scattering cross section (normalized to the Rutherford cross section) at the energy $E = 18.84$ MeV. See page 19 for Explanation of Tables

| $\vartheta_{\text{c.m.}}$ (deg) | $\sigma/\sigma_R$ | $\Delta(\sigma/\sigma_R)$ |
|---|---|---|
| 20.837 | 1.0084e+00 | 1.457e-02 |
| 21.834 | 1.0018e+00 | 1.440e-02 |
| 22.872 | 9.9926e-01 | 1.435e-02 |
| 23.901 | 9.7235e-01 | 1.393e-02 |
| 24.937 | 9.9452e-01 | 1.422e-02 |
| 25.913 | 9.7006e-01 | 1.383e-02 |
| 26.983 | 9.5455e-01 | 1.358e-02 |
| 28.015 | 9.5034e-01 | 1.355e-02 |
| 29.068 | 9.6082e-01 | 1.366e-02 |
| 30.129 | 9.7290e-01 | 1.384e-02 |
| 31.104 | 9.8540e-01 | 1.396e-02 |
| 31.150 | 9.9420e-01 | 1.339e-02 |
| 32.147 | 9.8944e-01 | 1.331e-02 |
| 33.181 | 1.0022e+00 | 1.349e-02 |
| 34.207 | 1.0145e+00 | 1.367e-02 |
| 35.239 | 1.0411e+00 | 1.401e-02 |
| 36.218 | 1.0315e+00 | 1.387e-02 |
| 37.280 | 1.0586e+00 | 1.422e-02 |
| 38.309 | 1.0729e+00 | 1.444e-02 |
| 39.356 | 1.0917e+00 | 1.469e-02 |
| 40.410 | 1.1057e+00 | 1.495e-02 |
| 41.387 | 1.1047e+00 | 1.481e-02 |
| 41.430 | 1.1041e+00 | 1.567e-02 |
| 42.460 | 1.1146e+00 | 1.583e-02 |
| 43.383 | 1.0891e+00 | 1.547e-02 |
| 44.460 | 1.0887e+00 | 1.545e-02 |
| 45.447 | 1.0852e+00 | 1.541e-02 |
| 46.511 | 1.0746e+00 | 1.526e-02 |
| 47.518 | 1.0759e+00 | 1.531e-02 |
| 48.565 | 1.0490e+00 | 1.492e-02 |
| 49.582 | 1.0283e+00 | 1.466e-02 |
| 50.573 | 1.0192e+00 | 1.446e-02 |
| 51.604 | 1.0135e+00 | 1.436e-02 |
| 51.664 | 1.0093e+00 | 1.374e-02 |
| 52.688 | 9.9158e-01 | 1.356e-02 |
| 53.625 | 9.6092e-01 | 1.314e-02 |
| 54.688 | 9.3924e-01 | 1.283e-02 |
| 55.677 | 9.1345e-01 | 1.250e-02 |
| 56.729 | 8.8815e-01 | 1.216e-02 |
| 57.734 | 8.6600e-01 | 1.194e-02 |
| 58.772 | 8.4015e-01 | 1.156e-02 |
| 59.785 | 8.0479e-01 | 1.115e-02 |
| 60.777 | 7.8853e-01 | 1.080e-02 |
| 61.801 | 7.6513e-01 | 1.046e-02 |
| 61.803 | 7.6843e-01 | 1.101e-02 |
| 62.833 | 7.4119e-01 | 1.060e-02 |
| 63.838 | 7.0688e-01 | 1.015e-02 |
| 64.878 | 6.8666e-01 | 9.820e-03 |
| 65.888 | 6.6116e-01 | 9.460e-03 |
| 66.890 | 6.3702e-01 | 9.120e-03 |
| 67.892 | 6.1850e-01 | 8.910e-03 |
| 68.920 | 5.9948e-01 | 8.570e-03 |
| 69.928 | 5.7347e-01 | 8.230e-03 |
| 70.947 | 5.5575e-01 | 8.030e-03 |
| 71.945 | 5.3773e-01 | 7.560e-03 |
| 71.950 | 5.3319e-01 | 7.780e-03 |
| 71.999 | 5.3171e-01 | 7.900e-03 |
| 72.965 | 5.2353e-01 | 7.320e-03 |
| 73.968 | 4.9317e-01 | 6.970e-03 |
| 74.993 | 4.7607e-01 | 6.670e-03 |
| 75.999 | 4.5739e-01 | 6.420e-03 |
| 77.000 | 4.4419e-01 | 6.230e-03 |
| 78.000 | 4.2276e-01 | 6.030e-03 |
| 79.016 | 4.1023e-01 | 5.740e-03 |
| 80.020 | 3.9289e-01 | 5.550e-03 |
| 80.969 | 3.7159e-01 | 5.780e-03 |
| 81.030 | 3.7843e-01 | 5.420e-03 |
| 81.981 | 3.5955e-01 | 5.640e-03 |
| 82.031 | 3.6386e-01 | 5.320e-03 |
| 82.040 | 3.7327e-01 | 5.520e-03 |
| 82.056 | 3.7003e-01 | 5.630e-03 |
| 82.057 | 3.6668e-01 | 5.840e-03 |
| 83.041 | 3.5371e-01 | 5.290e-03 |
| 84.047 | 3.4122e-01 | 5.120e-03 |
| 85.018 | 3.3771e-01 | 5.110e-03 |
| 86.050 | 3.1123e-01 | 4.750e-03 |
| 87.053 | 3.0430e-01 | 4.670e-03 |
| 88.053 | 2.8711e-01 | 4.400e-03 |
| 89.053 | 2.7945e-01 | 4.240e-03 |
| 90.052 | 2.7114e-01 | 4.150e-03 |
| 91.052 | 2.6216e-01 | 3.930e-03 |
| 92.050 | 2.4948e-01 | 4.290e-03 |
| 92.050 | 2.5000e-01 | 3.830e-03 |
| 92.050 | 2.5150e-01 | 3.760e-03 |
| 93.047 | 2.4228e-01 | 3.700e-03 |
| 94.044 | 2.3642e-01 | 3.620e-03 |
| 95.054 | 2.3451e-01 | 3.650e-03 |
| 96.037 | 2.2006e-01 | 3.470e-03 |
| 97.031 | 2.1327e-01 | 3.400e-03 |
| 98.027 | 2.0655e-01 | 3.240e-03 |
| 99.021 | 1.9485e-01 | 3.040e-03 |
| 100.015 | 1.8839e-01 | 2.990e-03 |
| 101.005 | 1.8020e-01 | 2.750e-03 |
| 102.002 | 1.7491e-01 | 2.770e-03 |
| 102.002 | 1.7231e-01 | 2.720e-03 |
| 103.488 | 1.6106e-01 | 2.570e-03 |
| 104.973 | 1.5512e-01 | 2.470e-03 |
| 106.460 | 1.4639e-01 | 2.350e-03 |
| 107.937 | 1.3935e-01 | 2.240e-03 |
| 109.411 | 1.3123e-01 | 2.130e-03 |
| 110.894 | 1.2664e-01 | 2.050e-03 |
| 111.895 | 1.2495e-01 | 2.050e-03 |
| 112.378 | 1.1998e-01 | 1.980e-03 |
| 113.369 | 1.1683e-01 | 1.940e-03 |
| 113.857 | 1.1675e-01 | 1.950e-03 |
| 114.845 | 1.1194e-01 | 1.860e-03 |
| 115.337 | 1.1217e-01 | 1.920e-03 |
| 116.325 | 1.0444e-01 | 1.750e-03 |
| 116.809 | 1.0519e-01 | 1.800e-03 |
| 117.789 | 1.0456e-01 | 1.750e-03 |
| 119.252 | 9.7540e-02 | 1.650e-03 |
| 120.728 | 9.3680e-02 | 1.600e-03 |
| 122.206 | 9.0650e-02 | 1.560e-03 |
| 123.677 | 8.7420e-02 | 1.540e-03 |
| 125.150 | 8.2470e-02 | 1.500e-03 |
| 126.613 | 8.1080e-02 | 1.450e-03 |
| 126.739 | 8.1160e-02 | 1.410e-03 |
| 128.208 | 7.8530e-02 | 1.540e-03 |
| 129.680 | 7.5100e-02 | 1.470e-03 |
| 131.143 | 6.9990e-02 | 1.380e-03 |
| 132.625 | 6.8980e-02 | 1.360e-03 |
| 134.107 | 6.6790e-02 | 1.320e-03 |
| 135.566 | 6.3940e-02 | 1.290e-03 |
| 136.523 | 6.2090e-02 | 1.460e-03 |
| 137.020 | 6.1200e-02 | 1.240e-03 |
| 137.984 | 5.9410e-02 | 1.550e-03 |
| 138.481 | 6.0670e-02 | 1.250e-03 |
| 139.449 | 5.8360e-02 | 1.510e-03 |
| 139.937 | 5.6490e-02 | 1.220e-03 |
| 140.904 | 5.5990e-02 | 1.460e-03 |
| 141.404 | 5.5760e-02 | 1.180e-03 |
| 142.382 | 5.5590e-02 | 1.440e-03 |
| 143.859 | 5.2830e-02 | 1.380e-03 |
| 145.311 | 5.3560e-02 | 1.380e-03 |
| 146.757 | 5.1960e-02 | 1.350e-03 |
| 148.212 | 4.9170e-02 | 1.310e-03 |
| 149.660 | 5.0380e-02 | 1.360e-03 |
| 150.934 | 4.6900e-02 | 1.030e-03 |
| 151.122 | 4.8440e-02 | 1.290e-03 |
| 152.860 | 4.7660e-02 | 1.030e-03 |
| 154.988 | 4.5910e-02 | 8.961e-04 |
| 156.913 | 4.5820e-02 | 7.743e-04 |
| 158.840 | 4.2610e-02 | 8.075e-04 |
| 158.874 | 4.3750e-02 | 9.496e-04 |
| 160.602 | 4.1660e-02 | 9.476e-04 |
| 160.775 | 4.2880e-02 | 8.421e-04 |
| 162.524 | 4.0580e-02 | 9.068e-04 |
| 164.661 | 4.0220e-02 | 9.993e-04 |
| 166.580 | 4.0360e-02 | 9.137e-04 |
| 168.502 | 3.9430e-02 | 9.431e-04 |
| 168.538 | 3.8440e-02 | 1.030e-03 |
| 170.434 | 3.8780e-02 | 9.552e-04 |

**Table 16**

$^{124}$Sn($\alpha$,$\alpha$)$^{124}$Sn elastic scattering cross section (normalized to the Rutherford cross section) at the energy $E = 18.90$ MeV. See page 19 for Explanation of Tables

| $\vartheta_{\text{c.m.}}$ (deg) | $\sigma/\sigma_R$ | $\Delta(\sigma/\sigma_R)$ | $\vartheta_{\text{c.m.}}$ (deg) | $\sigma/\sigma_R$ | $\Delta(\sigma/\sigma_R)$ | $\vartheta_{\text{c.m.}}$ (deg) | $\sigma/\sigma_R$ | $\Delta(\sigma/\sigma_R)$ |
|---|---|---|---|---|---|---|---|---|
| 20.755 | 9.9945e-01 | 1.400e-02 | 77.834 | 3.7342e-01 | 5.390e-03 | 143.739 | 3.9730e-02 | 1.370e-03 |
| 21.806 | 9.9851e-01 | 1.395e-02 | 78.837 | 3.5055e-01 | 5.060e-03 | 145.193 | 3.7720e-02 | 1.310e-03 |
| 22.781 | 9.6804e-01 | 1.350e-02 | 79.844 | 3.3508e-01 | 4.780e-03 | 146.657 | 3.7890e-02 | 1.340e-03 |
| 23.877 | 9.9293e-01 | 1.382e-02 | 80.843 | 3.2126e-01 | 4.620e-03 | 148.113 | 3.4900e-02 | 1.250e-03 |
| 23.913 | 9.9293e-01 | 1.384e-02 | 81.844 | 3.0653e-01 | 4.490e-03 | 149.580 | 3.5640e-02 | 1.240e-03 |
| 24.854 | 9.4869e-01 | 1.319e-02 | 81.845 | 3.0476e-01 | 4.480e-03 | 151.037 | 3.5070e-02 | 1.240e-03 |
| 24.904 | 9.6870e-01 | 1.346e-02 | 82.846 | 2.9317e-01 | 4.320e-03 | 152.983 | 3.2820e-02 | 7.305e-04 |
| 25.874 | 9.6135e-01 | 1.333e-02 | 83.851 | 2.8308e-01 | 4.190e-03 | 154.920 | 3.2370e-02 | 6.963e-04 |
| 25.944 | 9.5557e-01 | 1.326e-02 | 84.853 | 2.7100e-01 | 4.040e-03 | 156.884 | 3.2310e-02 | 6.496e-04 |
| 26.895 | 9.6440e-01 | 1.334e-02 | 85.854 | 2.6119e-01 | 3.900e-03 | 158.806 | 3.1270e-02 | 7.310e-04 |
| 26.948 | 9.7871e-01 | 1.358e-02 | 86.856 | 2.4926e-01 | 3.760e-03 | 160.763 | 2.7020e-02 | 8.030e-04 |
| 27.892 | 9.4872e-01 | 1.312e-02 | 87.856 | 2.3741e-01 | 3.600e-03 | 162.694 | 3.1150e-02 | 1.060e-03 |
| 29.005 | 9.7004e-01 | 1.340e-02 | 88.855 | 2.2898e-01 | 3.470e-03 | 164.626 | 2.8960e-02 | 9.606e-04 |
| 30.123 | 9.7763e-01 | 1.350e-02 | 89.855 | 2.2112e-01 | 3.370e-03 | 166.586 | 2.8910e-02 | 9.642e-04 |
| 31.038 | 9.9148e-01 | 1.340e-02 | 90.853 | 2.1521e-01 | 3.280e-03 | 168.503 | 2.9150e-02 | 9.958e-04 |
| 31.108 | 1.0152e+00 | 1.401e-02 | 91.851 | 2.0359e-01 | 3.050e-03 | 170.457 | 2.9160e-02 | 1.110e-03 |
| 32.084 | 1.0115e+00 | 1.365e-02 | 91.851 | 2.0438e-01 | 3.180e-03 | | | |
| 33.061 | 1.0056e+00 | 1.358e-02 | 92.849 | 1.9734e-01 | 3.080e-03 | | | |
| 34.181 | 1.0653e+00 | 1.440e-02 | 93.845 | 1.8980e-01 | 2.990e-03 | | | |
| 35.127 | 1.0563e+00 | 1.426e-02 | 94.842 | 1.8442e-01 | 2.940e-03 | | | |
| 36.208 | 1.0759e+00 | 1.452e-02 | 95.838 | 1.7326e-01 | 2.770e-03 | | | |
| 37.211 | 1.0922e+00 | 1.476e-02 | 96.832 | 1.6850e-01 | 2.730e-03 | | | |
| 38.160 | 1.1012e+00 | 1.482e-02 | 97.826 | 1.6293e-01 | 2.660e-03 | | | |
| 39.260 | 1.1160e+00 | 1.502e-02 | 98.823 | 1.5534e-01 | 2.530e-03 | | | |
| 40.364 | 1.1295e+00 | 1.522e-02 | 99.813 | 1.4970e-01 | 2.470e-03 | | | |
| 41.309 | 1.1033e+00 | 1.522e-02 | 100.808 | 1.4213e-01 | 2.330e-03 | | | |
| 41.350 | 1.1425e+00 | 1.540e-02 | 101.799 | 1.3700e-01 | 2.190e-03 | | | |
| 42.334 | 1.1111e+00 | 1.531e-02 | 101.805 | 1.3797e-01 | 2.290e-03 | | | |
| 43.366 | 1.1156e+00 | 1.543e-02 | 103.294 | 1.2892e-01 | 2.160e-03 | | | |
| 44.409 | 1.0986e+00 | 1.520e-02 | 104.777 | 1.2147e-01 | 2.040e-03 | | | |
| 45.265 | 1.0907e+00 | 1.511e-02 | 106.259 | 1.1662e-01 | 1.950e-03 | | | |
| 46.365 | 1.0672e+00 | 1.479e-02 | 107.739 | 1.1202e-01 | 1.880e-03 | | | |
| 47.456 | 1.0570e+00 | 1.466e-02 | 109.222 | 1.0513e-01 | 1.740e-03 | | | |
| 48.435 | 1.0293e+00 | 1.429e-02 | 110.707 | 1.0014e-01 | 1.690e-03 | | | |
| 49.471 | 1.0222e+00 | 1.413e-02 | 111.704 | 9.8150e-02 | 1.800e-03 | | | |
| 50.507 | 9.8458e-01 | 1.365e-02 | 112.187 | 9.5250e-02 | 1.660e-03 | | | |
| 51.479 | 9.7528e-01 | 1.351e-02 | 113.187 | 9.1400e-02 | 1.690e-03 | | | |
| 51.518 | 9.6952e-01 | 1.323e-02 | 113.668 | 8.9630e-02 | 1.570e-03 | | | |
| 52.538 | 9.5667e-01 | 1.304e-02 | 114.658 | 9.0380e-02 | 1.660e-03 | | | |
| 53.564 | 9.3857e-01 | 1.291e-02 | 115.144 | 8.7070e-02 | 1.510e-03 | | | |
| 54.598 | 9.0675e-01 | 1.251e-02 | 116.131 | 8.2920e-02 | 1.530e-03 | | | |
| 55.481 | 8.8734e-01 | 1.228e-02 | 116.622 | 8.0780e-02 | 1.440e-03 | | | |
| 56.561 | 8.5015e-01 | 1.178e-02 | 117.599 | 8.0780e-02 | 1.490e-03 | | | |
| 57.634 | 8.1912e-01 | 1.139e-02 | 119.076 | 7.4960e-02 | 1.360e-03 | | | |
| 58.617 | 7.7317e-01 | 1.079e-02 | 120.555 | 7.2810e-02 | 1.350e-03 | | | |
| 59.645 | 7.6029e-01 | 1.050e-02 | 122.027 | 6.9410e-02 | 1.340e-03 | | | |
| 60.673 | 7.2010e-01 | 1.002e-02 | 123.502 | 6.5360e-02 | 1.260e-03 | | | |
| 61.650 | 6.9886e-01 | 9.720e-03 | 124.969 | 6.2280e-02 | 1.200e-03 | | | |
| 61.658 | 6.9951e-01 | 9.780e-03 | 126.441 | 5.9140e-02 | 1.170e-03 | | | |
| 62.689 | 6.6987e-01 | 9.360e-03 | 126.575 | 5.9280e-02 | 1.390e-03 | | | |
| 63.699 | 6.4485e-01 | 9.050e-03 | 128.045 | 5.5800e-02 | 1.320e-03 | | | |
| 64.696 | 6.2730e-01 | 8.790e-03 | 129.529 | 5.5110e-02 | 1.260e-03 | | | |
| 65.737 | 5.9897e-01 | 8.430e-03 | 131.010 | 5.3700e-02 | 1.220e-03 | | | |
| 66.747 | 5.7452e-01 | 8.100e-03 | 132.493 | 5.0720e-02 | 1.160e-03 | | | |
| 67.755 | 5.5623e-01 | 7.840e-03 | 133.960 | 5.0030e-02 | 1.100e-03 | | | |
| 68.761 | 5.3432e-01 | 7.520e-03 | 135.422 | 4.8630e-02 | 1.080e-03 | | | |
| 69.777 | 5.1308e-01 | 7.180e-03 | 136.381 | 4.7800e-02 | 1.700e-03 | | | |
| 70.778 | 4.9470e-01 | 6.950e-03 | 136.892 | 4.7130e-02 | 1.100e-03 | | | |
| 71.777 | 4.6825e-01 | 6.680e-03 | 137.844 | 4.6750e-02 | 1.670e-03 | | | |
| 71.780 | 4.7327e-01 | 6.710e-03 | 138.354 | 4.5830e-02 | 1.060e-03 | | | |
| 72.797 | 4.5005e-01 | 6.400e-03 | 139.323 | 4.3940e-02 | 1.560e-03 | | | |
| 73.803 | 4.4106e-01 | 6.320e-03 | 139.826 | 4.4620e-02 | 1.020e-03 | | | |
| 74.800 | 4.2268e-01 | 6.040e-03 | 140.799 | 4.4510e-02 | 1.560e-03 | | | |
| 75.825 | 4.0303e-01 | 5.810e-03 | 141.289 | 4.3320e-02 | 1.010e-03 | | | |
| 76.830 | 3.8138e-01 | 5.520e-03 | 142.278 | 4.0570e-02 | 1.430e-03 | | | |

**Table 17**

$^{144}$Sm($\alpha$,$\alpha$)$^{144}$Sm elastic scattering cross section (normalized to the Rutherford cross section) at the energy $E = 19.45$ MeV. See page 19 for Explanation of Tables

| $\vartheta_{\text{c.m.}}$ (deg) | $\sigma/\sigma_R$ | $\Delta(\sigma/\sigma_R)$ |
|---:|---:|---:|
| 15.023 | 9.9443e-01 | 1.136e-02 |
| 16.050 | 1.0003e+00 | 1.137e-02 |
| 17.076 | 9.9475e-01 | 1.145e-02 |
| 18.103 | 9.9632e-01 | 1.148e-02 |
| 19.129 | 1.0040e+00 | 1.137e-02 |
| 20.156 | 1.0128e+00 | 1.100e-02 |
| 21.182 | 1.0036e+00 | 1.037e-02 |
| 22.208 | 9.9883e-01 | 1.032e-02 |
| 23.233 | 9.9291e-01 | 1.027e-02 |
| 24.259 | 1.0037e+00 | 1.025e-02 |
| 25.284 | 9.9131e-01 | 1.021e-02 |
| 26.309 | 1.0053e+00 | 1.034e-02 |
| 27.334 | 1.0085e+00 | 1.055e-02 |
| 28.359 | 1.0027e+00 | 1.029e-02 |
| 29.384 | 1.0066e+00 | 1.050e-02 |
| 30.408 | 1.0198e+00 | 1.507e-02 |
| 31.432 | 1.0206e+00 | 1.076e-02 |
| 32.456 | 1.0133e+00 | 1.070e-02 |
| 33.480 | 1.0101e+00 | 1.070e-02 |
| 34.503 | 1.0028e+00 | 1.041e-02 |
| 35.526 | 9.9627e-01 | 1.052e-02 |
| 36.549 | 9.9647e-01 | 1.050e-02 |
| 37.571 | 9.8968e-01 | 1.078e-02 |
| 38.593 | 9.7495e-01 | 1.026e-02 |
| 39.615 | 9.6950e-01 | 1.053e-02 |
| 40.637 | 9.6466e-01 | 9.774e-03 |
| 41.658 | 9.7528e-01 | 9.890e-03 |
| 42.679 | 9.7642e-01 | 9.888e-03 |
| 43.700 | 9.8185e-01 | 9.900e-03 |
| 44.720 | 9.9564e-01 | 1.074e-02 |
| 45.740 | 9.9389e-01 | 1.079e-02 |
| 46.760 | 1.0090e+00 | 1.032e-02 |
| 47.779 | 1.0311e+00 | 1.071e-02 |
| 48.798 | 1.0241e+00 | 1.043e-02 |
| 49.816 | 1.0356e+00 | 1.062e-02 |
| 50.834 | 1.0309e+00 | 1.492e-02 |
| 51.852 | 1.0264e+00 | 1.054e-02 |
| 52.870 | 1.0372e+00 | 1.062e-02 |
| 53.887 | 1.0473e+00 | 1.063e-02 |
| 54.904 | 1.0615e+00 | 1.211e-02 |
| 55.920 | 1.0585e+00 | 1.219e-02 |
| 56.936 | 1.0729e+00 | 1.117e-02 |
| 57.951 | 1.0859e+00 | 1.161e-02 |
| 58.966 | 1.0707e+00 | 1.106e-02 |
| 59.981 | 1.0765e+00 | 1.126e-02 |
| 60.995 | 1.0784e+00 | 1.244e-02 |
| 62.009 | 1.0856e+00 | 1.107e-02 |
| 63.023 | 1.0811e+00 | 1.110e-02 |
| 64.036 | 1.0562e+00 | 1.089e-02 |
| 65.048 | 1.0508e+00 | 1.067e-02 |
| 66.060 | 1.0530e+00 | 1.090e-02 |
| 67.072 | 1.0813e+00 | 1.139e-02 |
| 68.083 | 1.0539e+00 | 1.114e-02 |
| 69.094 | 1.0510e+00 | 1.115e-02 |
| 70.105 | 1.0272e+00 | 1.085e-02 |
| 71.114 | 9.9017e-01 | 1.971e-02 |
| 72.124 | 9.5337e-01 | 9.888e-03 |
| 73.133 | 9.7721e-01 | 1.027e-02 |
| 74.141 | 9.3970e-01 | 9.940e-03 |
| 75.150 | 9.0827e-01 | 9.355e-03 |
| 76.157 | 9.0651e-01 | 9.656e-03 |
| 77.164 | 9.4688e-01 | 1.041e-02 |
| 78.171 | 9.0078e-01 | 9.967e-03 |
| 79.177 | 8.8001e-01 | 9.813e-03 |
| 80.183 | 8.7745e-01 | 9.689e-03 |
| 81.188 | 8.2501e-01 | 1.129e-02 |
| 82.193 | 8.0272e-01 | 8.556e-03 |
| 83.197 | 7.8205e-01 | 8.455e-03 |
| 84.201 | 7.7795e-01 | 8.465e-03 |
| 85.204 | 7.5133e-01 | 8.211e-03 |
| 86.207 | 7.3524e-01 | 7.913e-03 |
| 87.210 | 7.1104e-01 | 7.781e-03 |
| 88.211 | 6.9320e-01 | 7.676e-03 |
| 89.213 | 6.6963e-01 | 7.223e-03 |
| 90.214 | 6.4842e-01 | 7.207e-03 |
| 91.214 | 6.4119e-01 | 7.379e-03 |
| 92.214 | 6.2289e-01 | 6.993e-03 |
| 93.213 | 5.9840e-01 | 6.885e-03 |
| 94.213 | 5.8820e-01 | 6.838e-03 |
| 95.211 | 5.7078e-01 | 6.674e-03 |
| 96.209 | 5.5617e-01 | 6.342e-03 |
| 97.207 | 5.4371e-01 | 6.362e-03 |
| 98.204 | 5.2301e-01 | 6.245e-03 |
| 99.200 | 5.0597e-01 | 5.776e-03 |
| 100.196 | 4.8451e-01 | 5.816e-03 |
| 101.192 | 4.7642e-01 | 5.135e-03 |
| 102.187 | 4.5164e-01 | 5.075e-03 |
| 103.181 | 4.3703e-01 | 4.814e-03 |
| 104.176 | 4.2290e-01 | 4.765e-03 |
| 105.169 | 4.1079e-01 | 4.641e-03 |
| 106.162 | 3.9585e-01 | 4.459e-03 |
| 107.155 | 3.8909e-01 | 4.381e-03 |
| 108.147 | 3.7559e-01 | 4.237e-03 |
| 109.139 | 3.7004e-01 | 4.182e-03 |
| 110.131 | 3.5743e-01 | 4.072e-03 |
| 111.122 | 3.5313e-01 | 4.444e-03 |
| 112.112 | 3.4082e-01 | 4.114e-03 |
| 113.102 | 3.2933e-01 | 3.854e-03 |
| 114.091 | 3.2274e-01 | 3.899e-03 |
| 115.081 | 3.1234e-01 | 3.788e-03 |
| 116.069 | 3.0205e-01 | 3.646e-03 |
| 117.057 | 2.9361e-01 | 3.544e-03 |
| 118.045 | 2.8855e-01 | 3.479e-03 |
| 119.032 | 2.8037e-01 | 3.401e-03 |
| 120.019 | 2.7391e-01 | 3.347e-03 |
| 121.006 | 2.6823e-01 | 3.082e-03 |
| 121.992 | 2.6231e-01 | 3.344e-03 |
| 122.977 | 2.5435e-01 | 3.211e-03 |
| 123.963 | 2.4514e-01 | 3.143e-03 |
| 124.947 | 2.4257e-01 | 3.096e-03 |
| 125.932 | 2.3291e-01 | 2.998e-03 |
| 126.916 | 2.2770e-01 | 2.937e-03 |
| 127.899 | 2.2438e-01 | 2.859e-03 |
| 128.883 | 2.1325e-01 | 2.783e-03 |
| 129.865 | 2.0998e-01 | 2.741e-03 |
| 130.848 | 2.0899e-01 | 2.460e-03 |
| 131.830 | 2.0525e-01 | 2.878e-03 |
| 132.812 | 1.9583e-01 | 2.720e-03 |
| 133.793 | 1.9263e-01 | 2.712e-03 |
| 134.774 | 1.8840e-01 | 2.651e-03 |
| 135.755 | 1.8559e-01 | 2.613e-03 |
| 136.735 | 1.8482e-01 | 2.600e-03 |
| 137.715 | 1.7488e-01 | 2.366e-03 |
| 138.695 | 1.7477e-01 | 2.488e-03 |
| 139.674 | 1.7163e-01 | 2.437e-03 |
| 140.653 | 1.7070e-01 | 2.410e-03 |
| 141.334 | 1.7327e-01 | 2.587e-03 |
| 143.291 | 1.6624e-01 | 2.627e-03 |
| 145.246 | 1.6039e-01 | 2.033e-03 |
| 147.201 | 1.5589e-01 | 1.931e-03 |
| 149.154 | 1.5125e-01 | 1.919e-03 |
| 151.106 | 1.4843e-01 | 2.374e-03 |
| 153.057 | 1.4558e-01 | 1.767e-03 |
| 155.007 | 1.4175e-01 | 1.525e-03 |
| 156.957 | 1.4222e-01 | 1.730e-03 |
| 158.905 | 1.3723e-01 | 1.522e-03 |
| 160.853 | 1.3005e-01 | 1.662e-03 |
| 162.123 | 1.2510e-01 | 1.947e-03 |
| 162.801 | 1.2879e-01 | 1.678e-03 |
| 164.747 | 1.3078e-01 | 1.454e-03 |
| 166.694 | 1.3469e-01 | 1.571e-03 |
| 168.639 | 1.3041e-01 | 1.533e-03 |
| 170.585 | 1.1894e-01 | 1.797e-03 |
| 171.852 | 1.2050e-01 | 1.930e-03 |
| 172.530 | 1.2304e-01 | 1.940e-03 |

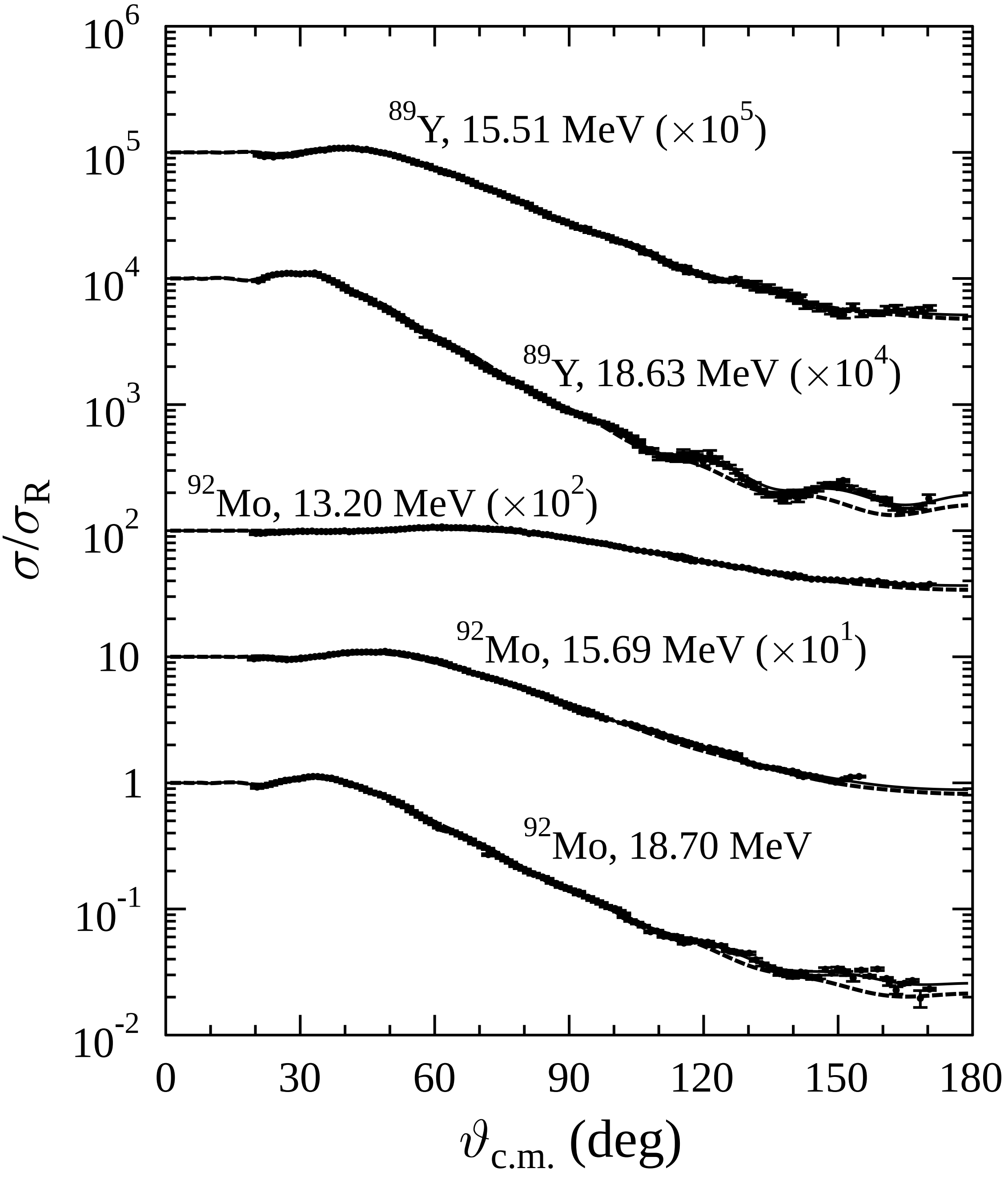

**Graph 1**. Elastic ($\alpha$,$\alpha$) scattering angular distributions of $^{89}$Y and $^{92}$Mo.

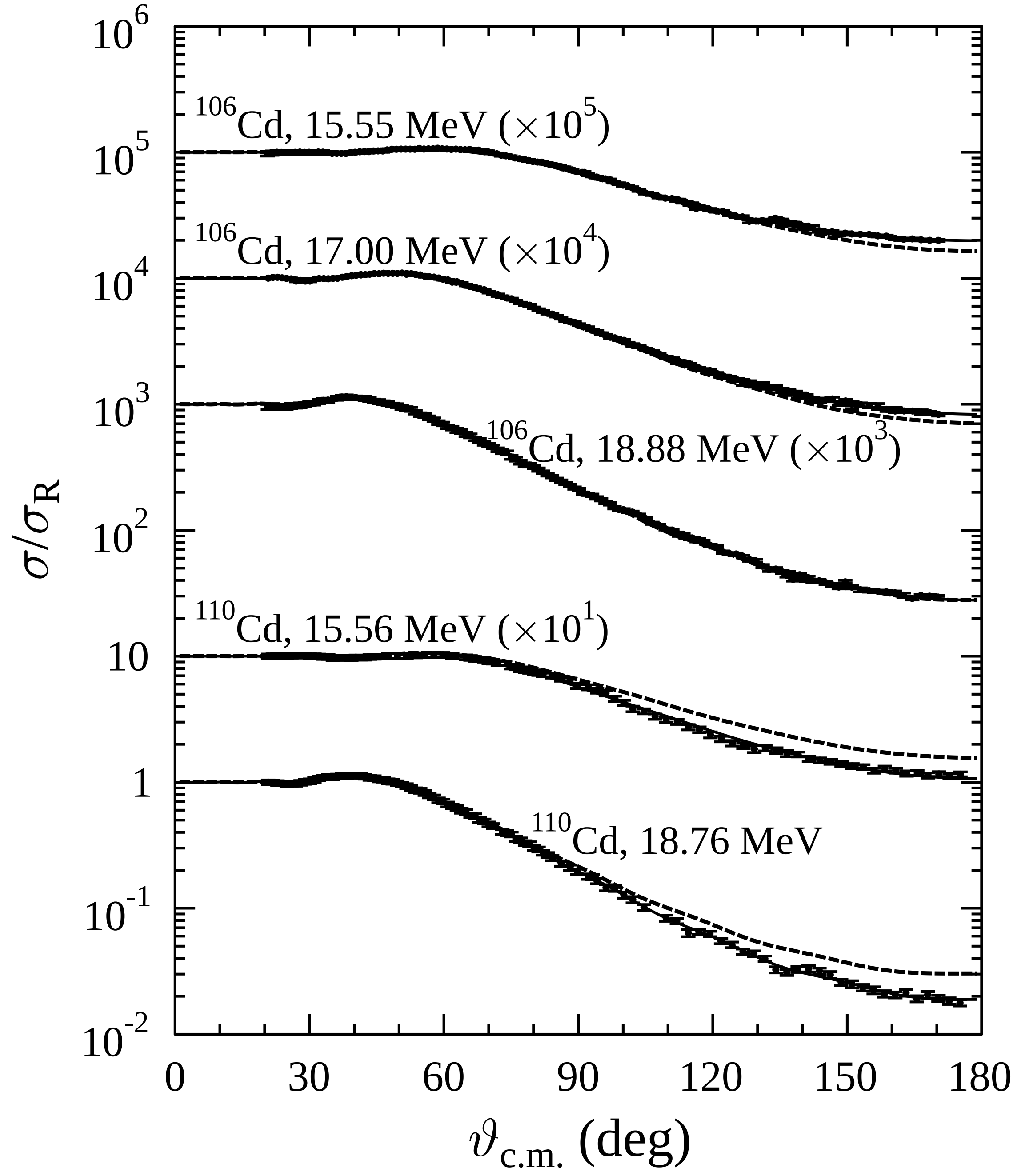

**Graph 2**. Elastic ($\alpha$,$\alpha$) scattering angular distributions of $^{106}$Cd and $^{110}$Cd.

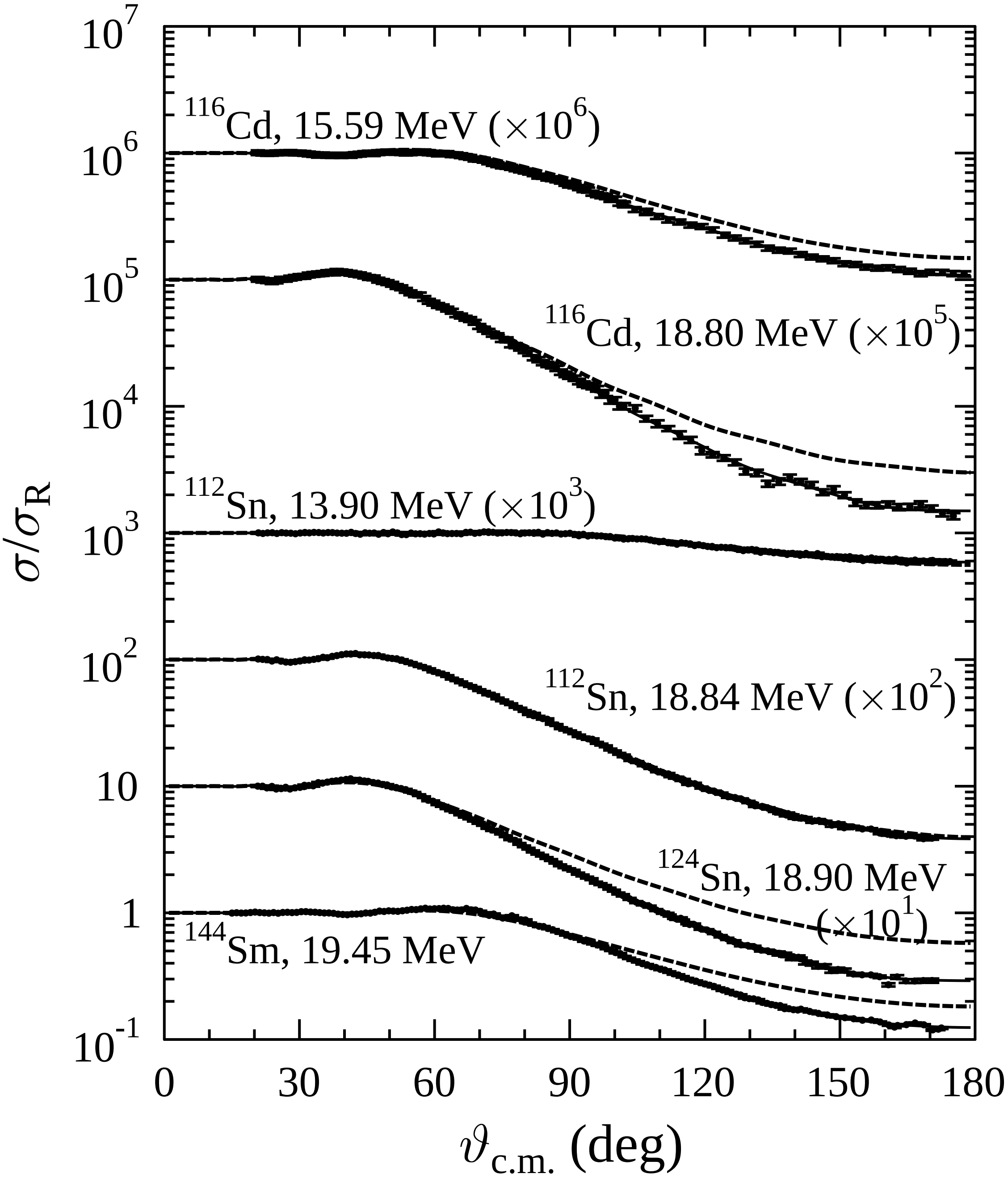

**Graph 3**. Elastic ($\alpha$,$\alpha$) scattering angular distributions of $^{116}$Cd, $^{112}$Sn, $^{124}$Sn, and $^{144}$Sm.